Use of Remotely Sensed Data to Quantify Plant Water Use from Irrigated Lands in Wolf Bay Watershed Area

by

Nishan Bhattarai

A thesis submitted to the Graduate Faculty of
Auburn University
in partial fulfillment of the
requirements for the Degree of
Master of Science

Auburn, Alabama
December 13, 2010

Keywords: plant water use, irrigation water demand, evapotranspiration, remote sensing,
SEBAL, Wolf Bay watershed area

Approved by

Mark Dougherty, Co-chair, Assistant Professor of Biosystems Engineering
Latif Kalin, Co-chair, Assistant Professor of Forestry
Luke Marzen, Associate Professor of Geography

Abstract

Irrigation is one of the major water uses in the US and the world. An attempt is made to quantify water use from irrigated plants using remotely sensed data. Objectives of the study are to 1) assess the validity of a modified surface energy balance algorithm for land (SEBAL) model in the humid southeastern US; 2) quantify seasonal volumetric ET as an estimate of plant water use in Wolf Bay watershed area during growing season (April to September) of 2005-2008 using remotely sensed data; and 3) derive water demand factors from remotely sensed data to project future irrigation water demand in Wolf Bay watershed area. Daily, monthly, and two-month ET from the modified SEBAL are validated with energy-budget eddy covariance ET measurements from four USGS stations in Florida. SEBAL estimated daily ET with a root mean square error (RMSE) of 0.48 mm/day, % RMSE of 10%, mean bias error (MBE) of 0.05 mm, Nash-Sutcliffe efficiency coefficient (ENS) of 0.82, and coefficient of determination (R^2) of 0.83. Monthly ET was estimated with a RMSE of 16 mm, % RMSE of 16%, MBE of -2 mm, ENS of 0.77 and R^2 of 0.77. Two-month ET was estimated with a RMSE of 30 mm, % RMSE of 16%, MBE of -5 mm, ENS of 0.71 and R^2 of 0.73. The validated SEBAL model is applied in Wolf Bay watershed area to estimate seasonal ET from irrigated areas during the growing season (April-September) in 2005-2008. Area of total irrigated agricultural land in Wolf Bay watershed area is estimated using high quality digital aerial photographs, Landsat 5 TM images, and SEBAL derived parameters: surface albedo, normalized difference vegetation index (NDVI), and evaporative fraction. Results confirm that volumetric ET (Plant water use) from irrigated areas was higher in

dry years (2006 and 2007) than in the wet year (2005). Estimated water use from irrigated area in Wolf Bay watershed area in 2005, 2006, 2007, and 2008 was 5.91, 6.26, 6.87, and 6.59 million cubic meters, respectively. Water demand factors derived for different crops and turf farms for years 2005 to 2008 confirmed that plants have higher water demand in dry years than in wet years. Water demand factors and landuse and land cover (LULC) projection maps of Wolf Bay watershed area for years 2010, 2020, 2030, and 2040 were utilized to project irrigation water demand under dry, normal and wet precipitation conditions. Future irrigation water demand is based on the extreme scenario that most crop land in Wolf bay watershed area is converted into golf courses and turf farms with the assumptions that 100% of agricultural land is irrigated in 2040. Results indicate that irrigation water demand for year 2010 will be increased by 59% (6.19 to 9.82 million cubic meters), 65% (6.76 to 11.12 million cubic meters), and 63% (6.45 to 10.52 million cubic meters), under wet, dry, and normal climatic conditions, respectively from 2010 to 2040. Remote sensing method has been found useful in estimating plant water use, deriving water demand factors for different plants, and projecting irrigation water demand. Planners can use the projected irrigation water demand information from remote sensing method to effectively manage water resources in Wolf Bay watershed area. A case study is provided showing how the methods can be used to project future water demand at a watershed scale.

Acknowledgments

Table of Contents

List of Tables

List of Figures

xi

CHAPTER 1

INTRODUCTION

Water is relatively inexpensive in terms of cost, but is certainly not free. Quantifying the

water demand for a region is essential to meet current and future needs. Studies of water supply

should be conducted at the regional scale (Dziegielewski and Choudhury, 2008). Historic water

use trend can provide an idea of future water demand in a region. Planners need accurate water

use statistics to effectively manage water resources at both the regional and national level.

Almost 60% of all fresh water withdrawal in the world is used for some kind of irrigation

(USGS, 2000) and 70% of total fresh water use in the US is by irrigation (Weibe and Gollehon,

2006). Hence, irrigation water demand study is required for better management of water

resources in the US and the world. In this study, a remote sensing method is used to estimate

historic plant water use from irrigated plants and project future irrigation water demand in Wolf

Bay watershed area.

1.1 Background

1.1.1 Wolf Bay watershed Area

Wolf Bay Watershed area is located in Baldwin County, Alabama, near the Gulf of

Mexico covering an area of approximately 126 km^2. The watershed is mostly rural with two

municipalities; Foley and Elberta. The towns of Gulf Shores and Orange Beach lie between Wolf

Bay watershed and the Gulf of Mexico. Gulf Coast tourism and retirement destinations have

attracted a large number of people in recent years causing a rapid increase in population and

1

considerable land use change in and around Wolf Bay watershed area. The general population trend of Wolf Bay watershed area is presented in Figure 1.1.
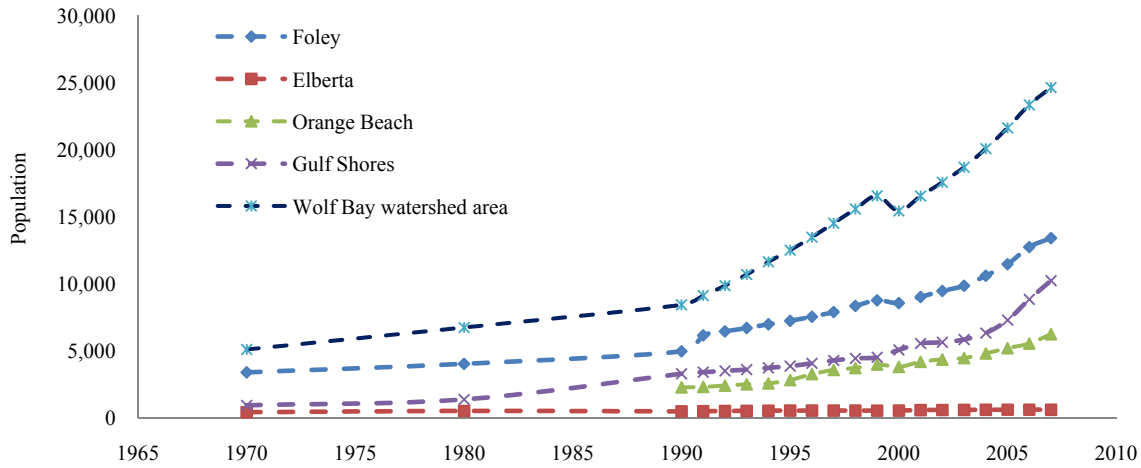
Figure 1.1. Population of four cities in and around Wolf Bay watershed area from 1970 to 2007 (Source: US Census Bureau for 1970, 1980, 1999, 2000; and 1990 to 2007 population from Baldwin County Planning Commission).

Wolf Bay watershed population area is estimated using a GIS layer of US Census Bureau Block level data for 1990 and 2000 (Appendix B.1). The population of Wolf Bay in other years is estimated using the annual population incremental rate from Baldwin County as described in Appendix B.1 and estimates shown in Appendix B.2 (Table B.2.3). Figure 1.1 indicates an increasing rate of population in Wolf Bay watershed area since 1970.

1.1.2 Water use

Based on water withdrawal data from Alabama Department of Economic and Community Affairs (ADECA) in 2005, major water use categories in Baldwin County that are most applicable for water use study in Wolf Bay watershed area are listed below:

- Public water use – All water withdrawals by public water companies, including municipal irrigation of parks and city golf courses, and recreation areas.

- Private-supplied water use – All non-irrigation private-supplied water withdrawals for domestic water use.

- Irrigation water use – Water withdrawals for irrigation use in center pivot systems, croplands, turf farms, golf courses, and nurseries are considered as irrigation water use.

ADECA reported population and water withdrawal figures for Baldwin County in 2005. The population served by public water was 136,892, whereas the rest of the population, 25,694 (about 16% of total population), was private-supplied. The total water withdrawal in 2005 was 69.01 million gallons per day (MGD). Major water withdrawal categories (% of total volume of water use) in Baldwin County in 2005 are shown as in Figure 1.2. Irrigation water withdrawal makes up 63% of total estimated water withdrawals in Baldwin County, followed by public water use which comprises 31% of water withdrawals. It can be assumed that three major water use categories in Wolf Bay watershed area are public, private-supplied and irrigation.
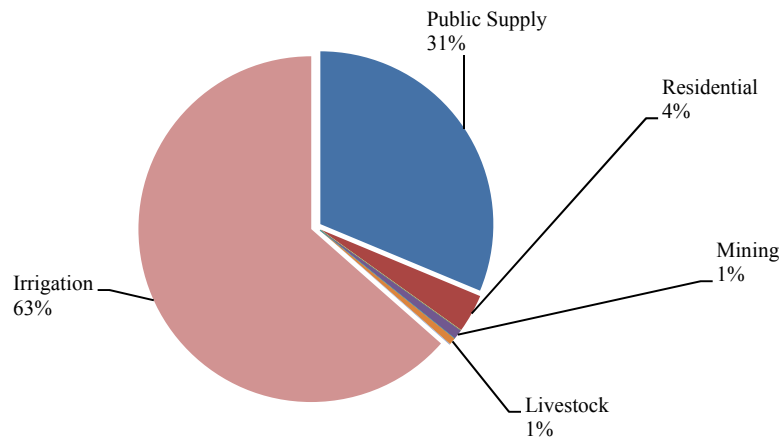
Figure 1.2. Water withdrawals (MGD) in Baldwin County, 2005 (Source: ADECA).

This study is focused on plant water use, however, public and private-supplied water use in Wolf Bay watershed area make up a large component of water use in the area. Public water use is estimated using monthly and annual water withdrawal data from public water companies in Wolf Bay watershed area. Available water structure data from Riviera Utilities in Foley, AL is used to estimate per capita residential water use (gallons per person per day, GPCD). Total

population served by public water is estimated using total urban area population. Population not served by public water is considered as private-supplied water use population. Per capita residential water use from Riviera Utilities is used to estimate total annual private-supplied water use. The estimates of public and private-supplied water use as well as the methods used are described in Appendix B.1 and B.2. Three major water use types in Wolf Bay watershed area are discussed below:

Public water use

Five water companies supply water in and around the Wolf Bay watershed area: Riviera Utilities; Elberta Water; Gulf Shores Water & Sewer; Orange Beach Water & Sewer; and Perdido Bay Water. Public water companies within Wolf Bay watershed boundary are Riviera Utilities, Elberta Water, and a small portion of Perdido Bay water. According to National Land Cover dataset (NLCD) land use/land cover (LULC) map and Natural Resource Conservation Service (NRCS) digital aerial photographs (2006 and 2009), the area covered by Perdido Bay Water inside Wolf Bay boundary is mostly rural (NLCD, 2001; NRCS, 2006; NRCS, 2009). Ground water withdrawal is the only reported source of water production for these five public water companies. The largest water company in terms of service area within Wolf Bay watershed is Riviera Utilities which is responsible for approximately half of the total water withdrawals by volume in the watershed area.

Both the per capita residential water use, gallons supplied per person, and gross per capita public water use, total public water supplied divided by the total population served by public water, from Riviera Utilities shows an increasing trend during summer, with expected decreasing trend in the winter. Recent Riviera Utilities records are compared to long-term average monthly

public withdrawals from the entire watershed (including adjacent cities) in Figure 1.3, providing a useful means to document historic and current fluctuation of water use.
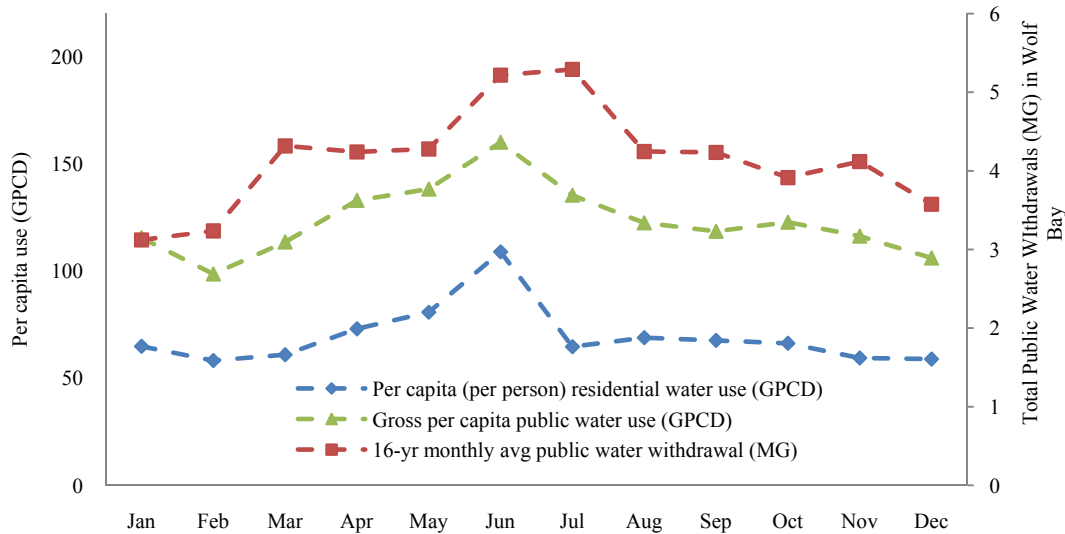
Figure 1.3. Estimated gross per capita public water use and per capita residential water use (GPCD), Riviera Utilities, from Sep 2008 showing seasonal fluctuation (Source: Riviera Utilities, ADECA, Perdido Bay water, US Census Bureau and Baldwin County Commission).

Private-supplied water use

Not all population in Wolf Bay watershed area is served by public water companies. A certain portion of the population uses privately owned wells for residential, irrigation, or other purposes. Private-supplied water withdrawals for residential use are estimated by multiplying private-supplied population by per capita residential water use. Figure 1.4 indicates that both public and private-supplied population has been increased rapidly in recent years, which indicates higher water use patterns for both public and private-supplied water users. Higher population also indicates that Foley is considerably expanding outside the boundary of Wolf Bay watershed. Foley is currently the largest city in the Wolf Bay watershed area with a population of 13,807 in 2008 (Baldwin County Commission, 2008).
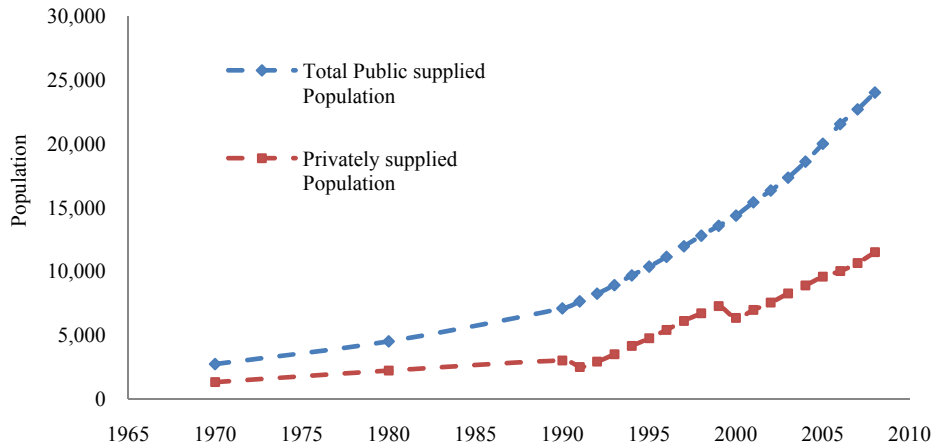
Figure 1.4. Population served by public and private water showing relatively higher service area coverage by public water in Wolf Bay (Sources: ADECA, Riviera Utilities, US Census Bureau, Baldwin County Commission).

Irrigation water use

Water withdrawals for irrigation use in center pivot systems, croplands, turf farms, golf courses, and nurseries are considered as irrigation water use. Plant water use in this study is defined as water used by irrigated plants in turf farms, nurseries, crop lands, and golf courses. Plant water use is quantified as actual water use from the plant. Hence, water lost in the irrigation system can be added to plant water use to get irrigation water use. GIS point shapefiles of irrigation water withdrawal data (1993 to 2008) within Wolf Bay watershed boundary from ADECA indicates that approximately 72% of historic irrigation water withdrawal comes from ground water (Figure 1.5).

6
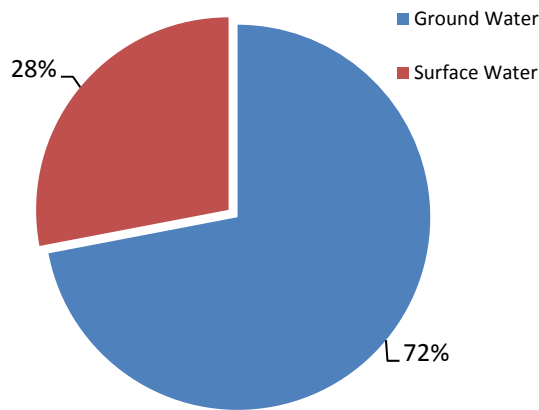
Figure 1.5. Sixteen -year (1993-2008) average ground water and surface water irrigation water withdrawals in Wolf Bay (Source: ADECA).

Figures 1.6 shows 16-year average monthly and yearly ground water irrigation withdrawals in Wolf Bay watershed, indicating the higher seasonal use expected during the warmer months of the growing season.
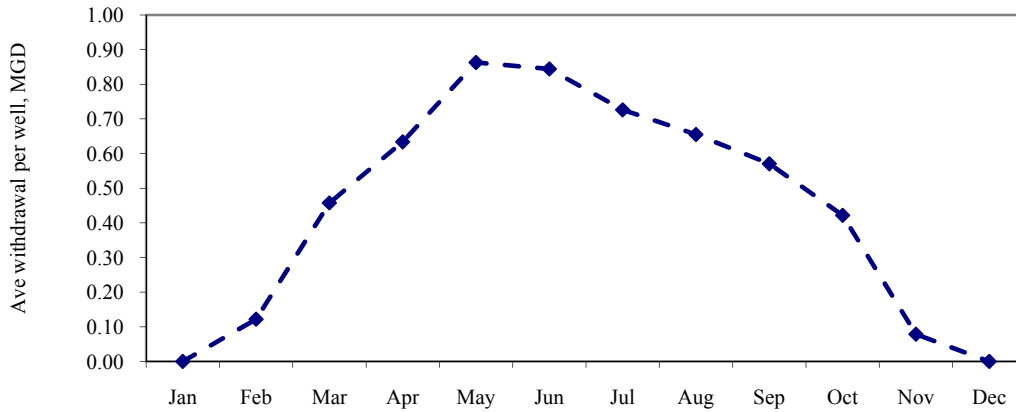
Figure 1.6. Average monthly ground water irrigation water withdrawals per well (4 to 5 wells) in million gallons per day (MGD) in Wolf Bay watershed from 1993 to 2008 showing historic seasonal fluctuation (Source: ADECA).

1.1.3 Agricultural lands in Wolf Bay watershed area

Crop lands and pastures covered 54% of Wolf bay watershed area in 1992. This value was reduced to 43% in 2001 (NLCD 1992 and 2001) and 34% in 2005 (Baldwin County Commission, 2005). According to Natural Resource Conservation Service (NRCS) data gateway crop land data layer by state, in 2008, about 30% of total area of Wolf Bay was covered by cropland, seed/sod grasses, nurseries, golf courses, and tree crops and pastures (NRCS, 2008). This decreasing trend in crop and pastures in Wolf Bay may have been caused by increasing urbanization.

Approximately, 17% of the total area (21.97 km^2) in Wolf Bay watershed area included potentially irrigated lands (Lands that are likely to be irrigated during growing season especially crop lands, golf courses and seed/sod farms and turf farms) in 2008 not including pasture. Figure

1.7 shows major crops in Wolf Bay watershed area by percentage of total potential irrigated area in 2008.
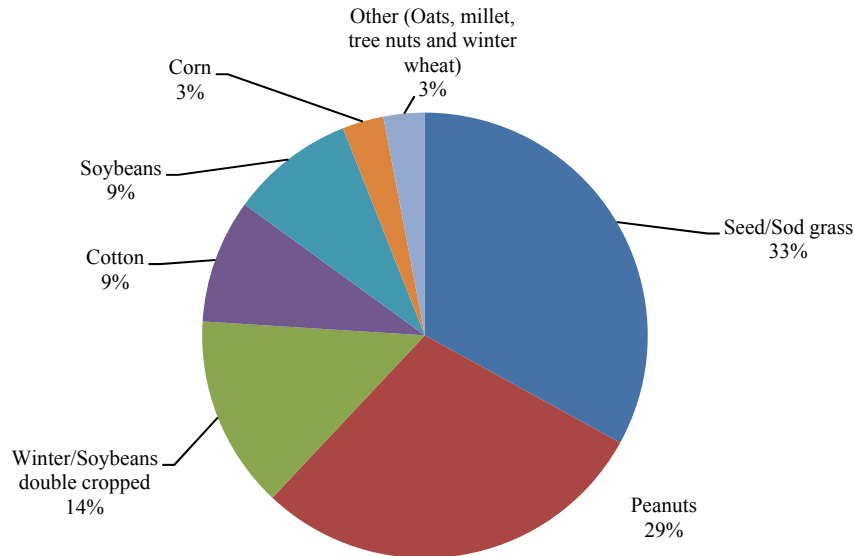
Figure 1.7. Major crops in Wolf Bay watershed area in 2008 as of total potential irrigated area (21.97 km^2) present in 2008 (Source: NRCS, 2008).

Figure 1.7 indicates that major crops in Baldwin County are soybeans, peanuts, corn, cotton, and winter wheat for grains. Major irrigated crops in Wolf Bay include soybeans, peanuts, cotton and corn (US Census of Agriculture, 2007). Irrigation of golf courses and seed/sod grass farms is also a common practice in Baldwin County. Most of the planting season starts in April with harvest ending in September. Winter wheat is the exception, as it is planted in September/October and harvested in May-April. Winter wheat is planted during the cool season when irrigation is not likely required. Wolf Bay watershed area includes only one golf course (Glenlakes golf course) which is irrigated through surface water withdrawal (ADECA, 2008).

1.2 Problem justification

Historic and recent trends in agricultural land use indicate that irrigation continues to be one of the major water uses in Wolf Bay watershed area. An efficient method of evaluating plant water use and future water demand is to study the historic and current plant water use in the Wolf

8

Bay watershed area. As increasing urbanization in Wolf Bay watershed area creates future water demand, projections of irrigation water demand provide necessary information. Planning efforts work to ensure that sufficient water resources will be available for irrigated areas in the Wolf Bay watershed area as well as consumption and other use by residents of businesses and municipality.

In recent decades, the use of remote sensing methods using satellite imagery for estimating evapotranspiration (ET) has gained popularity. ET, defined as a combined process of evaporation and transpiration, refers to the water consumed by agricultural plants and normally refers to all water evaporated from plant and soil surfaces plus that retained within plant tissues which is less than 1% of the total evaporated during a normal growing season (Jensen, 1969). ET maps generated from remotely sensed data reflect actual plant water use over a large coverage. Hence, estimation of ET from irrigated lands in Wolf Bay can provide a good estimate of plant water use in Wolf Bay watershed area.

Surface Energy Balance Algorithm for Land (SEBAL) model developed by Bastiaanssen (Bastiaanssen et al., 1998a; Bastiaanssen et al., 1998b, Bastiaanssen, 2000; Bastiaanssen et al., 2005) and modified by Allen et al. (Allen et al., 2002a; Allen et al., 2005a) has been widely used to provide accurate estimates of ET from the agricultural crops in the last decade. In the US, the modified SEBAL model has been used in Idaho, California, New Mexico, Minnesota, Texas, and Nebraska (Allen et al., 2005b; Melesse et al., 2006; Soppe et al, 2006; Gowda et al, 2008a; Singh et al., 2008). However, much less research about the SEBAL model has been done in humid southeastern US. A study applying the modified SEBAL model to determine water use from agricultural lands can be useful for water demand related studies in the humid southeastern US.

This research to estimate plant water use supports efforts underway by others to conduct comprehensive water use analysis in Wolf Bay watershed. Estimation of public and private-supplied water use can be done using water withdrawal data from water companies and population data from US Census Bureau (Appendix B.1). Historic trends of public and private-supplied water use can be used to project future public and private-supplied water use in Wolf Bay watershed area using projected population data. Total annual water demand projection in Wolf bay watershed can be estimated as the sum of projected public, private-supplied and plant water demand. Hence, this study is useful for planners seeking information regarding current water supplied available under extreme conditions such as drought and climate change.

1.3 Research objectives

1.3.1 Research questions

Irrigation water use studies are usually done by survey, using ground based studies and irrigation records. However in the absence of ground based data, it is difficult to estimate historic plant water use. Remote sensing methods using high- to low- resolution satellite imagery and aerial photography may provide an alternative. Given that we have minimal ground data due to lack of field based water use studies at the small watershed level, this research is conducted to answer the following two research questions:

1. Can remotely sensed data provide an estimate of historic plant water use in Wolf Bay watershed?

2. Can historic remotely sensed data be used in Wolf Bay watershed to derive water demand factors for agricultural lands that can be used for projecting irrigation water demand? Water demand factor is defined as unit depth or volume of water associated with per unit area of land (discussed in chapter 2).

1.3.2 Research objectives

The main goal of this research is to estimate historic and current plant water use in the Wolf Bay watershed area using remotely sensed data. The three research objectives of the research are:

1. Assess the validity of a modified surface energy balance algorithm for land (SEBAL) model in the humid southeastern US.

2. Quantify seasonal volumetric ET as an estimate of plant water use in Wolf Bay watershed area during selected wet and dry growing season (April-September) between 2005 and 2008 using remotely sensed data.

3. Derive water demand factors (mm per growing season) for major irrigated plants in Wolf Bay watershed area using remotely sensed data to project future irrigation water demand.

1.4 Thesis outline

This study focuses on three main objectives, mentioned above. The first objective is covered in Chapter 3. Objectives 2 and 3 are covered in Chapter 4. Both chapters 3 and 4 are written in a manuscript format.

Chapter 2 reviews literature related to evapotranspiration estimation, use of remotely sensed data, the Surface Balance Algorithm for Land (SEBAL) model, and land use-based projection of irrigation water use.

Chapter 3 describes validation of the Surface Balance Algorithm for Land (SEBAL) model to estimate ET using Landsat 5 TM images of Florida.

Chapter 4 describes application of the validated remote sensing method used to estimate plant water use in Wolf Bay watershed area.

Chapter 5 provides conclusions as well as recommendations for future research.

CHAPTER 2

LITERATURE REVIEW: REMOTE SENSING METHOD FOR QUANTIFYING PLANT
WATER USE

Water is a basic requirement of life. Major sources of water supply such as groundwater

aquifers, lakes, and rivers are shared by users in many localities. Water use planning is important

to assure the future need of the population. Historical water use scenarios and current population

trends are important components of prediction for future water demand. This chapter reviews

relevant literature regarding remote sensing methods for estimating evapotranspiration (ET), and

plant water use, and land use based irrigation water demand projection.

2.1 Plant water use and evapotranspiration

Irrigation is the application of water to the soil to provide adequate moisture for plant

growth. Approximately 70% of world water use is for agriculture (World Bank, 1992). Similarly,

70% of total fresh water use in the US is by irrigation (Weibe and Gollehon, 2006). Plant water

use includes extraction of ground water through springs or wells, surface water withdrawal from

reservoirs, rivers, lakes, and drainage water. Worldwide, irrigated area has increased rapidly over

the last 30 years to provide for increased agricultural output and to maintain a growing

population (Cai et al., 2001). Evapotranspiration (ET) is defined as the transport of water into the

atmosphere through the combined processes of evaporation and transpiration. ET is an important

component of the earth's energy and water budget and critical in regulating the water cycle.

Jenson (1969) stated that water consumption by agricultural plants normally refers to all water

evaporated from plant and soil surfaces plus that retained within plant tissues. However, the amount of water retained within the tissue of agricultural plants is generally less than 1% of the total evaporated during a normal growing season. Therefore, water consumption by agricultural plants, termed ET, essentially involves water evaporated from both plant and soil surfaces. Thus, ET and plant consumptive use are typically considered equal.

Crop water requirement is the amount of water required to compensate evapotranspiration loss from a cropped field. It is the amount of water that needs to be supplied to a crop either by rainfall or by irrigation. The irrigation water requirement and crop evapotranspiration have slightly different definitions. The irrigation water requirement can be defined as the difference between the crop water requirement and effective precipitation plus additional water for leaching of salts and to compensate for non-uniformity of water application (FAO, 2009). Effective precipitation is the amount of rainfall that contributes to root zone moisture (Fangmeier et al., 2005).

Crop ET provides information about irrigation water requirement of the plant (FAO, 1998). Crop ET is a function of different factors such as number and types of plants, soil moisture, soil type, season, air and surface temperature, and precipitation (Morton, 1968; FAO, 2009). As a result, estimation of ET is a relatively complicated process (Xu and Singh, 1998).

2.2 Evapotranspiration estimation methods

Evapotranspiration estimates can be made by quantifying all the components of the hydrologic budget (Musick et al., 1994; Li et al., 2000; Sadeh and Ravina, 2000; Aase and Pikul, 2000; and Wang et al., 2001). The components of hydrologic budget can be written as equation 1 (Viessman and Lewis, 2002) and also shown in Figure 2.1:

$$P - R - ET - G - I = \Delta S \qquad (1)$$

P   ET

                          R

ΔS

                    G
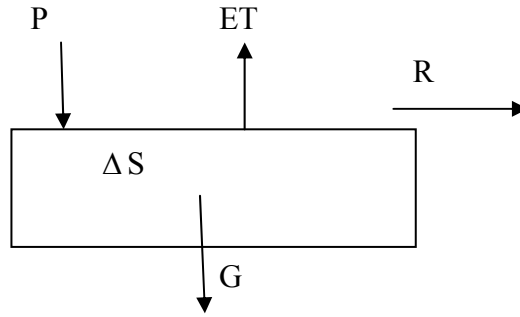
Figure 2.1. Hydrologic budget or fundamental equation used in hydrology.

where; R is surface runoff, G is the ground water influx, P is the precipitation, ΔS is the change

in storage, I is the interflow or subsurface flow, and ET is evapotranspiration. All components

are volumes per unit of time.

Evapotranspiration is the residual term in the Equation 1 and can be modified and written as:

$$ET \ = \ P - R - G - I - \Delta S \qquad\qquad (2)$$

Hydrological budget methods for ET estimation method include estimation or

measurement of all components on right hand side of equation 2. Studies related to the

hydrologic budget method have potential for high errors as it is difficult to measure all the

components of hydrologic budget accurately (Musick et al., 1994; Li et al., 2000; Wang et al.,

2001; Kang et al., 2002). Hydrological budget methods are applicable to small plots (10 m^2) or to

large catchments (>106 m^2) and they may cover periods ranging from a week to a year (Rosa and

Sharma, 1984). For large river basins measured in thousands of kilometers, the groundwater

inflow and change in storage can typically be neglected. Hence the water budget equation for

evapotranspiration in large watersheds becomes, $ET \ = \ P - Q,$ where Q is the stream flow

which equals to sum of surface runoff, interflow, and baseflow.

Various field measurement based methods have also been used for ET estimation. Some

examples include soil (Daamen et al., 1993) and plant weighing lysimeters (Edwards, 1986), soil

water budgets (Eastham, 1988; Jaeger et al., 1997; Cuenca et al., 1997), sap flow (Smith and

14

Allen, 1996), chemical tracing (Calder et al., 1986; Kalma et al., 1998), the Bowen ratio energy balance (Denmead et al., 1993), eddy covariance (Baldocchi et al., 1988) and catchment water balance (Bosch and Hewlett, 1982; Swift et al., 1988). The complexity associated with the estimation of ET has driven the development of new methods (Doorenbos and Pruitt, 1977; Allen et al., 1998). Empirical formulas were used early on to relate evaporation to one or more meteorological parameters and fair agreement with evaporation pans has been achieved (Penman, 1948; Thornthwaite, 1948; Blaney and Criddle, 1950; Van Bavel, 1966). ET is also measured by analysis of water and energy fluxes at flux towers on a short-period or daily basis. Resulting values are converted into short-period ET or daily ET using the surface energy balance equation described later (Wilson et al., 2001; Sun et al., 2008; Law et al., 2002). ET measured at flux towers has been widely used to estimate evapotranspiration and validate ET results from other models (Wilson et al., 2001; Sun et al, 2008). Similarly, the Bowen ratio-energy balance method (BREB) has been widely used to estimate vegetation evapotranspiration and validate ET results from other models (Fritschen, 1966; Malek et al., 1990; Wight et al., 1993; Hou et al, 2010; Ortega-Farias et al., 1993; Farahani and Bausch, 1995).

The conventional method of ET or crop water requirement involves use of routinely collected climate data to compute a reference evapotranspiration (ET_{ref}) for a reference crop, which is multiplied by an area-specific crop coefficient, K_c, (Allen et al., 1998). Reference ET is defined as evapotranspiration from a standard crop under well watered and fully shaded conditions (Allen et al., 1998). The conventional method provides only a point estimate of ET, and is subjected to errors due to variations in season, crop growth stage, planting period, and root-zone moisture condition (Ahmad et al., 2006). Quantifying the spatial variation of ET over large areas at regular intervals is very useful in hydrological applications (Stisen et al., 2008),

crop yield forecasting (Rosema et al, 2001), drought monitoring (Anderson et al., 2007), climatic analysis (Wood and Lakshmi, 1993), and irrigation scheduling (Allen, 1998).

2.3 Remote sensing methods of estimating evapotranspiration

In recent decades, the use of remote sensing (RS) methods using airborne or satellite imagery to estimate ET has gained popularity. RS methods offer an indirect measurement of ET typically using a set of equations in a strict hierarchical sequence to convert reflected spectral radiances into estimates of actual ET (Bastiaanssen et al., 2005). RS methods have played a great role in water resource management because of the enhanced ability to indirectly measure fundamental ET processes from satellites or other airborne platforms (Bastiaanssen and Bos, 1999; Bastiaanssen et al., 2005; Menenti, 2000). Synoptic coverage is now available at a variety of scales and temporal coverages and is less costly and vastly superior to field measurement of comparable data (Bastiaanssen et al., 2005).

Literature indicates that estimation of ET using remote sensing provides a unique synoptic alternative to quantify actual irrigation water use (Senay et. al., 2007; Kramer et al., 2008). Murray et al. (2009) used the Enhanced Vegetation Index (EVI) from MODIS sensors on board the Terra satellite (NASA, 2010) to scale ET over agricultural and riparian areas along the Lower Colorado River in the southwestern U.S. A linear regression model was developed by plotting crop coefficients derived from ground based ET divided by potential (reference crop) versus EVI scaled between bare soil (0) and full vegetation cover (1). The model for actual ET had an error or uncertainty of approximately 20%. The algorithm was applied to irrigation districts and riparian areas from Lake Mead to the US/Mexico border along the Colorado River. Results from RS data for agricultural crop ET were similar to results produced by crop coefficients developed for the irrigation districts along the river. Through RS techniques, riparian

ET was found to be only half that of crop coefficient estimates set by expert opinion, equal to about 40% of reference crop evapotranspiration (Murray et al., 2009).

Ray and Dadhwal (2001) used satellite-based RS data and GIS tools to estimate seasonal crop ET in the Mahi Right Bank Canal area of Gujarat, India. RS derived soil adjusted vegetation index (SAVI) values were used to estimate crop coefficients (K_c) for various major crops grown in the canal area through an empirical equation developed from regression analysis. The RS derived crop coefficient can be more useful than traditional crop coefficients in the sense that it represents a real-time crop coefficient that responds to actual crop conditions in the field and captures between-field variability. A reference crop evapotranspiration map using the FAO-24 modified Blaney–Criddle method (Allen and Pruitt, 1986) was generated from point meteorological observations through interpolation using the inverse-square-distance approach available in ARC/INFO GIS (ESRI, CA). The K_c and reference crop ET maps were combined to generate a seasonal crop evapotranspiration (ET_{crop}) map which highlighted spatial variation in ET_{crop} ranging from more than 600 mm per season for healthy tobacco crops to less than 150 mm per season for very poor wheat crops. RS based crop ET estimates were 7.2 to 12.8% lower than ET estimates derived from corresponding weather station data using reported crop coefficients by Water Technology Center (WTC, 1983) and reference ET at weather station.

Other research using remote sensing methods to map ET has been completed at a regional or global scale (Roerink et al., 1997; Kite and Droogers, 2000; Alhhab et al., 2007; Zhang et al., 1995; Chen et al., 2001; Tsoubi et al., 2008; Romaguera, et al., 2010; Nourbaeva et al., 2003; Jia et al., 2009). Use of high resolution images can be particularly useful for mapping ET at a local scale. The availability of high- resolution Landsat images with thermal bands has provided this opportunity with Landsat pixel sizes small enough to locate and quantify diversity from

individual agricultural fields (Kramber et al., 2008). Since Landsat images with thermal bands are available back to 1984, the available imagery database provides a good source for estimating crop water use at a local scale even in the past.

2.4 Surface Energy Balance Algorithm for Land (SEBAL)

The SEBAL model developed by Bastiaanssen (Bastiaanssen et al., 1998a; Bastiaanssen et al., 1998b; Bastiaanssen 2000; Bastiaanssen et al., 2002, 2005) and modified by Allen et al. (Allen et al., 2002) can be used to map the spatial variation of ET across a range of land uses at a local and regional scale. The Idaho Department of Water Resources (IDWR), for example, uses a Mapping Evapotranspiration at high Resolution with Internalized Calibration (METRIC) model, a modification of SEBAL model, to map evapotranspiration in the Snake River basin of Idaho. SEBAL and METRIC models use Landsat thermal data as a low-cost, high-quality alternative to traditional methods for monitoring water use from irrigation wells.

The main advantage of SEBAL model over other remote sensing methods is that it requires minimum ground data and can accurately measure seasonal or annual ET. The accuracy can be 85% on a daily basis and 95% on a seasonal basis (Bastiaanssen, et al., 2005). SEBAL method has been used in various studies to estimate evapotranspiration rates in Spain, US, China, Niger, Sri Lanka, Kenya, Morocco, The Netherlands and Turkey (Pelgrum and Bastiaanssen, 1996; Schmugge et al. , 2003; Morse et al, 2000; Wang et al., 1995; Roerink, 1995; Hemakumara et al., 2003; Jacob et al., 2002;; Lagouarde et al., 2002; Bastiaanssen and Bos, 1999; Farah, 2001; van den Kroonenberg, 2003; Kohsiek et al., 2002; Kite and Droogers, 2000).

Remotely sensed estimates of surface albedo, ground temperature and thermal infrared emissivity are used to compute reflected short wave and emitted long wave radiation away from the surface. A combination of short- and longwave radiation provides a measure of net radiation

absorbed at the surface of every pixel. The surface balance equation is based on the theory that incoming net solar radiation drives all relevant energy exchanges on earth's surface including ET, as shown below:

$$\Delta\theta/\Delta t = R_n - G + H + \lambda ET \tag{3}$$

$$[R_n = G + H + \lambda ET] \tag{4}$$

where; $\Delta\theta/\Delta t$ is the net energy storage which is assumed to be 0 for the time of the image taken. R_n (Wm^{-2}) represents the net surface radiation which is the actual amount of energy available at the surface. G (Wm^{-2}) represents the soil heat flux which is the rate of heat storage in the soil and vegetation. H (Wm^{-2}) represents the sensible heat flux which is the rate of heat loss to the air from the surface due to the temperature difference between the surface and air above the surface. λET (Wm^{-2}) is the latent heat flux, a measure of the amount of energy available to change available water from liquid to vapor, associated with ET.

Ahmad et al. (2005) used SEBAL to assess daily evapotranspiration across a range of land uses in the middle of the Olifants Basin in South Africa. Their study indicates that Landsat TM images can be used to derive a temporal series of evapotranspiration maps for a wide variety of water resource related studies. Tasumi et al. (2003) validated SEBAL model in the western United States and also conducted sensitivity and repeatability analyses. Their validation studies indicated that the ET estimates from SEBAL correspond well with lysimeter-measured ET for agricultural crops in the semi-arid study area. A repeatability test using two independent images and weather datasets indicated that seasonal estimation by SEBAL has a high repeatability. Seasonal estimates of evaporative fraction (ET_rF), defined as estimated seasonal ET divided by reference ET, and instantaneous evaporative fraction, defined as estimated instantaneous ET divided by reference ET, were relatively consistent with standard deviations of 0.06 and 0.05,

respectively. Tasumi et al. (2003) also demonstrated that SEBAL results can be used to validate traditionally applied crop coefficient curves.

Complex and time consuming atmospheric corrections can be avoided using the SEBAL model. ET estimation in SEBAL is not affected by errors in intermediate estimations. The SEBAL method uses surface temperature without correcting atmospheric effects on the measurement of longwave radiance. Two major atmospheric effects on the longwave radiance are path thermal radiance which is electromagnetic radiation emitted from a material due to heat and thermal transmittance which is rate of transfer of heat through one square meter divided by difference in temperature (Tasumi et al., 2003; Bartolucci et al., 1988). Simple atmospheric correction is applied in calculating albedo. Literature shows that there is no need of atmospheric correction for albedo and land surface temperature in SEBAL model. SEBAL has the ability to automatically calibrate in absence of atmospheric correction (Bastiaanssen et al. 1998). Tasumi et al. (2003) compared errors on ET estimation by using surface temperature and albedo derived from SEBAL with ET estimation from surface temperature and albedo derived from MODTRAN (Abreu and Anderson, 1998). The results showed that SEBAL ET is not sensitive to errors in surface temperature and albedo estimation.

Singh et al. (2008) conducted a study to assess the operational characteristics and performance of the SEBAL model for estimating crop ET and other energy balance components. They mapped spatial distribution and seasonal variation of crop ET on a large scale in south-central Nebraska climatic conditions. ET estimates from the SEBAL model were compared with measured fluxes from the Bowen ratio energy balance system (BREBS) on an instantaneous and daily basis. The BREBS measures surface energy fluxes (solar and net radiation, latent heat, sensible heat, and soil heat flux), air temperature, relative humidity, wind speed, wind, direction,

20

precipitation, and atmospheric pressure at a dedicated ET gauge station. Crop ET maps generated by SEBAL model for seven Landsat overpass days showed a very good progression of crop ET with time during the growing season in 2005 as documented surface conditions continuously changed. A good R^2 of 0.73 and a root-mean-square difference (RMSD) of 1.04 mm day^{-1} was found between the BREBS-measured and SEBAL-estimated ET.

SEBAL has been modified by Allen et al. (2002) using a ground base reference ET (ET_{ref}) to inversely and internally calibrate the surface energy balance. This modification eliminates the need for accurate surface temperature and air temperature data and also eliminates the need for complex estimation of the sensible heat component of the surface energy balance. The details of SEBAL algorithms with modifications are explained in the SEBAL expert training guide (Allen et al., 2002) and the SEBAL advance training and user manual (Waters et al., 2002) which are the same as the METRIC model used by Allen et al. (2005), Allen et al. (2007a), Allen et al. (2007b), Tasumi et al. (2005a), Tasumi et al. (2005b), Gowda et al. (2008a), Gowda et al., (2008b), Trezza et al. (2006), and Singh et al. (2008). It is concluded that since the method described in SEBAL expert training guide (Allen et al., 2002) and SEBAL advance training and user manual (Waters et al., 2002) is best fitted for the present study, the model used is described as the modified SEBAL explained later in chapter 3 and 4.

2.5 Identification of Irrigated agricultural lands

From the late 1980s, vegetation indices derived from remotely sensed data have been used to determine actual irrigated land (Lin et al., 2008). According to numerous authors, the normalized difference vegetation index (NDVI) derived from multi-spectral imagery is a sufficiently good indicator of irrigation as well as crop condition (Kolm and Case, 1984; Eckhardt et al., 1990; Abuzar et al., 2001; Martinez-Beltran and Calera-Belmonte, 2001). Single

date imagery acquired at the peak of the growing season may be sufficient to identify irrigation area, but multi-temporal data is needed to distinguish different irrigated crop types (Rundquist et al., 1989; Abuzar et al., 2001). Surface albedo (0.14 to 0.22 for corn, 0.17-0.22 for rice) (Allen et al., 2002) and NDVI > 0.7 (Tasumi and Allen, 2007) can be used to identify fully grown crops. Crop production can be expressed as a function of the relative evapotranspiration (ET_r) (Kassam and Doorenbos, 1983; Roerink et al., 1997) which is actual ET divided by potential ET. A value of $ET_r \geq 0.75$ is well acceptable for irrigated agriculture in the growing season, although this is not constant with time (Roerink et al., 1997). Since all parameters above are derived during SEBAL model processing, SEBAL is used with satellite imagery on irrigated area as a data processing tool.

2.6 Water demand factor

Quantifying water use and water demand for a region is essential to plan for the needs of the future population. Review of literature indicates that the two most common water demand projection methods are; population-based projections and land use-based projections (Duchon et al., 1991; Dziegielewski and Chowdhury, 2008; Baumberger et al., 2007). Population-based projection methods use projected population and per-capita water use estimates. The land use - based projection methods use projected land use area and per area water usage estimates.
In their study of regional water demand scenarios for Northeastern Illinois from 2005-2050, Dziegielewski and Chowdhury (2008) defined a water demand model based on a unit use coefficient which can be expressed as;

$$Q_{cit} = N_{cit} \times q_{cit} \qquad (5)$$

where; Q_{cit} is water withdrawal (or demand) in user sector c of study area i in year t; N_{cit} is the number of users (or demand drivers) such as population, employment, or area; and q_{cit} is the

average water requirement or water usage in gallons per capita-day or gallons per employee-day. This model assumes that future water demand will be proportional to the number of users N_{cit} while the future average rate of water use, q_{cit}, is assumed to either remain constant or change based on independent variables such as affluence, economic conditions, and social or other governmental drivers.

Duchon et al. (1991) presented a paper at the Georgia Water Resources Conference explaining that a land use-based water and wastewater demand forecast method is a more appropriate forecasting method than the commonly used population and unit water usage method. They described a land use-based approach to project water and wastewater demand in Gwinnett County, Georgia. Land use categories obtained from the Department of Planning and Development were correlated to customer categories used by the Department of Public Utilities to determine the most likely set of relationships between the two types of data. Information was used to estimate specific water and wastewater demand coefficients (mgd/acre) associated with one acre of each type of land use. After adjusting for expected changes in future development densities, calculated utility coefficients were applied to three future development scenarios (low, medium, and high density) to forecast the future utility demand of each.

Baumberger et al. (2007) conducted a study in 2005 on the effect of GIS-based demand allocation on water distribution system modeling. They used extended period simulations for the city of Olathe, Kansas, projecting water demand on three different metrics; population, land use, and customer billing. The spatial extents of different land use types, accurate historic water use patterns, and individual water use records were used to develop land use-based water demand projections. The city of Olathe's 2005 land use plan was used to identify nine land use types. The water demand for each land use was calculated by multiplying gross developable acres by

23

projected average water demand coefficients (gpm/acre) from Olathe's 2005 Water Master Plan Update Draft Report. The summary of billing reports for this period provided total monthly billed water use by meter size and customer category. Customer billing records were totaled for various user categories including institutional, industrial, commercial, and residential. Water consumption subtotals were adjusted to account for unmetered water use and water losses. Results were aggregated to determine total water demand projections for the city. Resulting projected water demands in million gallons per day (MGD) for the city in 2005 were 13.33, 13.24 and13.21 using population, land use and billing reports based projections, respectively. Actual water use during 2005 was 13.2 MGD. The Baumberger et al. (2007) study indicates that water demand can be allocated to a particular land use category for projecting future water demand.

A land use-based approach was also used by the Water Forum (2000) to estimate current demand and projection of 2030 water demand for Sacramento County, California. The water demand is based on 1) the number of acres in Sacramento County in various land use types; 2) the amount of water which is used per acre for a given land use type; and 3) adjustments for weather and for water conservation. The model can be expressed as below:

$$\text{Water Demand} = LU \times WDF \times WNF \times CF \qquad (6)$$

where; LU is the land use acreage in acres for each land use type, WDF is the water demand factor (acre-feet per day per acre) associated with each land use type, WNF is the weather normalization factor expressed as a percentage change in overall water demand, and CF is the conservation factor expressed in percentage reduction in overall water demand.

Irrigation water demand can be projected using a per irrigated acre unit-use approach (Dziegielewski and Chowdhury, 2008; WHPA, 2007). Water use per irrigated area is the water

use associated with unit area of irrigated land. USGS uses a term, water application rate (acre-ft per acre), which is volume of water applied to unit acre of agricultural land (USGS, 2000). Marella et al. (1998) used a land use-based water use coefficient (inches per acre) to project water demand from golf courses in Florida. Dziegielewski and Chowdhury (2008) used depth of water application per unit area and projected irrigated area estimates to project future irrigation water demand in Northeastern Illinois. Wittman Hydro Planning Associates, Inc. (WHPA, 2007) used a unit use coefficient method to project irrigation and agricultural water demand scenarios to 2050 for a 15-county area in East Central Illinois. Irrigated area, irrigation efficiency, rainfall, and evapotranspiration were considered as significant variables for irrigation water demand (Alcamo et al., 1997). The literature on land use-based water demand indicates that evapotranspiration or crop water use can be allocated to a particular land use to derive land use based coefficient for future water demand projection. Hence, identification of particular irrigated land use is important to derive reliable water demand factor. Literature also indicates that warmer or dryer seasons increase agricultural water demand (Obermeyer, 2003). ET estimated through the SEBAL model provides ET or actual water use which is dependent on the weather at the time of the image. Hence, ET estimated through the SEBAL should reliably reflect weather conditions indicating higher ET in irrigated agricultural crop land during dry growing seasons.

2.7 Summary of literature review

Researchers have used numerous field based ET estimation methods including traditional ET estimation using crop coefficients. As these methods only provide point estimates of ET, researchers became more interested in using remotely sensed data to map the spatial extent of ET over varied land uses. SEBAL is an example of the successful development of a remote sensing method for ET estimation. Various applications of SEBAL model have demonstrated that

SEBAL can estimate daily and seasonal ET accurately with minimum ground, meteorological and land use information. The key input data for SEBAL consists of spectral radiance in the visible, near-infrared, and thermal infrared part of the spectrum. This type of data is readily available from historic archived Landsat imagery. In addition to satellite imagery, the SEBAL model requires the following routine weather data parameters; wind speed, humidity, solar radiation, elevation, and air temperature.

High resolution digital ortho-referenced aerial photograph can be used to accurately locate agricultural areas, with ET from agricultural lands consequently extracted using GIS. The total bounded area of agricultural lands can be derived easily from GIS which can be applied to develop land use-based coefficients for plant water use, called in this thesis a water demand factor. Literature indicates that water demand factors can be applied to project future water demand based on historic trends of plant water use. Hence, SEBAL model can be useful to project future irrigation water demand from agricultural lands in Wolf Bay watershed using derived water demand factor with future land use. The estimate of land use-based coefficient for irrigated land thus provides a means to project irrigation water use. The methodology described in this thesis is of use for planners managing future water supplies in Wolf Bay and other watershed.

CHAPTER 3

VALIDATION OF A MODIFIED SURFACE ENERGY BALANCE ALGORITHM (SEBAL)
MODEL IN FLORIDA

Abstract

This chapter describes validation of a modified Surface Energy Balance Algorithm

(SEBAL) model using Landsat 5 Thermal Mapper (TM) images of Florida. A modified SEBAL

model is used to estimate net surface radiation, surface heat flux, and sensible heat flux from 16

Landsat 5 TM images from April-September, 2000 to 2006, are used for the study. The energy-

budget eddy covariance (EBEC) evapotranspiration (ET) estimates from four United States

Geological Survey (USGS) stations in Florida are used to validate daily and monthly ET

estimates from the model. The linear regression model of daily ET estimates from SEBAL model

versus measured daily ET explained 83% ($R^2 = 0.83$) of variation in measured daily ET at USGS

stations with a mean bias error (MBE) of 0.05 mm and root mean square error (RMSE) of 0.48

mm or (% RMSE of 10%). Monthly ET was estimated with a MBE of -2 mm and RMSE of 16

mm (% RMSE of 16%) and R^2 of 0.77. Two-month was estimated with a MBE of -5 mm, RMSE

of 30 mm or % RMSE of 16%, and R^2 of 0.73. The modified SEBAL model performed very well

in terms of Nash-Sutcliffe efficiency coefficient (ENS = 0.82, 0.77, and 0.71 for daily, monthly,

and two-month ET, respectively). It is concluded that the modified SEBAL can be used to

estimate ET in the humid subtropical climate of US.

3.1 Introduction

Evapotranspiration (ET) is the loss of water into the atmosphere through the combined processes of evaporation and transpiration. As it is one of the most significant components of the hydrologic budget, quantification of ET is critical in hydrological studies. Conventional methods of ET estimation include use of routine climate data to compute reference evapotranspiration for a reference crop (ET_{ref}), which is multiplied by an area-specific crop coefficient (K_c) to estimate ET for the crop (Allen, 1998). ET_{ref} is defined as ET from a standardized crop (Allen, 1998). Conventional methods provide only a point estimate of ET, and are subjected to errors due to variation in season, crop growth stage, planting period, and root-zone moisture condition (Ahmad et al., 2006). Knowledge about the spatial variation of ET over large areas is useful in hydrological applications (Stisen et al., 2008), crop yield forecasting (Rosema et al, 2001), drought monitoring (Anderson et al., 2007), product modeling (Nemani et al., 2002), climatic analysis (Wood and Lakshmi, 1993), and irrigation scheduling (Allen, 1998). Moderate resolution satellite remote sensing provides a relatively cost effective method of obtaining spatial as well as temporal variation of ET over a large area.

ET is estimated from remotely sensed data using a set of equations in a strict hierarchical sequence by converting spectral radiances measured from satellite or airborne instruments (Bastiaanssen et al., 2005). Surface Energy Balance Algorithm for Land (SEBAL) model was developed by Bastiaanssen (Bastiaanssen et al., 1998a; Bastiaanssen et al., 1998b, Bastiaanssen, 2000; Bastiaanssen et al., 2005) to map spatial variation of ET across a range of land uses. The model was modified by Allen et al. (Allen et al., 2002a; Allen et al., 2005a) to provide accurate estimates of ET from the agricultural crops. The modification by Allen et al. (2002a; Allen et al., 2005a) utilized ground base reference ET (ET_{ref}) to inversely and internally calibrate the surface energy balance (Allen et al., 2005a; Allen et al., 2007a, Allen et al., 2007b; Tasumi et al.,

2005a; Tasumi et al., 2005b). This modification eliminates the need for accurate surface temperature and air temperature measurement and the subsequent estimation of the sensible heat component of the surface energy balance. The details of SEBAL algorithms with modifications are explained by Allen et al. (2002a), Waters et al., (2002). The modified SEBAL model, called Mapping Evapotranspiration at high Resolution with Internalized Calibration (METRIC), is described and used by Allen et al. (2005a), Allen et al. (2007a), Allen et al. (2007b), Tasumi et al. (2005a), Tasumi et al. (2005b), Allen et al.,(2008), Gowda et al. (2008a), Gowda et al., (2008b), Trezza et al. (2006a), and Singh et al. (2008). The two main advantages of SEBAL and METRIC models over other image data processing methods are 1) they require minimum ground data and 2) they can be used to estimate both seasonal and annual ET.

The SEBAL method has been used successfully in various studies to estimate evapotranspiration rates in Spain, US, China, Niger, Sri Lanka, Kenya, Morocco, the Netherlands and Turkey (Pelgrum and Bastiaanssen, 1996; Schmugge et al. , 2003; Allen et al., 2000; Morse et al, 2000; Wang et al., 1995; Roerink, 1995; Hemakumara et al., 2003; Jacob et al., 2002; Lagouarde et al., 2002; Bastiaanssen and Bos, 1999; Farah, 2001; van den Kroonenberg, 2003; Kohsiek et al., 2002; Kite and Droogers, 2000). In the context of US, most of the studies related with SEBAL and METRIC model are done in the west where whether is dry (Allen et al., 2002a; Allen et al., 2005a; Allen et al., 2007a, Allen et al., 2007b; Tasumi et al., 2005a; Tasumi et al., 2005b; Kramer et al., 2008; Morse et al., 2000; Morse et al., 2004). The Idaho Department of Water Resources (IDWR) uses METRIC model, to map evapotranspiration in Snake River basin of Idaho to monitor irrigation water use from agricultural lands. The modified SEBAL model or METRIC model has been used to estimate monthly and seasonal ET for water rights accounting and operation of ground water models in New Mexico, Southern

California, and Southern Idaho (Allen et al., 2005b). SEBAL and METRIC model have not been applied to the same degree in the humid southeastern US. Soppe et al (2006) applied SEBAL model in imperial irrigation district in dry Southern California. Gowda et al. (2008) used METRIC model to map ET in the Texas high plains in semi-arid climate of Ogallala Aquifer region. Melesse et al. (2006) used SEBAL model to drive spatiotemporal dynamics of ET at the Glacial Ridge prairie restoration in Northwestern Minnesota which has humid continental climate. Singh et al. (2008) used SEBAL model to for Mapping ET and estimating surface energy fluxes in South-Central Nebraska which has semi-arid steppe climate. A test of applicability of the modified SEBAL model in the humid southeastern US can be useful in conducting irrigation and drainage related studies in the southeast.

Gowda et al. (2008a) used 2 Landsat 5 TM images (2005) to validate daily ET estimates using METRIC model and observed ET from soil water balance method from five irrigated crop lands in Texas high plains. Singh et al. (2008) used 7 cloudfree Landsat 5 TM images (2005) to validate daily ET from Bowen ratio energy balance system (BREBS)-measured ET in South-Central Nebraska. Tasumi et al. (2005) validated daily and monthly ET from METRIC model using lysimeter data from 1988 to 1991 with 11 Landsat 5 TM data in semi-arid western US. Validation of SEBAL or METRIC ET with measured ET data on a daily or seasonal basis over a variety of climatic condition can provide us a good knowledge about the accuracy of the model. This can be done by using Landsat images from different years representing variety of climatic condition. Teixeira et al. (2009), for example, used 10 Landsat images from 2001 to 2007 to validate daily ET estimate from SEBAL with ET measured at Flux towers in northeast Brazil.

The overall goal of this study is to apply modified SEBAL or METRIC model in water use related studies in the humid subtropical southeast. The objective of this paper is to use the

SEBAL model, developed by Bastiaanssen (Bastiaanssen, 1998; Bastiaanssen et al., 2005) and modified by Allen et al. (Allen et al., 2002a) to estimate daily and monthly ET from Landsat 5 TM imagery, and validate the results with field data. This study provides applicability of the modified SEBAL model in the humid southeastern US.

3.2 Materials and methods

3.2.1 Study area and datasets

The study area selected has Landsat 5 TM images that cover USGS stations in Florida. Measured ET data is available online from the Hydrologic Data Web Portal (HDWP) (USGS, 2007) at the USGS stations in Florida. Landsat 5 TM images from path/row: 15/41, 16/40, and 17/40 cover the four USGS sites used in this study. The spatial coverage of the combined study areas and the Landsat 5 TM images is 107,964 km^2. The limitations during Landsat 5 TM selections was availability of cloud free images and measured ET data from USGS stations. Only four out of seven USGS stations (Figure 3.1) were suitable for this study because of following limitations:

- Availability of cloud free Landsat 5 TM images during growing season,

- Agricultural fields to set "Cold" and "Hot" pixels close to the weather station and USGS stations, explained later.

- Land cover of the station (grass, marsh or station with agricultural setting) as the major goal of the study is to assess the applicability of the model in agricultural lands,
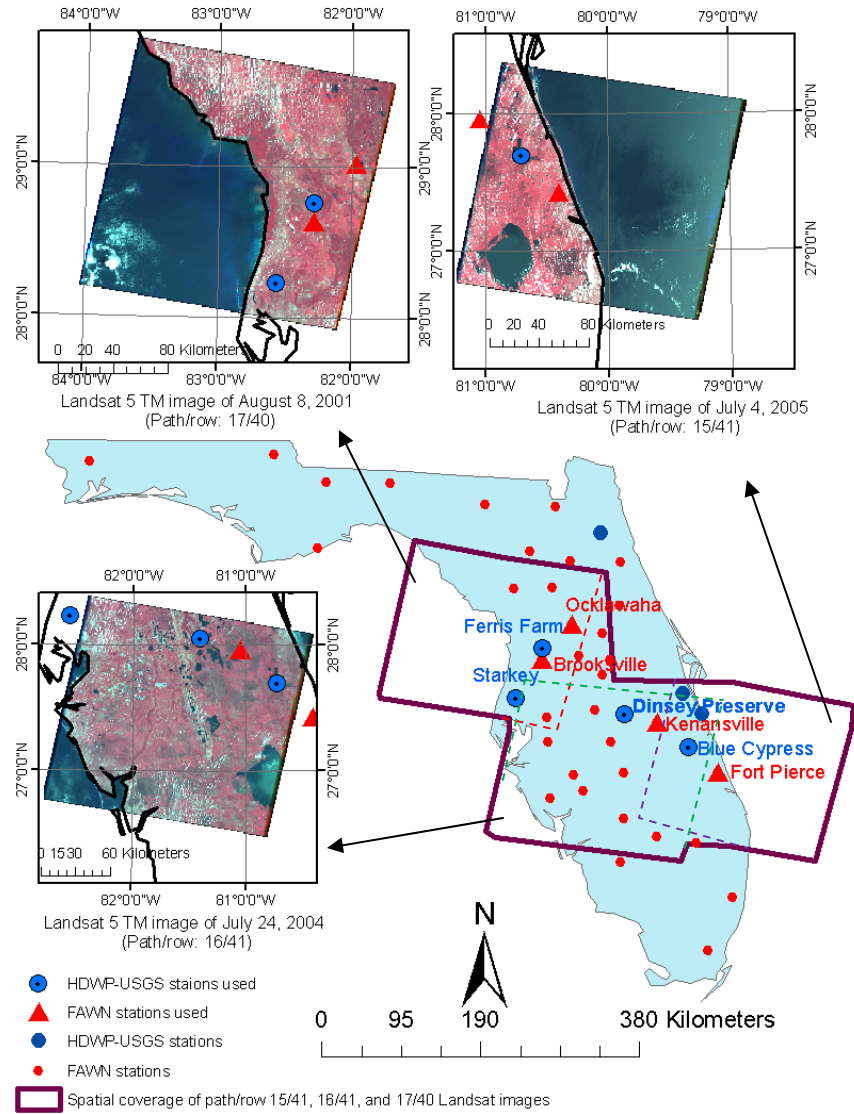
Figure 3.1. Landsat 5 TM Images and USGS and Florida Automated Weather Network (FAWN) weather stations in Florida (Source: USGS and FAWN).

The input data required for modified SEBAL ET processing includes; a digital satellite image with visible, near infra-red and thermal bands and basic weather parameters from a reference weather station including hourly or shorter period solar radiation, relative humidity, temperature, wind speed and precipitation. The weather parameters required for SEBAL processing is available from Florida Automated Weather Network (FAWN) stations (FAWN, 2010). The descriptions of USGS stations and FAWN stations are presented in Table 3.1 and Table 3.2, respectively.

32

Table 3.1. Description of USGS ET measurement site used during SEBAL validation method (Source: Douglas et. al., 2009).

Site	USGS Site ID	Site Full Name	Land Cover	Reference FAWN station	Longitude	Latitude	ET data available time period*	Landsat 5 TM coverage (Path/Row)
Blue Cypress, FL	274143080424100	ST.JOHNS RV MARSH AT BLUE CYPRESS NR FELLSMERE	Marsh	Kenansville, Fort Pierce	-80.7114	27.6953	January 2001-April 2005	15/41, 16/40
Disney Preserve, FL	280256081240100	DISNEY PRESERVE NR LAKE HATCHINEHA NR HAINES CITY	Grass	Kenansville	-81.4002	28.0488	July 2000-January 2006	16/40
Starkey, FL	295949081391400	STARKEY ADDITION PASTURE CLIMATE STA NR ODDESSA	Grass	Brookville	-81.6132	28.4161	April 2003-December 2004	17/40
Ferris Farms, FL	284541082163400	FERRIS FARMS NR FLORAL CITY	Grass	Brooksville, Ocklawaha	-82.776	28.7613	January 2003-February 2005	17/40

* USGS ET measurement data available online from USGS (USGS, 2007).

Table 3.2. Reference stations used during SEBAL validation (Source: FAWN, 2009).

Site	Site ID	Land Cover	Longitude	Latitude	Data available since	Landsat 5 TM coverage (Path/Row)
Kenansville	340	Grass	-81.050	27.963	March 2000	16/41
Fort Pierce	430	Grass	-80.402	27.427	April 1998	15/41
Brookville	310	Grass	-82.285	28.635	March 2000	17/40
Ocklawaha	280	Grass	-81.968	29.020	December 1998	17/40

3.2.2 Vegetation and Precipitation

Surface information with respect to vegetation and precipitation are critical component for determination of ET. According to Natural Resource Conservation Service (NRCS) data gateway crop land data layer by state major crops growing in the study area are citrus, sugarcane and peanuts (NRCS, 2010). Corn, rice, millet, water melon, soybeans and other crops are also grown in the area. The long-term precipitation data from Southwest Florida Management District and NOAA-NCDC were used for studying monthly ET variations in the study area. June to September receive more precipitation than April-May in the study area. Long-term average monthly precipitation in four counties, where the USGS stations are located, is shown in Figure 3.2. The figure shows 44-yr average monthly precipitation for Citrus, Pasco, and Polk County

(Southwest Florida Management District), and Indian River County (Vero Beach 4 SE station, maintained by NOAA-NCDC). All the counties have a similar pattern of precipitation except for July in Indian River County. Indian River County had received greater precipitation during winter than other counties.
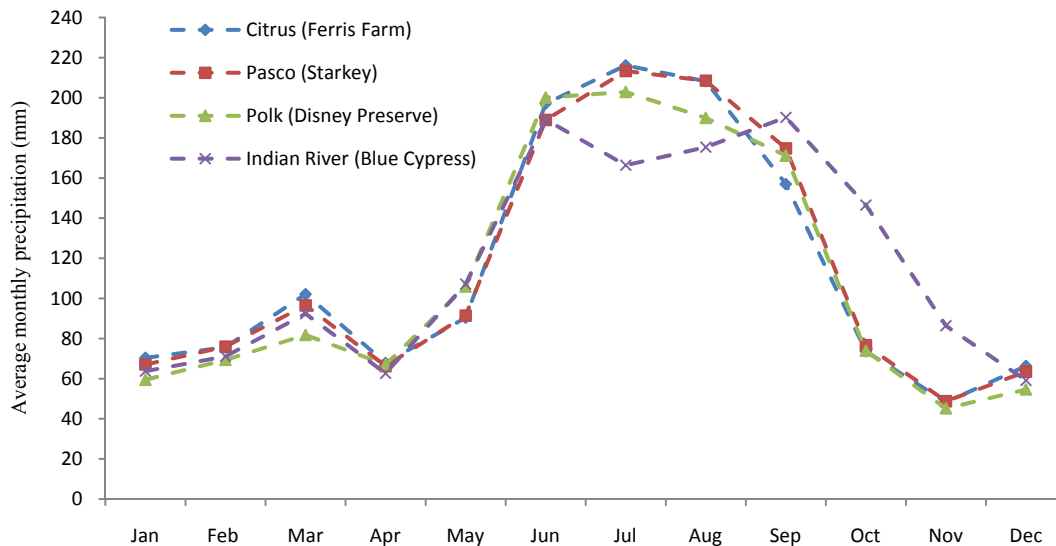
Figure 3.2. Average monthly precipitation for four counties in Florida (Source: Southwest Florida Management District and NOAA-NCDC).

3.2.3 Landsat 5 TM data

Landsat 5 TM has 7 spectral bands of which bands 1-5 and 7 provide data for the visible, near infra-red and mid infra-red bands; band 6 provides data for longwave (thermal) radiation. Bands 1-5 and 7 have a spatial resolution of 30 m and are used to derive vegetation indices, emissivity and albedo within SEBAL. TM band 6 has a spatial resolution of 120 m and provides input data for land surface temperature which is very useful for ET estimation.

Landsat 5 TM images are obtained online from USGS global visualization viewer (USGS, 2010). A total of sixteen Landsat 5 TM images including path/row 15/41, 17/40, and 16/41 are used for this (Table 3.3). A subset of each Landsat 5 TM image covering the corresponding USGS stations is used for processing.

Table 3.3. Landsat 5 TM images processed for ET validation (Source: USGS).

S.N.	Landsat 5 TM image acquisition date	Satellite overpass local time*	Path/row	Cloud cover %
1	5/19/2000	11:25	15/41	0
2	6/20/2000	11:25	15/41	10
3	4/2/2001	11:41	17/40	0
4	4/18/2001	11:41	17/40	0
5	6/21/2001	11:41	17/40	10
6	8/8/2001	11:41	17/40	0
7	8/24/2001	11:41	17/40	0
8	7/31/2003	11:26	15/41	0
9	9/15/2003	11:38	17/40	0
10	5/14/2004	11:29	15/41	10
11	6/29/2004	11:43	17/40	10
12	7/8/2004	11:37	16/41	0
13	7/24/2004	11:38	16/41	0
14	8/16/2004	11:44	17/40	10
15	9/1/2004	11:43	17/40	0
16	7/4/2005	11:37	15/41	0

* Eastern daylight time (GMT-4 hours).

3.2.4 Reference ET estimation

The SEBAL and METRIC models require some basic weather input such as solar radiation, temperature, relative humidity, wind speed, and precipitation. The four Florida Automated Weather Network (FAWN) stations used as reference stations in this study are shown in Figure 3.1. Fifteen-minute weather data are available at each of the stations. REF-ET software for windows (Allen et al., 2000a) is used to compute the ASCE Penman-Monteith standardized form of reference ET (ET_{ref}) for alfalfa (Allen et al., 2000b).

The output from REF-ET software was fifteen-minute ET_{ref} for the day. ET_{ref} for the satellite overpass local time is estimated using linear interpolation from the output. Similarly, wind speed at anemometer height (10 m for all FAWN stations) at the time of image capture is computed from available 15-minute data. ASCE Penman-Monteith standardized form of daily reference ET (ET_{ref_24}) was also computed using REF-ET software. Monthly reference ET and two-month reference ET were computed as a sum of daily ET_{ref} from the REF-ET software.

35

3.2.5 Modified SEBAL model

The modified SEBAL model used in this study is explained in Appendices A.1 and A.2. The surface energy balance equation is based on the theory that incoming net solar radiation drives all energy exchanges on the earth's surface including evapotranspiration, as shown below:

$$[R_n = G + H + \lambda ET] \tag{1}$$

where; R_n (Wm^{-2}) represents the net surface radiation which is the actual amount of energy available at the surface. G (Wm^{-2}) represents the soil heat flux which is the rate of heat storage in the soil and vegetation. H (Wm^{-2}) represents the sensible heat flux which is the rate of heat loss to the air due to temperature difference. λET (Wm^{-2}) is the latent heat flux associated with ET.

Surface energy balance algorithms from the modified SEBAL (Allen et al., 2002a; Waters et al., 2002) are used in this study. The algorithms are similar to the algorithms used in Mapping Evapotranspiration at high Resolution with Internalized Calibration (METRIC) model (Allen et al., 2005a; Allen et al., 2007a; Allen et al., 2007b; Tasumi et al., 2005a; Gowda et al.; 2008a; Gowda et al., 2008b; Trezza et al., 2006a). ERDAS Imagine 9.2 software (Leica Geosystems, 2008) is used to process Landsat 5 Thematic mapper (TM) images using SEBAL equations programmed in the Modeler Function of ERDAS.

A limitation of the modified SEBAL model is that a well irrigated pixel should be present serving as a "Cold" pixel from agricultural lands. Irrigation is done mainly during the crop growing season and ET estimation is most important during this season to calculate actual water use from the crops. Hence, Landsat 5 TM images from the growing season period are used exclusively for this study. One of the major constraints in the study was availability of cloud free images. However, only point estimates were important for this study for the validation purposes and all available Landsat 5 TM images in which USGS station locations were in cloud free area

of image are used for the analysis. The modified SEBAL model is used to derive spatial variation of monthly ET from subset images of 16 Landsat 5 TM images.

3.2.6 Validation of modified SEBAL method

Validation of estimates of instantaneous (at the time of image capture) surface balance parameters was not possible since instantaneous measured data was not available. Estimation of instantaneous surface balance energy parameters is not important for water managers unless daily estimates are derived from it and used for validation (Bastiaanssen, 2000). This study focuses on the validation of daily and monthly ET estimates from the model. Measured ET data at USGS stations are available online through the Hydrologic web data portal (HDWP). ET at USGS stations in this study are measured by the Energy-budget eddy covariance (EBEC) method (Sumner and Jacobs, 2005). Regression analysis is used to validate ET estimates from the model by plotting estimated ET versus observed ET values at USGS stations.

Root mean square error (RMSE) and % RMSE value are used as performance indicators of the model performance. RMSE and % RMSE provides information about actual deviation between the estimated and measured values. RMSE and % RMSE are calculated using equations below:

$$\text{RMSE} = \sqrt{\frac{1}{n}\sum_{i=1}^{n}\left(\text{ET}_{m,i} - \text{ET}_{o,i}\right)^2} \qquad (2)$$

$$\% \text{ RMSE} = \sqrt{\frac{1}{n}\sum_{i=1}^{n}\left\{\frac{\left(\text{ET}_{m,i} - \text{ET}_{o,i}\right)}{\text{ET}_{o,i}} \times 100\right\}^2} \qquad (3)$$

where; $\text{ET}_{m,i}$ and $\text{ET}_{o,i}$ are the modeled and observed ET values, respectively, for each day or month i; and n is the number of observations.

Nash-Sutcliffe efficiency (ENS) is used to determine how well the plot of observed versus simulated data fits the 1:1 line (Nash and Sutcliffe, 1970). NSE values ranges from $-\infty$ and

1, 1 being the optimal value. For ENS > 0.75, the model is considered very good, while ENS

values above 0.5 is considered to be satisfactory (Moriasi et al., 2007). ENS is computed as:

$$ENS = 1 - \frac{\sum_{i=1}^{n}(ET_{o,i} - ET_{m,i})^2}{\sum_{i=1}^{n}(ET_{o,i} - \overline{ET_o})^2} \qquad (4)$$

where; $ET_{m,i}$ and $ET_{o,i}$ are the modeled and observed ET values, respectively, for each day or

month i; and n is the number of observations; $\overline{ET_o}$ is the mean of observed ET values.

Mean bias error (MBE) value is used to determine if the model over estimated or

underestimated measured ET values. A positive MBE estimate provides the average amount of

overestimation in the estimated value, whereas a negative MBE provides the average amount of

underestimation in the estimated value. MBE is calculated as:

$$MBE = \frac{1}{n}\sum_{i=1}^{n}(ET_{m,i} - ET_{o,i}) \qquad (5)$$

US validation results of modified SEBAL model from other studies in US are compared

with the results from this study to assess the validity of the modified SEBAL model in the humid

southeastern US. Similar studies include modified SEBAL model application in Idaho (Allen et

al., 2003) and Southwestern California (Thoreson, 2009).

3.2.7 Data Analysis

AlaskaPak v2.2 tool for ArcGis 9.x (National Park Service, 2009) is used to select

random pixels in this study. Since this tool only works with polygon shapefiles, a polygon

covering the boundary of each raster image is created to select random pixels. Each randomly

selected pixel is viewed and assigned with a land use/land cover (LULC) value from the 2001

National Land Cover Dataset (NLCD) map (USGS, 2001) and the NRCS crop land data layer

(NRCS, 2004). Random selection of pixels was used for analyzing SEBAL derived albedo,

NDVI, LST and ET values for different LULC types on the August 8, 2001 image. The random

samples generated from AlaskaPak v2.2 tool did not generate enough sample pixels for water,

hence polygons of water body present in the image, Lake Weir (29.0169 N, -81.9790 W), Lake Panasoffkee (28.79 N, 82.13 W) and other small water bodies, were created and random samples were created from those polygon areas.

The goal of validation is to check the applicability of the modified SEBAL model to predict ET in agricultural lands of the humid southeast. Randomly selected pixels for agricultural lands are used for estimating average monthly ET from agricultural lands. Random pixels from agricultural lands are arranged with available precipitation data to see if there is a pattern in change in monthly ET from during high and low precipitation months.

3.3 Results and discussions

3.3.1 Normalized difference vegetation index, surface albedo and land surface temperature

Analysis of SEBAL derived Normalized difference vegetation index (NDVI), albedo and land surface temperature from a subset of the Landsat 5 TM August 8, 2001 image (Path/row: 17/40) showed decent results. The statistical analysis of albedo, NDVI, and land surface temperature (LST) values from random pixels of five LULC types are shown in Table 3.4. All the random pixels are taken from cloud free area. The surface albedo values are in agreement with other studies and literature (Allen et al., 2002a; Minor, 2009; Horiguchi, 1992; Betts and Ball, 1992; Tom and Castakzer, 2003). Negative NDVI with very low NDVI were found in sample pixels of water. Forest and water body absorb more incident solar radiation. i.e. less reflectance or lower albedo, than agricultural lands, urban areas and bare land and use it for evapotranspiration resulting into lower ET as shown in Figure 3.3. Forest and agricultural areas showed similar NDVI values with forest area having lower albedo values. Higher albedo and lower NDVI values were obtained for bare soil and urban areas, as expected.
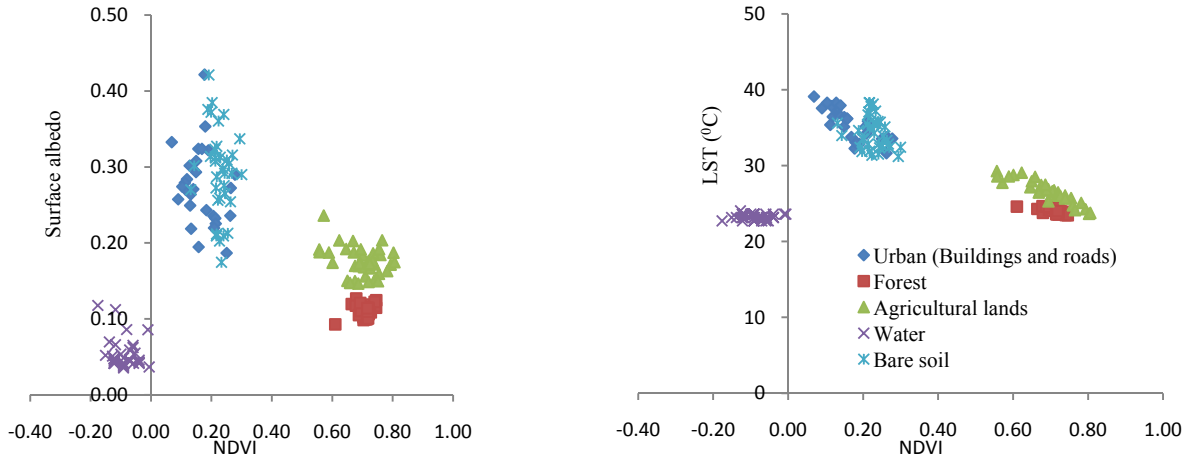
Figure 3.3. SEBAL derived surface albedo, NDVI and LST of sampled pixels from Landsat 5 TM image of August 8, 2001.

Table 3.4. Mean albedo, NDVI and LST (K) at the satellite overpass time for five LULC types derived from the Landsat 5 TM image of August 8, 2001. Mean with same letter in a column are not significantly different (Tukey-Kramer test, α =0.05).

Land use	No. of Pixels	albedo	NDVI	LST (^{o}C)
Bare soil	35	0.29A	0.22A	34.46A
Urban (Buildings and roads)	41	0.27A	0.14B	35.59A
Agricultural lands	41	0.18B	0.70C	26.69B
Forest	39	0.11C	0.71C	24.17C
Water	32	0.05D	-0.09D	23.25C

Estimated land surface temperature (LST) was the minimum and maximum for water and urban areas (Building and roads), respectively. The temperature of urban areas (building and roads) is usually higher because of no vegetation. Agriculture and forested land have lower temperature due to presence of higher biomass and associated ET. This result agrees with results from another study in the dry climate of Sudan (Ahmed et al., 2005).

3.3.2 Instantaneous surface energy balance parameters

All surface energy balance parameters are estimated on an instantaneous basis meaning at the time of image capture (Eastern Daylight Time). Instantaneous surface balance parameter estimates from SEBAL at USGS stations are shown in Figure 3.4.
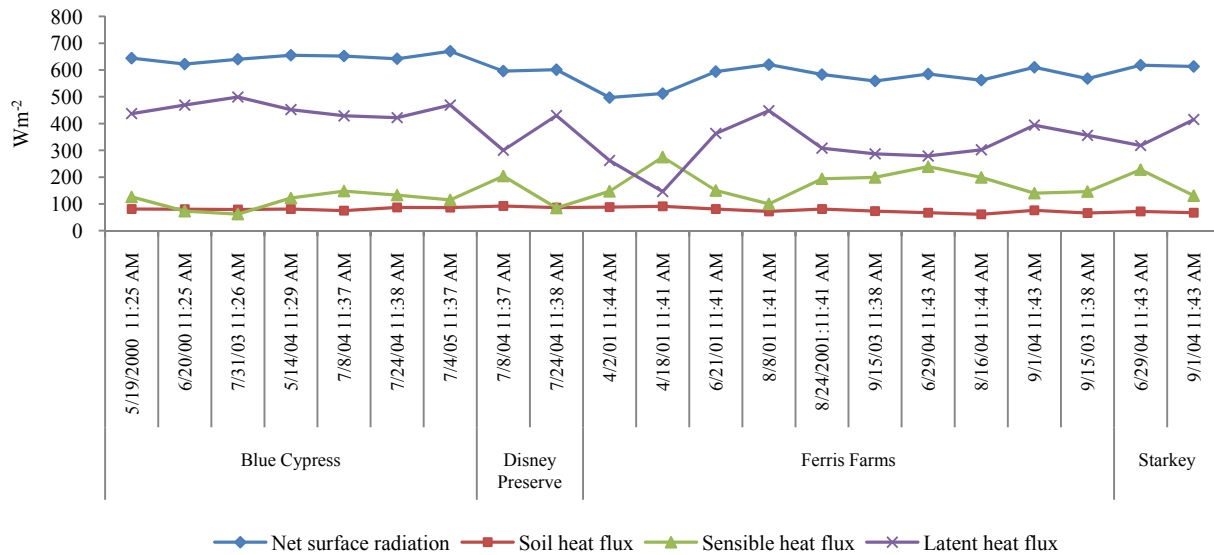
Figure 3.4. Instantaneous energy fluxes from SEBAL at four USGS stations.

Figure 3.4 indicates that during daytime most of the available net surface energy is used for latent heat flux transfer. All the images were taken at the similar time of day. Soil heat flux (G) at the USGS stations did not fluctuate much and is found to be the lowest of all energy fluxes, as expected. On average, estimated G was found to be $0.08R_n$ (Mean $G/Rn = 0.08$, standard deviation = 0.01, from $0.6R_n$ to $0.9R_n$). This finding supports generalization from previous research that G for short vegetation can be often approximated during the daylight period as $0.1R_n$ (Allen et al., 2002a, Allen et al., 1996; Clothier et al., 1986; Choudhary et al., 1987; Allen et al., 1994b; Debuin and Holtslag,1982). Latent heat flux (λET) fluctuated in a similar pattern as net surface radiation (R_n) and mirror image to the sensible heat flux at all four stations.

The analysis of April 2, 2001 and April 18, 2001 Landsat images showed that λET was lower and even lower than sensible heat flux at image capture time, indicating extremely dry conditions and a higher rate of convective heat transfer to the air. This was verified by precipitation data at the Brooksville FAWN station which is approximately 14 km south of Ferris

41

Farm station; indicating that the station received less than 1 mm of precipitation during the entire month of April, 2001 and no precipitation occurred in last five days from April 18, 2001.

A positive linear relationship between SEBAL derived R_n and λET was obtained (R^2=0.73) as shown in Figure 3.5 at USGS stations. This relationship held true with 1000 randomly selected pixels from the August 8, 2001 image ($R^2 = 0.77$) as shown in Figure 3.6 and confirms the fact that available net surface radiation energy drives the process of ET. Similar results have been found in other studies (de Silva et al.; 2007; Kaminsky and Dubayah; 1997; Silberstein et al., 2001; Alados et al., 2003).
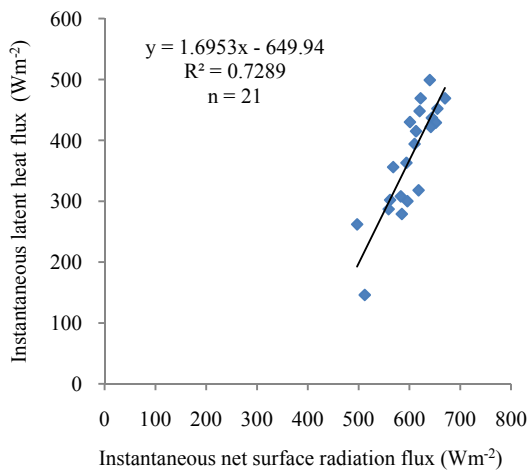
Figure 3.5. λET versus R_n at USGS stations on selected dates.
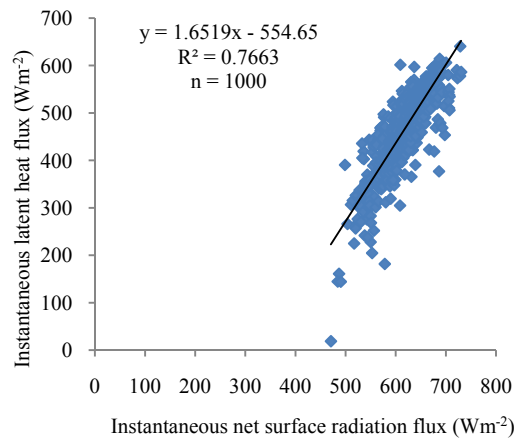
Figure 3.6. λET versus R_n at randomly selected pixels in August 8, 2001.

3.3.3 LST and daily ET

The plot of land surface temperature (LST) versus daily ET image indicated that higher ET is associated with lower surface temperature (Figure 3.7). The lower LST is due to the higher ET and availability of water. For, example, highest ET was obtained from open water body with lowest LST as shown in Figure 3.7. Strong negative correlation between LST and ET was also observed by Ahmed et al. (2005). Daily ET was found to be minimum and 0 in some cases for bare soil and urban areas. The area represented by the subset image received about 15 mm of rainfall in the last five days (FAWN, 2009) from August 8, 2001, which may have attributed to

42

the soil moisture content in bare lands and urban areas and evaporation may have occurred during the daytime.
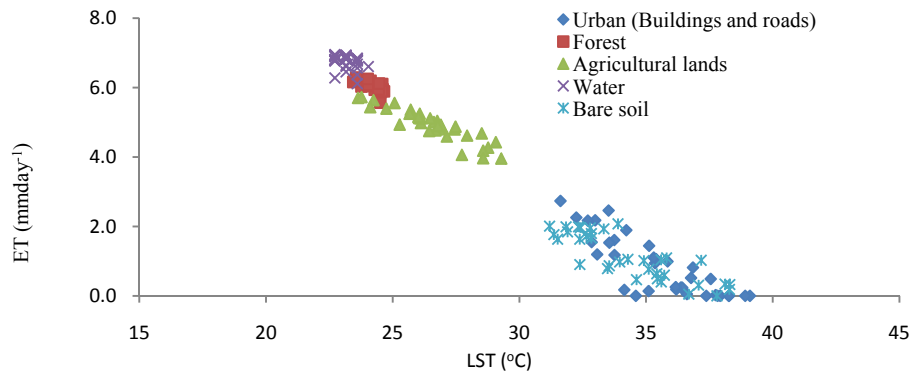
Figure 3.7. Daily ET and LST from sample pixels in August 8, 2001.

The daily ET map for August 8, 2001 image and NLCD land use/land cover map of 2001 is shown in Figure 3.8. The figures clearly indicates that daily ET is higher in wetlands and open water bodies. Forested area have higher ET than agricultural and pasture lands but lower than wetlands and open water body.
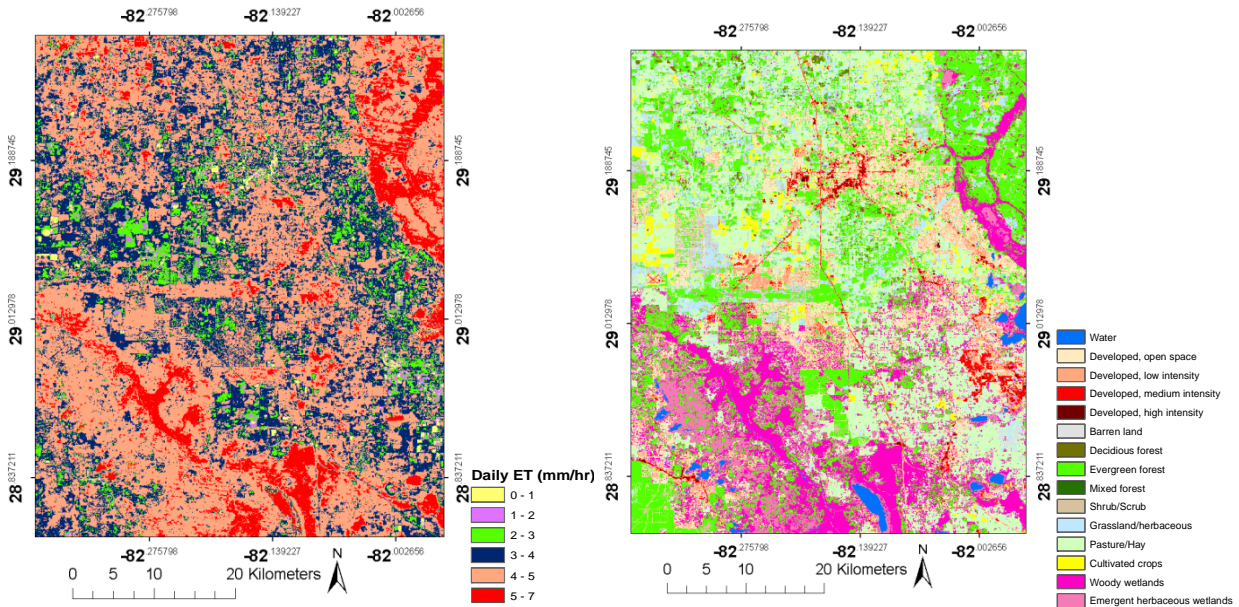
Figure 3.8. SEBAL derived daily ET map from August 8, 2001 Landsat 5 TM image in the left and land use/land cover map corresponding to the same coverage area in the right from NLCD 2001.

The statistical analysis of daily ET obtained from randomly selected sample pixels for these LULC classes are shown in Table 3.5. Daily reference ET for alfalfa grass was 5.47mm for

43

August 8, 2001 from the REF-ET software. Water was found to be lowest LST and highest daily

ET. Daily ET values from bare soil and urban area were not significantly different. Forested area

was found to have lower LST and higher daily ET values when compared to those from

agricultural land. This could be due to presence of higher green biomass which means higher rate

of transpiration and lower surface temperature but lower albedo.

Table 3.5. Mean LST at the satellite overpass time and daily ET, and monthly ET for five land
use types derived from Landsat 5 TM image of August 8, 2001. Mean with same letter in a
column are not significantly different (Tukey-Kramer test, α =0.05).

Land use	LST (^{o}C)	Daily ET (mm)
Bare soil	34.46A	1.12A
Urban	35.59A	1.02A
Agricultural lands	26.69B	4.98B
Forest	24.17C	6.04C
Water	23.25C	6.74D

3.3.4 Validation of daily and monthly ET estimates from the model

Daily and monthly SEBAL ET estimates from the pixels representing USGS stations are

located based on the latitude and longitude of the station. SEBAL performed well in terms of

estimating daily, monthly and two-month ET at USGS stations as shown in Figures 3.9, 3.10,

and 3.11, respectively. Error in daily SEBAL ET varied from -1.64 mm to 0.72 mm with mean

bias error (MBE) of 0.05 mm root mean square error (RMSE) of 0.48 mm/day (% RMSE =10%).

A strong linear relationship was found between estimated and measured daily ET with R^2 =0.83

and Nash-Sutcliffe Coefficient (ENS) of 0.82. Error in monthly ET varied from -39 mm to 28

mm with MBE of -2 mm and RMSE of 16 mm (% RMSE = 16%). Error in monthly ET varied

from -39 mm to 28 mm with MBE of -2 mm and RMSE of 16 mm (% RMSE = 16%). Two-

month ET (April-May, June-July, September-August) varied from -68 mm to 43 mm with a

MBE of -5 mm, RMSE of 30 mm (% RMSE = 16%). A good linear relationship was found

between estimated and measured monthly and two-month ET with (R^2 =0.77 and ENS of 0.77

for monthly ET, and $R^2 = 0.73$ and ENS of 0.71 for two-month ET. Based on R^2 and ENS the

model was considered good for estimating daily, monthly, and two-month ET.
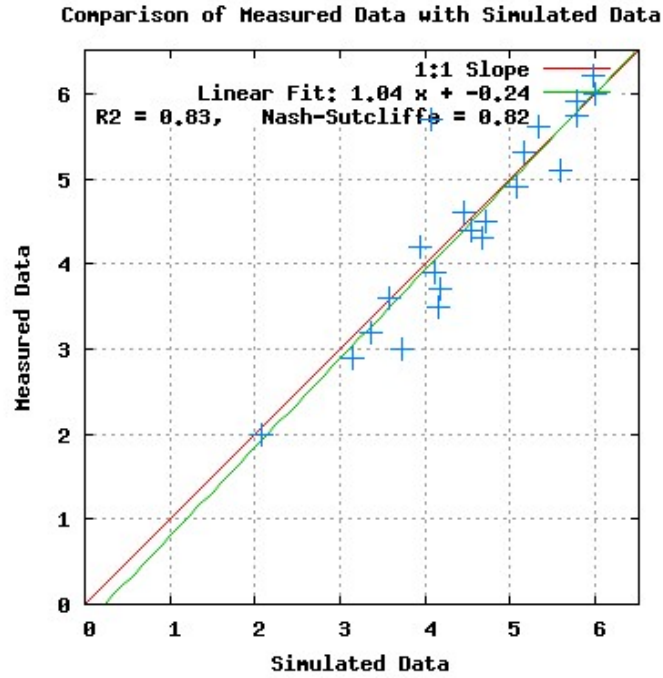
Figure 3.9. Estimated daily ET versus measured daily ET at USGS stations (Source: USGS).
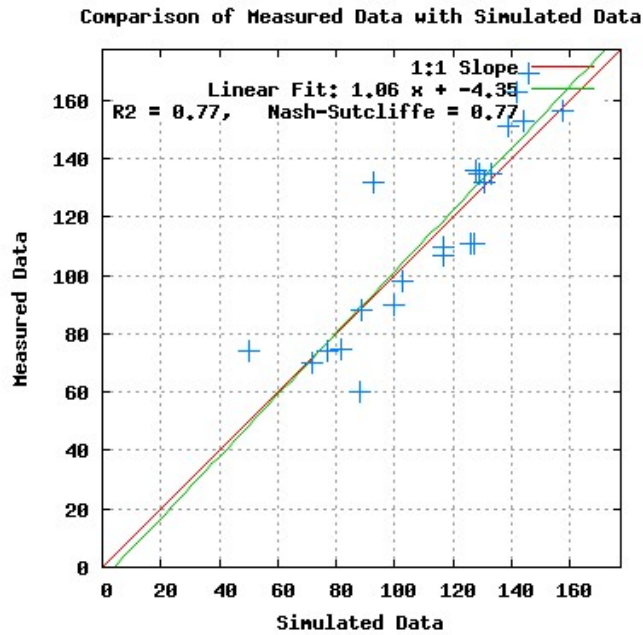
Figure 3.10. Estimated monthly ET versus measured ET at USGS stations (Source: USGS).
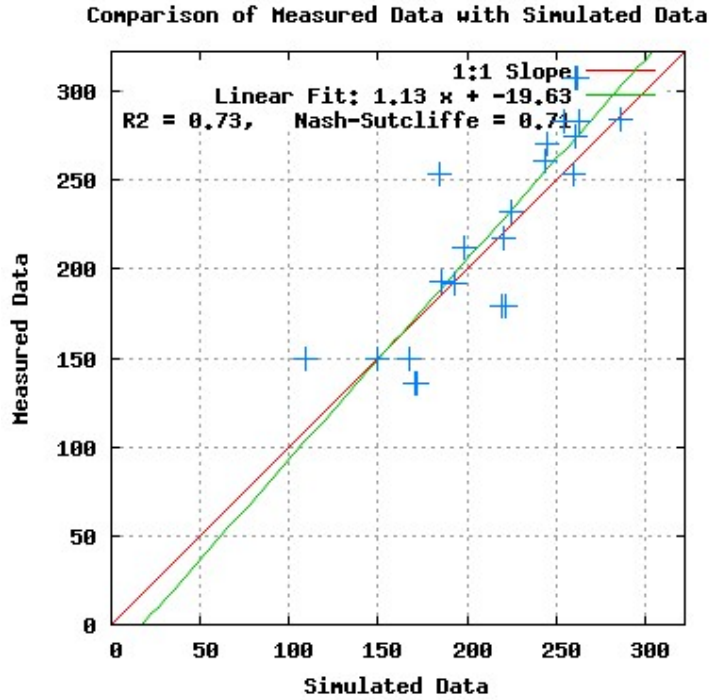
Figure 3.11. Estimated tw0-month ET versus measured ET at USGS stations (Source: USGS).

Both daily ET and monthly ET from the modified SEBAL model performed well in terms of explaining the variation in measured ET at USGS station. Figures 3.12, 3.13 and 3.14 show the temporal variation of estimated and measured daily, monthly and two-month ET, respectively. Estimated daily, monthly, and two-month ET followed similar pattern as measured ET at USGS stations over a different time periods from 2000 to 2005.
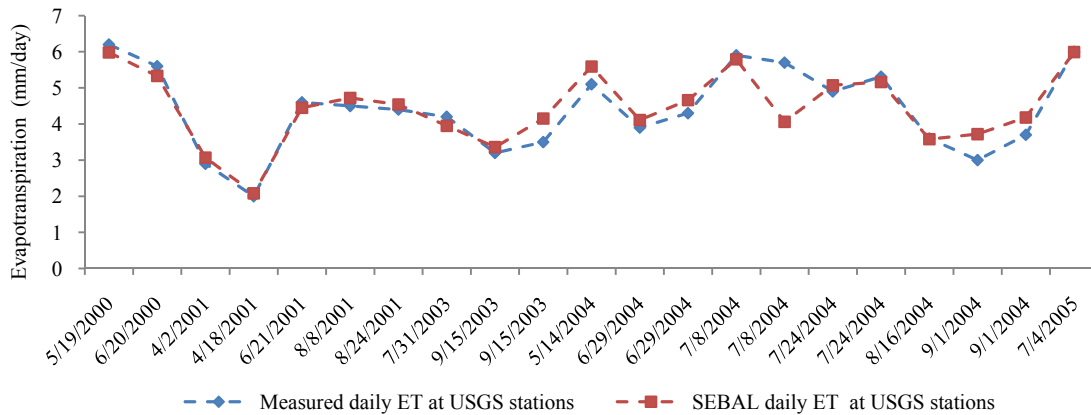
Figure 3.12. Temporal variation of estimated and measured daily ET at USGS stations (Source: USGS).

46
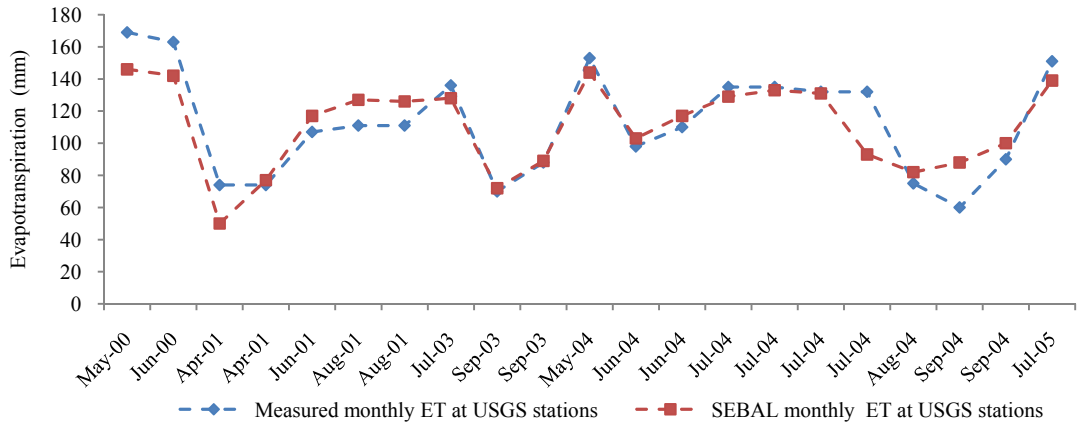
Figure 3.13. Temporal variation of estimated and measured monthly ET at USGS stations (Source: USGS).
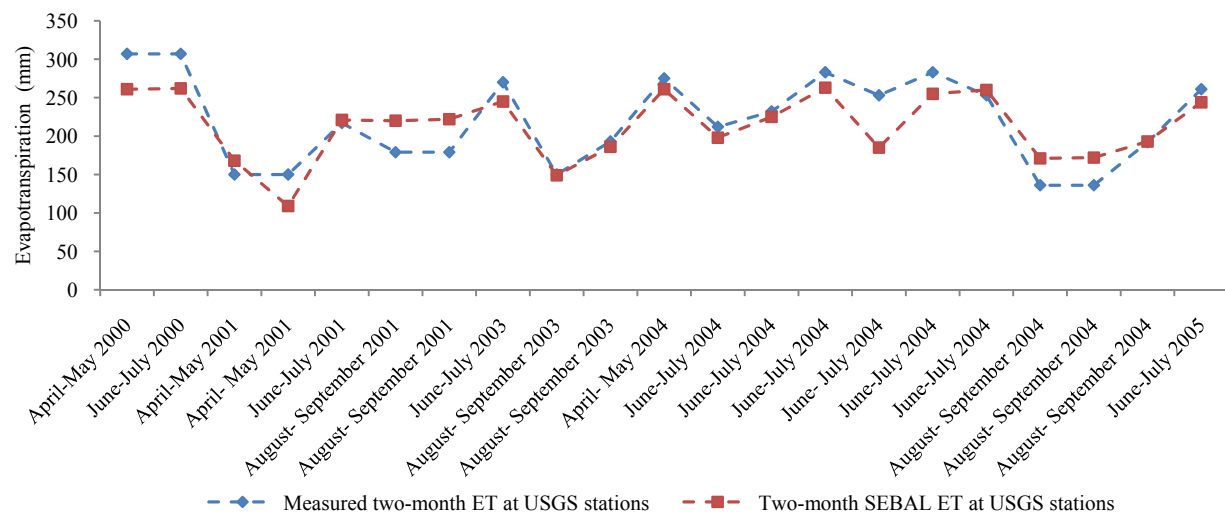
Figure 3.14. Temporal variation of estimated and measured two-month ET at USGS stations (Source: USGS).

US validation of modified SEBAL model showed RMSE of ± 16% when monthly SEBAL ET was compared with lysimeter measured data (Allen et al., 2003). Cumulative four month ET was estimated 4% higher than the measured ET. Thoreson et al. (2009) applied SEBAL model in imperial district in Southwestern California. Monthly SEBAL ET varied from -2.7 to 30.7% when compared to water balance ET. Cumulative 1-year ET (Oct-97 to Sep-98) was 0.6% more than Water Balance ET. These two studies show that the cumulative ET from SEBAL model is lower due to the reduction in the random errors components. The results are comparable with RMSE and % RMSE error in this study. Besides, MBE for daily monthly and

47

two-month ET was very low. Hence, the modified SEBAL model performed well in the humid southeastern US.

3.3.5 Monthly ET Analysis results

Figure 3.15 shows monthly ET from SEBAL from randomly sampled pixels of agricultural land. SEBAL monthly ET and measured monthly ET at USGS stations are arranged from the lowest to the highest precipitation months for each station. ET from agricultural land was more than ET from three stations where the vegetation was grass including Disney Preserve, Ferris Farm, and Starkey. SEBAL estimated average monthly ET from agricultural land was lower than ET from marshland at Blue Cypress station. During dry months, both measured ET and estimated ET were higher than precipitation indicating use of ground water or available soil moisture by plants. During wet conditions when enough water was available, plants use only a portion of available as indicated by monthly ET being less than precipitation (Figure 3.15). The gap between ET and precipitation is higher during periods when precipitation is low indicating higher water demand during dry months. This clearly indicates that agricultural crops were irrigated during the dry precipitation months.
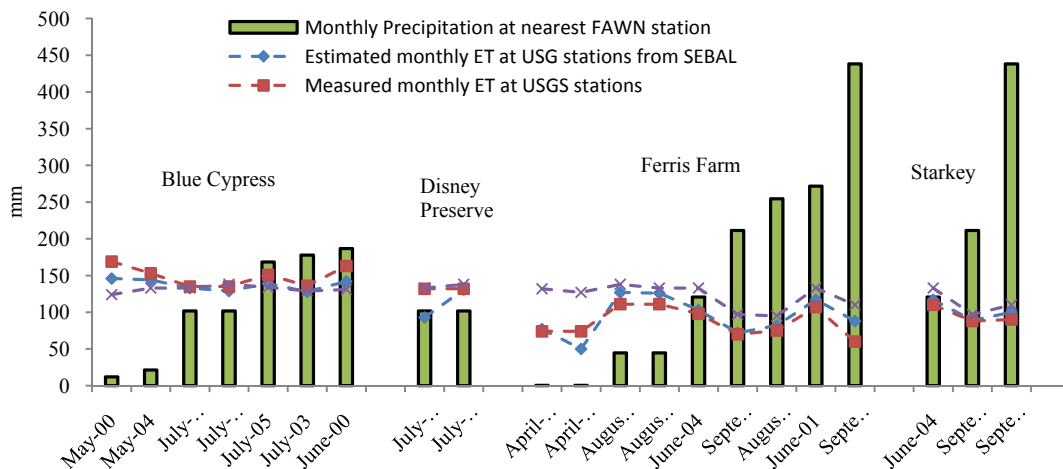
Figure 3.15. Monthly ET from USGS stations and agricultural lands with monthly precipitation (Source: USGS, FAWN).

July-04* = July 8, 2004 image, July-04** = July 24, 2004 image, Aprily-01* = April 2, 2001 image, April-01** = April 18, 2001 image, August-01* = August 8, 2001 image, August-01** = August 24, 2001 image.

Monthly ET maps for April 2001, August 2001, and July 2004 are shown in Figures 3.16, 3.17, and 3.18, respectively. Landsat TM image of April 2, 2001 and April 18, 2001 are independently used to derive spatial variation of monthly ET during April 2001. Figures 3.16, 3.17, and 3.18 indicate that monthly ET maps independently derived from two different images of the same month are similar. Similarly, for July 2004 and August 2001, two images are used to estimate monthly ET independently from two Landsat 5 TM images (July 8, 2004 and July 24, 2004 for July 2004 and August 8, 2001 and August 24, 2001 for August 2001). Location of USGS stations are also shown in Figure 3.16, 3.17 and 3.18.
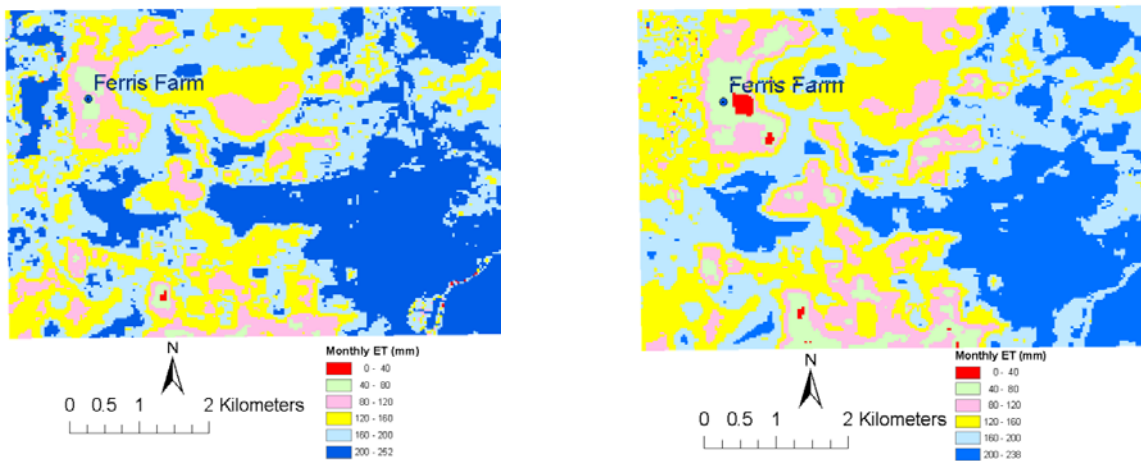
Figure 3.16. Monthly ET in April 2001 (left: derived from a subset image of Landsat 5 TM image of April 2, 2001, right: derived from a subset image of Landsat 5 TM image of April 18, 2001).
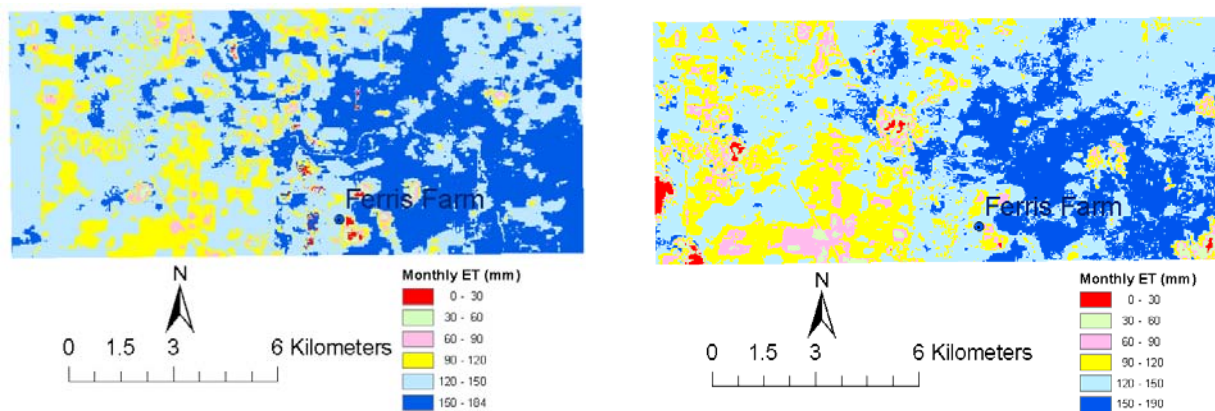
Figure 3.17. Monthly ET in August 2001 (left: derived from a subset image of Landsat 5 TM image of August 8, 2001, right: derived from a subset image of Landsat 5 TM image of August 24, 2001).

49
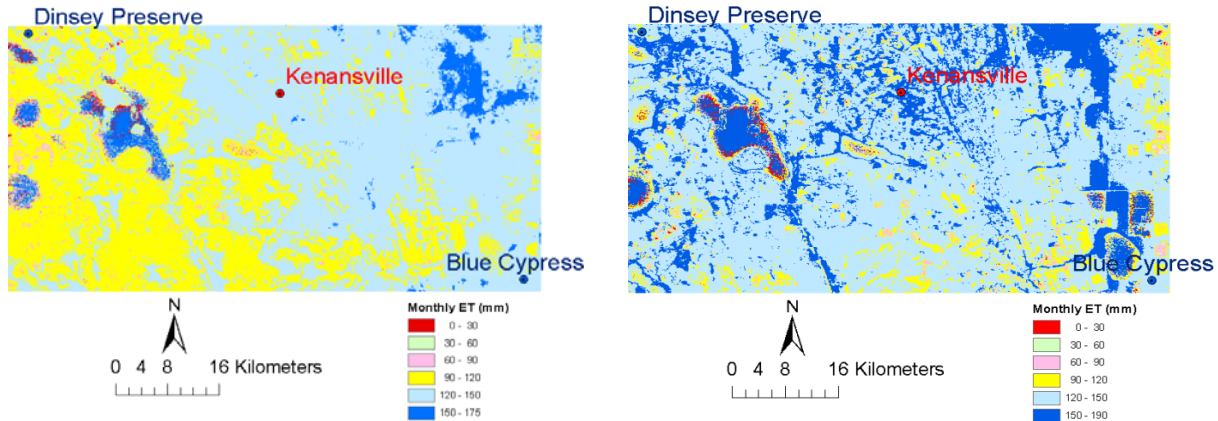
Figure 3.18. Monthly ET in July 2004 (left: derived from a subset image of Landsat 5 TM image of July 8, 2004, right: derived from a subset image of Landsat 5 TM image of July 24, 2004).

3.4 Summary and conclusions

A modified SEBAL model is used to estimate daily and monthly evapotranspiration (ET) from sixteen Landsat 5 TM images of Florida. A subset of Landsat 5 TM image of August 8, 2001 (path/row: 17/40) is used to derive surface albedo, normalized difference vegetation index (NDVI), land surface temperature (LST), daily and monthly ET from different land use/land cover (LULC) types for the day. Results from SEBAL analysis showed that daily ET was higher in water bodies followed by forests, agriculture lands, urban land, and bare soil in an August 8, 2001 image. Instantaneous surface energy parameters estimated from SEBAL model are in agreement with results from other studies. Daily ET and monthly ET are validated with measured ET data from energy-budget eddy covariance method at four USGS stations in Florida. The modified SEBAL model performed well in terms of predicting and explaining the temporal variation of daily ET and monthly ET at four USGS station. Daily ET are estimated at a RMSE of 0.48 mm/day, % RMSE of 10%, MBE of 0.05 mm/day and R^2 was 0.83 from the regression plot of SEBAL ET versus energy budget eddy covariance (EBEC) ET at USGS stations. Monthly ET are estimated at a RMSE of 16 mm and % RMSE of 16% ($r^2 = 0.77$) and a MBE of -2 mm. Two-month ET (April-May, June-July, September-August) are estimated at a RMSE of

50

30 mm or % RMSE of 16% ($R^2 = 0.73$) and a MBE of -5 mm. Nash-Sutcliffe efficiency coefficients (ENS) of the model for estimating ET was good for daily (ENS=0.82), monthly (ENS=0.77) and two-month (ENS=0.71) basis. The modified SEBAL model can be applied to estimate ET from agricultural lands in daily, monthly or seasonal basis if enough cloud free images are available. Three major limitations of the model are 1) availability of cloud free images, 2) presence of well irrigated agricultural land in the image 3) need of a reference weather station. In spite of limitations of the model, it provides a unique and accurate way to derive spatial distribution of ET in a single application. The results of this study suggested that the modified SEBAL model can be applied in the humid southeastern US to quantify actual ET from irrigated agriculture. Hence, modified SEBAL model can be useful in irrigation water use related studies in the humid southeastern US.

References

Ahmad, M. D., Biggs, T., Turral, H., and Scott, C.A., 2006, Application of SEBAL approach and MODIS time-series to map vegetation water use patterns in the data scarce Krishna river basin of India. Water Science & Technology, 53 (10), 83-90.

Ahmed, B.M., Hata, T., Tanakamaru, H., Abdelhadi, A.W., and Tada, A., 2005, Spatial analysis of land surface temperature and evapotranspiration for some land use/cover types in the Gezira area, Sudan, Nogyo Doboku Gakkai Kyushu Shibu Koenshu, 86, 264-265.

Alados, I., Foyo-Moreno, I., Olmo, F.J., and Alados-Arboledas, L., 2003, Relationship between net radiation and solar radiation for semi-arid shrub-land, Agricultural and Forest Meteorology, 116, 221–227.

Allen, R. G., Morse, A., Tasumi, M., Trezza, R., Bastiaanssen, W.G.M., Wright, J., and Kramber, W., 2002b, Evapotranspiration from a satellite-BASED surface energy balance for the Snake Plain Aquifer in Idaho, Proceedings of USCID Conference, USCID, Denver.

Allen, R. G., Pereira, L. S., Raes, D., and Smith, M., 1998, Crop evapotranspiration - guidelines for computing crop water requirements - FAO Irrigation & Drainage Paper 56, FAO, 1998, 301 Agriculture Organization of the U. N. (FAO), Rome, Italy.

Allen, R. G., Pruitt, W.O., Businger, J.A., Fritschen, L.J., Jensen, M.E., and Quinn, F.H., 1996, Chap. 4 Evaporation and transpiration, Wootton et al., eds., ASCE handbook of hydrology, ASCE, Reston, Va., 125–252.

Allen, R., Waters, R., and Bastiaanseen, W.G.M., 2002a, SEBAL Expert training, Idaho State University, August 19, 2002.

Allen, R.G, Tasumi, M, Morse, A., and Trezza, R., 2005a, A Landsat-based energy balance and evapotranspiration model in Western US water rights regulation and planning, Journal of Irrigation and Drainage Systems, 19 (3-4), 251-268.

Allen, R.G., 2000a, REF-ET: Reference Evapotranspiration Calculation Software for FAO and ASCE standardized Equations, University of Idaho, www.kimberly.uidaho.edu/ref-et/ (last accessed on April 30, 2009).

Allen, R.G., 2000b, Manual: REF-ET: Reference Evapotranspiration Calculation Software for FAO and ASCE standardized Equations. University of Idaho, http://www.kimberly.uidaho.edu/ref-et/manual.pdf (last accessed on April 30, 2009).

Allen, R.G., Smith, M., Pereira, L.S., and Perrier A., 1994, An update for the calculation of reference evapotranspiration. ICID Bulletin, 43, 35-91.

Allen, R.G., Tasumi, M. and Trezza, R., 2005b, Benefits from Tying Satellite-based Energy Balance to Reference Evapotranspiration, Earth Observation for Vegetation Monitoring and Water Management. (D'Urso, G., A. Jochum, and J.Moreno (eds.). The American Institute of Physics, 127-137.

Allen, R.G., Tasumi, M. and Trezza, R., 2007a, Satellite-based energy balance for mapping evapotranspiration with internalized calibration (METRIC) – Model, ASCE journal of Irrigation and Drainage Engineering, 133(4), 380-394.

Allen, R.G., Tasumi, M. Morse, A.T., Trezza, R., Kramber, W., Lorite I., and Robison, C.W., 2007b, Satellite-based energy balance for mapping evapotranspiration with internalized calibration (METRIC) – Applications. ASCE journal of Irrigation and Drainage Engineering, 133(4), 395-406.

Allen, R.G., Tasumi, M., Morse, A., and Trezza, R., 2005a, A landsat-based energy balance and evapotranspiration model in Western US water rights regulation and Basin estimated from remote sensing measurements, Hydrological Processes, 15(9), 1585–1607.

Allen, R.G., Morse, A., and Tasumi, M., 2003, Application of SEBAL for Western US Water Water Rights Regulation and Planning, ICID Workshop on Remote Sensing of ET for Large Regions, 17 September, 2003.

Anderson, M.C., Norman, J.M., Mecikalski,J.R., Otkin J.A., and Kustas, W.P, 2007, A climatological study of evapotranspiration and moisture stress across the continental United States based on thermal remote sensing: 2. Surface moisture climatology, Journal of Geophysical Research 112(D11112), 1–13.

Bastiaanssen, W. G. M., and Bos, M. G, 1999, Irrigation performance indicators based on remotely sensed data: a review of literature, Irrigation and Drainage Systems, 13(4), 291–311.

Bastiaanssen, W. G. M., Menenti, M., Feddes, R. A., and Holtslag, A. A. M., 1998a, A remote sensing surface energy balance algorithm for Land (SEBAL), Part 1: Formulation, Journal of Hydroogy, 212-213, 198–212.

Bastiaanssen, W. G. M., Noordman, E.J.M., Pelgrum, H., Davids, G., Thoreson, B.P., and Allen, R.G., 2005, SEBAL Model with Remotely Sensed Data to Improve Water-Resources Management under Actual Field Conditions, Journal of Irrigation and Drainage engineering, 131(1), 85-93.

Bastiaanssen, W. G. M., Pelgrum, H., Wang, J., Ma, Y., Moreno, J., Roerink, G. J., and Van der Wal, T., 1998b, The surface energy balance algorithm for land (SEBAL), Part 2: Validation." Journal of Hydroogy, 212-213, 213–229.

Bastiaanssen, W. G. M., Ud-din-Ahmed, M., and Chemin, Y., 2002, Satellite surveillance of water use across the Indus Basin, Water Resources Research, 38(12), 1273–1282.

Bastiaanssen, W.G.M, 2000, SEBAL-based sensible and latent heat fluxes in the irrigated Gediz Basin, Turkey. Journal of Hydrology, 229, 87-100.

Bastiaanssen, W.G.M., 1995, Regionalization of surface flux densities and moisture indicators in composite terrain. A remote sensing approach under clear skies in Mediterranean climates. 271, SC-DLO Report, Wageningen, The Netherlands.

Betts, A.K., and Ball, J.H., 1997, Albedo over the boreal forest, Journal of Geophysical Research,102 (D24), 28,901-28,909.

Chander G., and Markham, B., 2003, Revised Landsat-5 TM radiometric calibration procedures and postcalibration dynamic ranges, IEEE Transactions on Geoscience and Remote Sensing, 41, 2674-2677.

Chemin, Y., 2001, The application of the surface energy balance algorithm for land (SEBAL) for estimating daily evaporation - A handbook of published methodologies, Version 0.6.7, International Water Management Institute: Colombo, Sri Lanka.

Choudhury, Ri., Idso, S.B., and Reginato., J.R., 1987, Analysis of an empirical model for soil heat flux under a growing wheat crop for estimating evaporation by an infrared-temperature based energy balance equation, Agricultural and Forest Meteorology, 39, 283-297.

Clothier, B. E., Clawson, K. L., Pinter Jr, P. J., Moran, M. S., Reginato,R. J., and Jackson, R. D., 1986, Estimation of soil heat flux from net radiation during the Growth of alfalfa. Agricultural and Forest Meteorology, 37, 319-329.

Conard, C., Dech, S.W., Hafeez, M., Lamers, J., Martius, C., and Strunz, G., 2007, Mapping and assessing water use in a Central Asian irrigation system by utilizing MODIS remote sensing products, Irrigation and Drainage Systems, 21, 197-218.

da Silva, V.d.P.R., de Azevedo, P.V., and da Silva, B.B., 2007, Surface Energy Fluxes and Evapotranspiration of a Mango Orchard Grown in a Semiarid Environment, Agronomy Journal, 99, 1391-1396.

De Bruin, H.A.R., and Holtslag, A.A.M., 1982, A simple parameterization of the surface fluxes of sensible and latent heat during daytime compared with the Penman- Monteith concept, Journal of Applied meteorology, 21, 1610-1621.

Druce, P., Spano, D., Syner R.L., and Paw U, K.T., 1997, Surface renewal estimates of evapotranspiration. Short canopies. Acta Horticulturae, 449, 57-62.

Farah, H. O., 2001, Estimation of regional evaporation under all sky conditions with satellite and routine weather data, PhD thesis,Wageningen University, The Netherlands.

Florida Automated Weather Network, University of Florida Extension, 2010, http://fawn.ifas.ufl.edu/ (Last accessed on June 10, 2010).

Gowda, P.H., Howell, T.A., and Allen, R.G., 2008b, Deriving hourly surface fluxes and ET from landsat thematic mapper data using METRIC, Pecora 17 – The Future of Land Imaging…Going Operational November 18 – 20, 2008, Denver, Colorado.

Gowda, P.H., Howell, T.A., Chavez, J.L., Marek, T.H., and New, L.L., 2008a, Surface Energy Balance Based Evapotranspiration Mapping in the Texas High Plains. Sensors, 8, 5186-5201.

Hemakumara, H. M., Chandrapala, L., and Moene, A., 2003, Evapotranspiration fluxes over mixed vegetation areas measured from large aperture scintillometer, Agricultural Water Management, 58, 109–122.

Horiguchi, Ikuo (Ed.) 1992, Agricultural Meteorology, Buneidou, Tokyo, Japan

Jacob, F., Olioso, A., Gu, X. F., Su, Z., and Seguin, B., 2002, Mapping surface fluxes using airborne visible, near infrared, thermal infrared remote sensing data and a spatialized surface energy balance model, Agronomie, 22, 669–680.

Jensen, M.E., 1969, Chapter IV: Plant and Irrigation Water requirements. USDA-ARS-SWC, Snake River Conservation Research Center, Kimberly, Idaho.

Kaminsky, K.Z., and R. Dubayah. 1997. Estimation of surface net radiation in the boreal forest and northen prairie from shortwave flux measurements. Journal of Geophysical Research, 102, 29707–29716.

Kite, G. W., and Droogers, P, 2000, Comparing evapotranspiration estimates from satellites, hydrological models and field data, Journal of Hydroogy, 229(1-2), 3–18.

Kohsiek, W., Meijninger, W., and de Bruin, H. A. R., 2002, Long range scintillometry. Proceedings of International Symposium on Boundary Layer Physics.

Kramber, W.J., Morse, A., Allen, R.G., and Trezza, R., 2008, Landsat thermal data for water resources management in Idaho. ASPRS 2008 Annual Conference Portland, Oregon. April 28 - May 2, 2008.

Lagouarde, J. P., Jacob, F., Gu, X. F., Olioso, A., Bonnefond, J. M., Kerr, Y. H., McAneney, K. J., and Irvine, M., 2002, Spatialization of sensible heat flux over a heterogeneous landscape." Agronomie, 22, 627–633.

Leica Geosystems, 2008, http://gi.leica-geosystems.com/documents/pdf/SML.pdf (last accessed on June 10, 2010).

Markham, B. L., and Baker, J. L., 1986, Landsat MSS and TM Post-Calibration Dynamic Ranges, Atmospheric Reflectance and At-Satellite Temperatures, pp.3-7. Laboratory for Terrestrial Physics-NASA/Goddard Space Flight Center, Greenbelt, MD. 20771.

Melesse, A. M., Oberg, J., Nangia, V., Berri, O., and Baumgartner, D., 2006, Spatiotemporal dynamics of evapotranspiration at the Glacial Ridge prairie restoration in northwestern Minnesota, Hydrologial Processes, 20, 1451-1464.

Mengistu, M.G., and Savage, M.J., 2010, Surface renewal method for estimating sensible heat flux, Water SA, 36 (1), 9-18.

Moriasi, D.N., Arnold, J.G., Van Liew, M.W., Bingner, R.L, Harmel, R.D. and Veith, T.L., 2007, Model evaluation guidelines for systematic quantification of accuracy in watershed simulations. Transactions of the ASABE 50(3), 885-900.

Morse, A., Tasumi, M., Allen, R. G., and Kramber, W. J., 2000, Application of the SEBAL methodology for estimating consumptive use of water and streamflow depletion in the Bear River basin of Idaho through remote sensing, Final Rep., Phase I, Submitted to Raytheon Systems, Earth Observation System Data and Information System Project, by Idaho Dept. of Water Resources and Univ. of Idaho planning. Irrigation and Drainage Systems 19, 251–268.

Morse, A., Kramber W.J., Allen, R.G., and Tasumi, M., 2004, Use of the METRIC Evapotranspiration Model to Compute Water Use by Irrigated Agriculture in Idaho. Proceedings of the 2004, IGARSS Symposium, Anchorage, AK.

Nash, J. E. and Sutcliffe, J. V. 1970, River flow forecasting through conceptual models, Part 1 - A discussion of principles. Journal of Hydrology 10(3): 282-290.

National Aeronautics and Space Administration (NASA), 2000, http://earthobservatory.nasa.gov/GlobalMaps/view.php?d1=MOD11C1_M_LSTDA (last accessed on July 12, 2010).

National Climatic Data Center (NCDC), NOAA-NCDC, http://www4.ncdc.noaa.gov/cgi-win/wwcgi.dll?wwDI~StnSrch~StnID~20004380 (last accessed on June 15, 2010).

National Park Service, 2009, AlaskaPak v2.2 for ArcGIS 9.x, http://science.nature.nps.gov/nrgis/applications/gisapps/gis_tools/8x/alaskapak.aspx (last accessed on June 25, 2010).

Natural Resource Conservation Service, USDA, 2004,

http://datagateway.nrcs.usda.gov/GDGOrder.aspx (last accessed on July 9, 2010).

Nemani, R.R., White, M.A., Thornton, P., Nishida, K., Reddy, S., Jenkins, J. and Running, S.W., 2002, Recent trends in hydrologic changes have enhanced the carbon sink in the United States,Geophysical Research Letter 29 (10) (2002), 1468.

Natural Resource Conservation Service, USDA, 2004,

http://datagateway.nrcs.usda.gov/GDGOrder.aspx (last accessed on July 9, 2010).

Paulson, C.A, 1970, The mathematical representation of wind speed and temperature profiles in unstable atmospheric surface layer, Applied meteorology, 96, 587-861.

Pelgrum, H., and Bastiaanssen, W. G. M., 1996, An intercomparison of techniques to determine the area-averaged latent heat flux from individual in situ observations: A remote sensing approach using EFEDA data, Water Resources Research, 32(9), 2775–2786.

Roerink, G. J., 1995, SEBAL estimates of the areal patterns of sensible and latent heat fluxes over the HAPEX-Sahel grid, a case study on 18 September 1992, DLO-Staring Centre Interne Mededeling 364, Alterra, Wageningen.

Rosema, A., Verhees, L., Putten, E., Gielen, H., Lack, T., Wood, J., Lane, A., Fannon, J., Estrela, T., Dimas, M., Bruin, H., Moene, A., and Meijninger, W., 2001, European energy and water balance monitoring system final report April 2001. The European Community Fourth Framework Programme for Research, Technological Development and Demonstration in The Field of Environment and Climate, Theme 3, Space Techniques Applied to Environmental Monitoring and Research Area 3.1.2: Pilot Projects, ENV4-CT97-0478, Scientific Report.

Schmugge, T. J., Jacob, F., French, A., and Kustas, W. P., 2003, Surface flux estimates with ASTER thermal infrared data, ASTER Workshop.

Soppe, R. W.; Bastiaanssen, W.; Keller, A.; Clark, B.; Thoreson, B.; Eckhardt, J.; Davids, G., 2006, Use of High Resolution Thermal Landsat Data to Estimate Evapotranspiration Within the Imperial Irrigation District in Southern California, American Geophysical Union, Fall Meeting 2006.

Seguin, B., Courault, D., and Gu´erif, M., 1994, Surface temperature and evapotranspiration: application of local scale methods to regional scales using satellite data. Remote Sensing of Environment, 49, 287–295.

Silberstein, R., Held, A., Hatton, T., Viney, N., and Sivapalan, M., 2001, Energy balance of a natural jarrah (Eucalyptus marginata) forest in Western Australia: Measurements during the spring and summer, Agricultural and Forest Meteorology, 109, 79–104.

Singh, R. K., Irmak, A., Irmak, S., and Martin, D.L., 2008, Application of SEBAL Model for Mapping Evapotranspiration and Estimating Surface Energy Fluxes in South-Central Nebraska, Journal of Irrigation and Drain Engineering, 134, 273.

Snyder R.L., Spano, D., and Paw U, K.T., 1996, Surface renewal analysis for sensible heat and latent heat flux density. Boundary- Layer Meteoroogy, 77, 249-266.

Southwest Florida Management District, http://www.swfwmd.state.fl.us/data/ (last accessed on June 24, 2010).

Stisen, S., Jensen, K.H., Sandholt, I., and Grimes, D.I.F., 2008, A remote sensing driven distributed hydrological model of the Senegal River basin, Journal of Hydrology, 354, 131–148.

Sumner, D.M., and Jacobs, J.M., 2005, Utility of Penman–Monteith, Priestley–Taylor, reference evapotranspiration, and pan evaporation methods to estimate pasture evapotranspiration. Journal of Hydrology, 308, 81–104.

Tasumi, M., Allen, R. G., Trezza, R., and Wright, J. L., 2005a, Satellite-based energy balance to assess within population variance of crop coefficient curves, ASCE journal of Irrigation and Drainage Engineering, 131(1), 94-109.

Tasumi, M., Trezza, R., Allen, R.G. and Wright, J. L., 2005b, Operational aspects of satellite-based energy balance models for irrigated crops in the semi-arid U.S. Journal of Irrigation and Drainage Systems, 19, 355-376.

Teixeira, A.H. de C., Bastiaanssen, W.G.M., Bassoi, L.H., 2007, Crop water parameters of irrigated wine and table grapes to support water productivity analysis in Sao Francisco River basin, Brazil. Agricultural Water Management, 94, 31–42.

Thoreson, B., Clark, B., Soppe, R., Keller, A., Bastiaanssen, W., and Eckhardt, J., 2009, Comparison of Evapotranspiration Estimates from Remote Sensing (SEBAL), Water Balance, and Crop Coefficient Approaches, World Environmental and Water Resources Congress 2009: Great Rivers, 4347- 4361.

Tom Markvart, T., and CastaŁżer, L. (eds.), 2003, Practical Handbook of Photovoltaics: Fundamentals and Applications, Oxford, UK, Elsevier, 999.

58

Trezza, R., 2006a, Estimation of Evapotranspiration from Satellite-Based Surface Energy
Balance Models For Water Management in the Rio Guarico Irrigation System,
Venezuela, AIP Conference. Proceedings, 852, 162-169.

Trezza, R., 2006b, Evapotranspiration from a Remote Sensing Model for Water Management in
an irrigation system in Venezuela, Interciencia, 31(6), 417-423.

USGS, 2001, http://gisdata.usgs.gov/website/mrlc/viewer.htm (last accessed on March 10, 2010).

USGS- Hydrologic Data Web Portal (HDWP), 2007, http://dataport.er.usgs.gov/et.html (last
accessed on June 10, 2010).

Van den Kroonenberg, A., 2003, Surface flux estimates over an olive yard: SEBAL method
applied to NOAA-KLM and Landsat-7, MS thesis, Wageningen University,
Department of Meteorology.

Wang, J., Ma, Y., Menenti, M., Bastiaanssen, W. G. M., and Mitsuta, Y., 1995, The scaling up of
land surface processes over a heterogeneous landscape with satellite observations,
Journal of the Meteorological Society of Japan, 73(6), 1235–1244.

Waters, R., Allen, R., Tasumi, M., Trezza, R., and Bastiaanssen, W.G.M., 2002, SEBAL Surface
Energy Balance Algorithms for Land, Idaho implementation, Advance Training and
Users Manual, Department of Water Resources: Boise, ID, USA, 2002.

Webb, E.K., 1970, Profile relationships: the log-linear range, and extension to strong stability.
Quarterly Journal of the Royal Meteorological Society, 96, 67-90.

Wieringa, J., Davenport, A.G., Grimmond, C.S.B., and Oke, T.R., 2001, New Revision of
Davenport Roughness Classification. Proceedings of the 3rd European & African
Conference on Wind Engineering, Eindoven, Netherlands, July 2001, 8.

Wood, E. F., and Lakshmi, E., 1993, Scaling water and energy fluxes in climate systems: Three
land-atmospheric modeling experiments, Journal of Climate, 6, 839−857.

CHAPTER 4

A SURFACE ENERGY BALANCE METHOD TO ESTIMATE PLANT WATER USE IN
WOLF BAY WATERSHED AREA

Abstract

This chapter describes the use of remote sensing in estimating evapotranspiration (ET)

and plant water use at a watershed scale. The Surface Energy Balance Algorithm (SEBAL)

model has been widely used in western US but with limited research in the southeast and not a

single work published in Alabama. A study using a modified SEBAL model is conducted in an

approximately 126 km^2 watershed in Baldwin County, AL to estimate total plant water use

through volumetric ET estimation from Landsat 5 Thematic Mapper (TM) imagery. The

potential to project future water demand in the watershed with these data is discussed. SEBAL

model is validated with energy-budget eddy covariance data by comparing ET estimates from

USGS stations in Florida. The validated methodology is applied in Wolf Bay watershed area in

Alabama, focusing on recent four years from 2005 to 2008, which included one wet year, 2005;

two dry years, 2006 and 2007; and one normal year in 2008. Daily, monthly, seasonal ET maps

and total ET estimates are derived from the SEBAL model using historic Landsat 5 TM images.

Irrigated areas are identified using 1m resolution aerial images, surface albedo, NDVI, and

evaporative fraction. Results confirmed that plant water use was higher during dry years than in

wet years. Estimated plant water use in 2005, 2006, 2007, and 2008 were 5.91, 6.26, 6.87, and

6.59 in million cubic meters, respectively. Water demand factors are derived for major irrigated

plants in Wolf Bay watershed area based on recent plant water use. Results confirm that plants have higher water demand in dry years than in wet years. Projected landuse and land cover (LULC) projection map of Wolf Bay watershed area for years 2010, 2020, 2030, and 2040 are utilized to project irrigation water demand for dry, normal and wet precipitation conditions based on a scenario that most of the crop lands in Wolf bay watershed area are converted into golf courses and turf farms, and that by 2040, 100% of agricultural land is irrigated. Results indicate that irrigation water demand is expected to increase from 2010 to 2040 from 6.19 to 9.82 million cubic meters, 6.76 to 11.12 million cubic meters, 6.45 to 10.52 million cubic meters under wet, dry, and normal precipitation conditions, respectively. Remote sensing methods can be useful in estimating ET for plant water use in Alabama and also for deriving water demand factors for the projection of future water demand without the need for detailed ground survey data. A case study is presented showing how the method is used to plan for future water needs at the watershed scale.

4.1 Introduction

Irrigation is one of the major water use categories in the US and the world. Seventy percentage of total fresh water use in the US is accounted by irrigation (Weibe and Gollehon, 2006). Worldwide, 70% of total water use in the world is for agriculture (World Bank, 1992). Plant water use in this study is defined and quantified as the actual water used by turf farms, nurseries, crop, golf courses, and other irrigated plants. Traditional methods of irrigation water use estimation such as collection of water pumping records and conduction of field surveys involve significant amount of cost. Literature indicates that estimates of evapotranspiration (ET) provide a good measure of the amount of water utilized by plants (Jensen, 1969). Conventional methods of ET estimation include use of routine climate data to compute ET from a reference

crop (Reference ET, ET_{ref}, defined as evapotranspiration from a standardized crop under standard conditions) and an area-specific crop coefficient (K_c), provide only a point estimate of ET, and are subjected to many errors (Allen et. al., 1998; Ahmad et al., 2006). Mapping of ET using satellite imagery provides an estimate of ET or water used by irrigated crops, at relatively low cost and over large coverage area.

Estimation of evapotranspiration using remotely sensed data has attracted many researchers in last two decades. One of the main advantages of use of satellite imagery in estimating ET is the possibility for extending point measurement data or empirical relationships to much larger areas (Seguin et al., 1994; Kustas and Norman, 1996; Carlson and Buffum, 1989; Allen et al., 2005a; Garatuza-Payan and Watts, 2005, Zhang et al, 2009). Most of the studies using remote sensing methods to map ET estimation or plant water use are done at the regional or global scale. The availability of high resolution Landsat images that include thermal bands provides an opportunity to also study land surface at a local scale. Landsat has a pixel size small enough to locate individual agricultural fields (Kramber et al., 2000).

Surface Energy Balance Algorithm for Land (SEBAL) model developed by Bastiaanssen (Bastiaanssen et al., 1998a; Bastiaanssen et al., 1998b; Bastiaanssen et al., 2002; Bastiaanssen et al., 2005) and modified by Allen et al. (Allen et al., 2002a) can be used to map spatial variation of ET across a range of land uses. The modification by Allen et al. (2002a) utilized ground base reference ET (ET_{ref}) to inversely and internally calibrate surface energy balance (Allen et al., 2005a; Allen et al., 2007a, Allen et al., 2007b; Tasumi et al., 2005a; Tasumi et al., 2005b). This modification eliminates the need for accurate surface temperature and air temperature measurement and the subsequent estimation of sensible heat. After modification, the model is called Mapping Evapotranspiration at high Resolution with Internalized Calibration (METRIC)

in papers (Allen et al., 2005a; Allen et al., 2007a; Allen et al., 2007b; Tasumi et al., 2005a, b; Gowda et al., 2008a; Gowda et al., 2008b; Trezza et al., 2006a; Singh et al., 2008). The two main advantages of SEBAL and METRIC model over other image data processing methods are 1) that it requires minimum ground data and 2) it can accurately estimate both seasonal and annual ET. The instantaneous and daily ET fluxes from SEBAL method has been validated with fair accuracy in Spain, US, China, Niger, Sri Lanka, Kenya, Morocco, The Netherlands, and Turkey (Pelgrum and Bastiaanssen, 1996; Schmugge et al. , 2003; Morse et al, 2000; Wang et al., 1995; Roerink, 1995; Hemakumara et al., 2003; Jacob et al., 2002;; Lagouarde et al., 2002; Bastiaanssen and Bos, 1999; Farah, 2001; van den Kroonenberg, 2003; Kohsiek et al., 2002; and Kite and Droogers, 2000).

From the late 1980s, various vegetation indices derived from remotely sensed data have been used to determine actual irrigated land (Lin et al., 2008). NDVI derived from multi-spectral imagery is a sufficiently good indicator of irrigation presence, irrigation status and crop condition (Kolm and Case, 1984; Eckhardt et al., 1990; Abuzar et al., 2001; Martinez-Beltran and Calera-Belmonte, 2001). Literature indicates that single date imagery acquired at the peak of the growing season may be sufficient to identify irrigation area, while multi-date data is needed to distinguish between different irrigated crop types (Rundquist et al., 1989; Abuzar et al., 2001). Surface albedo (0.14 to 0.22 for corn, 0.17-0.22 for rice) (Allen et al., 2002a) and NDVI > 0.7 (Tasumi and Allen, 2007) can be used for identifying vegetated crop area. Crop production can be expressed as a function of the relative evapotranspiration (Kassam and Doorenbos, 1983; Roerink et al., 1997) which is actual ET divided by potential ET. A value of $ET_r \geq 0.75$ is well acceptable for irrigated agriculture, although this value is not constant through time (Roerink et

al., 1997). The parameters explained above can be derived during SEBAL model processing. SEBAL can be used to identify and extract irrigated land from satellite imagery.

SEBAL model can be useful in estimating seasonal or annual ET or plant water use from agricultural lands at a small watershed level. In this study, SEBAL model is used to land use-based water use coefficient. Water demand factor represent average water use associated with a unit area for a particular land use type (Water Forum, 2000; Baumberger et al. 2007, Duchon et al. 1991, WHPA, 2007). This demand metric is commonly referred as irrigation water demand (Asokan and Dutta, 2008; Alcamo et al., 1997) or depth of water application per unit area (Dziegielewski and Chowdhury, 2008; Hook et al., 2010). USGS uses the terms irrigated water use per acre or application rate for denoting irrigation water applied to a unit area of irrigated land. The estimate of a land use-based water use coefficient for irrigated land can provide an estimate of projected irrigation demand utilizing projected land use maps. This information is very useful for planners to allocate future water demand in an area.

A remote sensing method, SEBAL model, to estimate plant water use is explained in this chapter. In addition, derivation of land use-based water use coefficient for future water demand projection in a watershed is discussed. The objective of this paper is to use SEBAL model, developed by Bastiaanssen (Bastiaanssen, 1998; Bastiaanssen et al., 2005) and modified by Allen et al. (Allen et al., 2002a; Waters et al., 2002) to estimate volumetric ET to quantify seasonal plant water use during the growing season of 2005-2008 in Wolf bay watershed area. Another objective of the paper is to derive water demand factors for year 2000-2005 to project future irrigation water demand in the watershed.

4.2 Materials and methods

4.2.1 Study Area

Wolf Bay watershed is located in Baldwin County, Alabama, near the Gulf of Mexico as shown in Figure 4.1. The watershed is spread over 126 km^2 covering two municipalities; Foley and Elberta. Gulf Coast tourism and retirement destinations have attracted a large number of people in recent years resulting in a rapid increase in population accompanied by considerable land use change. The average annual and growing season (April to September) precipitation is 1753 mm and 928 mm, respectively, based on 39-yr rainfall data from the National Oceanic and Atmospheric Administration-National Climatic Data Center (NOAA-NCDC) at three local stations (Pensacola Regional Airport, Robertsdale station and Fairhope 2 E station). This study focuses on growing season ET from 2005-2008. During 2005-2008, 2005 received the maximum amount of growing season rainfall (1493 mm), which is 565 mm higher than the 39-yr average growing season rainfall. Years 2006 (662 mm) and 2007 (709 mm) received lowest growing season rainfall. 2008 (1030 mm) was a normal year in terms of growing season rainfall.
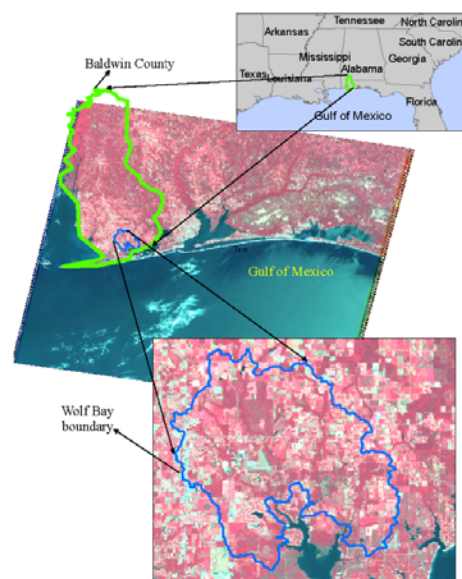
Figure 4.1. Location of Wolf Bay watershed boundary in Baldwin County, AL using False Color Composite Landsat 5 TM image (Path/row: 39/20) acquired on July 15, 2008 (Source: USGS).

According to Natural Resource Conservation Service (NRCS) data gateway crop land data layer by state, major crops in Baldwin County are soybeans, peanuts, corns, cotton, and winter wheat for grain (NRCS, 2008). Major irrigated crops include soybeans, peanuts, cotton and corn. Irrigation of golf courses, seed/sod grass farms and nurseries, is also a common practice in Baldwin County especially in coastal areas. Crop planting season generally starts in April and harvesting ending in September, except winter wheat which is planted in September/October and harvested in May/April. About 30% of total area of Wolf Bay watershed area is covered by croplands, seed/sod grasses, nurseries, golf courses, and tree crops and pastures. Approximately, 17% of the total area in Wolf Bay watershed area includes potentially irrigated land not including pasture. The main agricultural crops considered for this study are peanuts, soybeans, corn and cottons. Wolf Bay watershed area covers one golf course (Glenlakes golf course) where irrigation is supplied through surface water.

4.2.2 Imagery data

A total of 17 Landsat 5 TM images during the 2005 to 2008 growing season are obtained from USGS-Glovis webpage for the dates shown in Table 4.2. One image is used to extrapolate ET for one month or two month depending on the availability of sufficient cloud free images.

Table 4.1. Landsat 5 TM images used for SEBAL analysis (Source: USGS).

SN	Landsat Image date	Cloud cover %	ET mapping period
1	2005/04/02	0	April 2005
2	2005/5/20	10	May 2005
3	2005/6/21	10	June 2005
4	2005/7/7	0	July 2005
5	2005/8/8	10	August 2005
6	2005/9/9	0	September 2005
7	2006/4/5	0	April 2006
8	2006/5/23	10	May 2006
9	2006/6/8	10	June -July 2006
10	2006/9/28	0	August-September 2006
11	2007/4/24	0	April-May 2007
12	2007/6/27	10	June-July 2007
13	2007/8/30	0	August-September 2007
14	2008/4/26	0	April 2008
15	2008/5/12	0	May 2008
16	2008/7/15	1	June-July 2008
17	2008/9/17	28	August-September 2008

66

4.2.3 Weather data and reference ET estimation

SEBAL algorithms require some basic weather information from a reference station as input. Jay weather station (location: 30.775 N, -87.14 W, elevation: 63 m) from Florida Automated Weather Network (FAWN) is used as a reference station, as 15-minute interval weather data (air temperature, wind speed, solar radiation, relative humidity, and precipitation) from the station is readily available since 2002 (FAWN, 2010). REF-ET software developed by Allen et al. (2000a) is used to compute the ASCE Penman-Monteith standardized (Allen et al., 2000b) form of reference ET (ET_{ref}) for alfalfa using actual weather data. Computed fifteen-minute ET_{ref} data from REF-ET software is used to compute the ET_{ref} for the satellite overpass local time using linear interpolation. Similarly, wind speed at anemometer height (10 m) at the time of image capture is computed from available 15-minute data. REF-ET software is also used to compute ASCE Penman-Monteith standardized daily form of reference ET (ET_{ref_24}) and monthly reference ET (ET_{ref_month}), sum of daily ET_{ref_24} from April-September from 2005-2008.

4.2.4 The modified SEBAL Model

The SEBAL model, developed by Bastiaanssen (Bastiaanssen, 1998; Bastiaanssen et al., 2005) and modified by Allen et al. (Allen et al., 2002a; Allen et al., 2007a) is applied in this study to estimate volumetric ET to quantify plant water use for growing season (April to September) or 2005-2008. The surface energy balance equation is based on the theory that incoming net solar radiation drives all energy exchanges on the earth's surface including evapotranspiration, as shown below:

$$[R_n = G + H + \lambda ET] \tag{1}$$

where; R_n (Wm^{-2}) represents the net surface radiation which is the actual amount of energy available at the surface. G (Wm^{-2}) represents the soil heat flux which is the rate of heat storage in

67

the soil and vegetation. H (Wm^{-2}) represents the sensible heat flux which is the rate of heat loss to the air due to temperature difference. λET (Wm^{-2}) is the latent heat flux associated with ET.

The modified SEBAL model used in this study is explained in Appendices A.1 and A.3. ERDAS Imagine 9.2 software (Leica Geosystems, 2008) is used to process Landsat images using SEBAL algorithms programmed in the Modeler function of ERDAS. The input data required for SEBAL ET processing include; a digital satellite image with visible, near infra-red and thermal bands and basic weather parameters including hourly or shorter period solar radiation, relative humidity, temperature, wind speed and precipitation. Estimation of ET using SEBAL provides a unique synoptic alternative to quantify actual plant water use. Three major limitations of the model are 1) availability of cloud free images, 2) presence of well irrigated agricultural land in the image 3) need of a reference weather station.

Random pixels representing agricultural lands generated by AlaskaPak v2.0 tool for ArcGis 9.x (National Park Service, 2009) are used to extract seasonal ET for each year. Pixels covered by clouds are omitted from the calculation. For year 2005, 2006 and 2007 random pixels from agricultural lands were also collected from area outside the Wolf Bay boundary as most of the area inside the Wolf Bay boundary were covered by clouds.

4.2.5 Validation of modified SEBAL model

Validation of SEBAL ET estimates are done with Florida 30 m pixel data representing either grass or marsh land, although SEBAL methodology was used in Wolf Bay for estimating ET from irrigated lands. It is assumed that if SEBAL model provided better results for grass or marsh conditions then it should also provide good results for agricultural lands as algorithms in SEBAL model is applied independently to each pixel of the image. Daily, monthly and two-month ET from SEBAL model were validated with measured ET data from energy-budget eddy

68

covariance method at four USGS stations in Florida as explained in Chapter 3. The modified

SEBAL model performed well in terms of predicting and explain temporal variation in daily,

monthly and two-month (April-May, June-July, and September-August) ET when compared to

energy budget eddy covariance (EBEC) ET at USGS stations in South- Central Florida. The

mean bias error (MBE), root mean square error (RMSE), % RMSE, coefficient of determination

(R^2), and Nash-Sutcliffe Coefficient (ENS) from modified SBEAL model validation study are

shown in Table 4.2. The SEBAL model validation site and Wolf Bay watershed study area are in

humid subtropical climatic region. Long term growing season temperature and mean growing

season precipitation in both study areas are similar as shown in Table 4.3.

Table 4.2 SEBAL validation results in South-Central Florida

ET Period	MBE	RMSE	% RMSE	R^2	ENS
Daily	0.05 mm	± 0.48 mm	± 10	0.83	0.82
Monthly	-2 mm	± 16 mm	± 16	0.77	0.77
Two-month	-5 mm	± 30 mm	± 16	0.73	0.71

Table 4.3 Thirty-year average (1980-2009) growing season temperature and mean growing season precipitation from three closest NOAA stations from Wolf Bay watershed area and four NOAA stations closest from the USGS stations used for SEBAL validation (Source: NOAA-NCDC).

	South-Central Florida (SEBAL validation site)	Wolf bay watershed area	NOAA stations used
Mean growing season temperature (^{o}C)	25.1	25.9	Pensacola Regional Airport, Fairhope 2 NE, and Roberstdale
Mean growing season Precipitation (mm)	926	891	Vero Beach SE, Inverness 3 SE. Mountain Lake, and St Leo

4.2.6 Analysis of SEBAL ET estimates

Comparison of SEBAL ET with Potential ET, Pan ET

Estimated ET is compared and plotted against monthly AWIS (Agricultural Weather

Information Service) potential and Pan ET estimates to see if there is any correlation between

them. Estimated monthly ET from AWIS stations are derived from the 30 m pixel representing location of the AWIS station in Landsat 5 TM image. Potential ET is defined as the amount of water transpired in a given time by a short green crop, completely shading the ground, of uniform height and with adequate water status in the soil profile (Penman, 1948). AWIS uses the modified Bair and Robertson model (AWIS, 2009) to estimate Potential ET for three weather stations (KPNS- Pensacola Regional Airport, KHRT- Hurlburt Field, and KCEW- Crestview Bob Sherman station). Data Input for the AWIS model includes: maximum dry bulb temperature, minimum dry bulb temperature, total solar energy at the top of the atmosphere, hours of sunshine, day length, wind speed, and vapor pressure deficit.

SEBAL ET versus water withdrawal data

Monthly SEBAL ET estimates are plotted against water withdrawal data from three golf courses available from Alabama Department of Economic and Community Affairs (ADECA). The pumping data from the golf courses were converted into depth by estimating irrigated area in golf course through digitization. The reason behind plotting SEBAL ET against water withdrawal is to see if there is any correlation between them.

4.2.7 Estimation of irrigated area

Extraction of irrigated area required manual digitizing and great care. Irrigated lands were identified for each Landsat image processed for ET estimation. The 2005 land use shapefile from Baldwin County Planning Commission is used to extract all agricultural lands in Wolf Bay. This shapefile was modified by overlaying high resolution 1 m resolution aerial photographs (2006 and 2009) and crop layers (2008) from NRCS. The resulting base map provided irrigated areas for volumetric ET estimation purpose. Manual editing of individual polygons was possible, since the study area was relatively small (126 km^2).

The Landsat image was viewed as a 4-3-2 false color composite (FCC) band combination to modify the shapefile by identifying and deleting all bare lands. The Erdas Imagine Modeler function was used to set up the criteria of albedo, normalized difference vegetation index (NDVI) and evaporative fraction (ETrF) for separating irrigated lands, as follows; Albedo > 0.14, NDVI > 0.5, and $ET_rF > 0.75$. Values of albedo and NDVI are chosen in such a way that most of the forested area is eliminated from analysis and low vegetated area, such as crop lands, seed/sod grasses, turf farms, are covered. The resulting polygon of agricultural land from Baldwin County Planning Commission, 2008 and 2009 crop layers from NRCS, and 1 m aerial digital photograph are used for extraction and assignment of agricultural lands (Figure 4.2). Some area which are inside the polygon but do not meet all criteria are summed up and subtracted from total area to estimate total irrigated area. The process is shown in Figure 4.3.

(i) 3-2-1 Aerial image 2006   (ii) 4-3-2 aerial image 2009   (iii) 4-3-2 Landsat 5 TM image of 2008/7/15 image.

(iv) ETrF image from SEBAL dark blue showing higher ETrF values (0 to 1.35 for 2008/7/15 image.   (v) Erdas Imagine map showing irrigated lands (dark blue color indicating region which met all criteria).
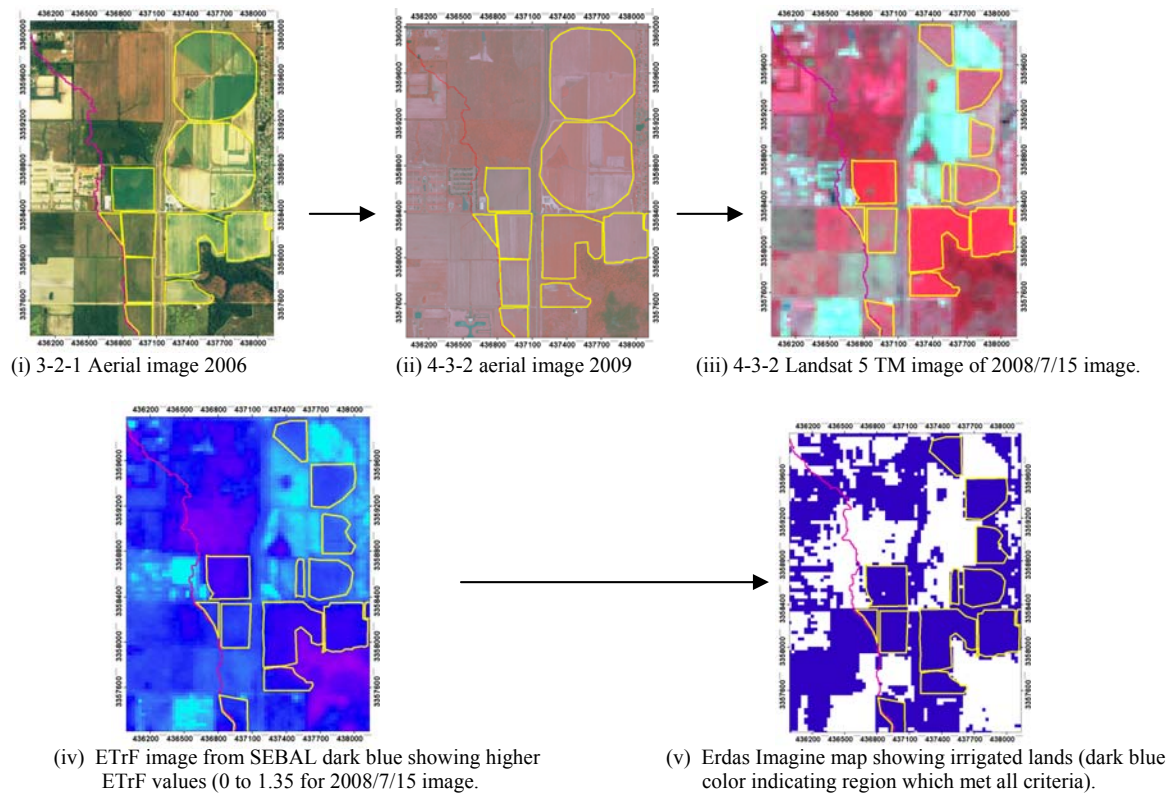
Figure 4.2. Preparation of polygon shape file for irrigated area in a small part of Wolf Bay watershed area (red line denotes part of the Wolf Bay watershed boundary), first the shape file is overlaid with aerial image, and then with Landsat 5 TM image, ETrF Map generated from SEBAL, and finally with ERDAS Imagine map created using criteria used for potential irrigated areas.
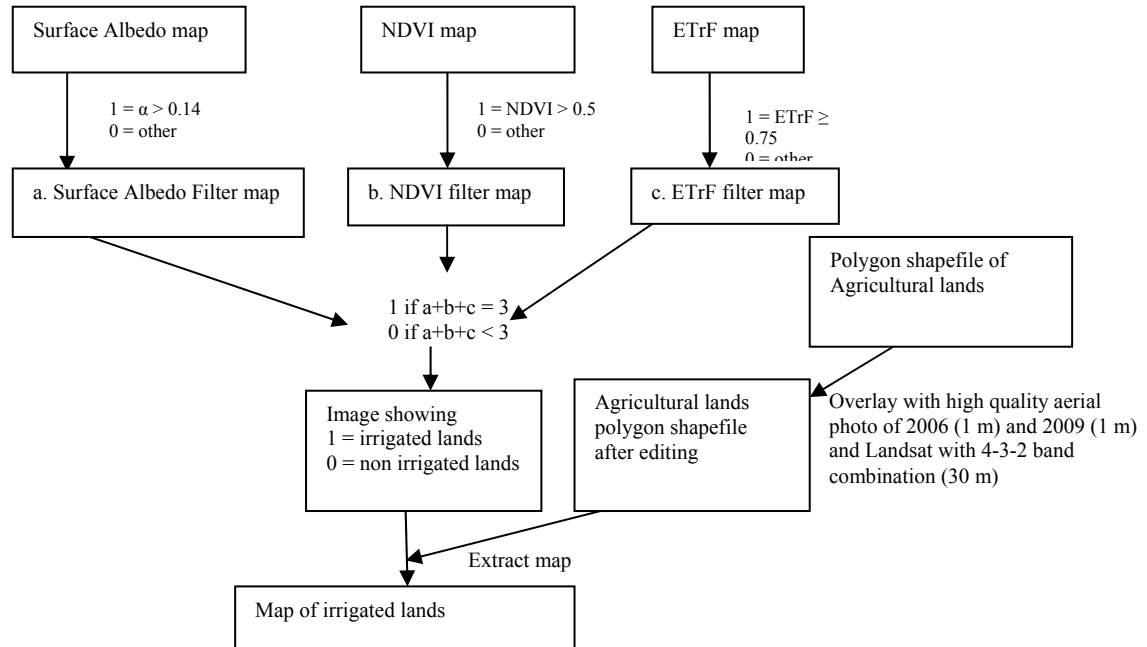
Figure 4.3. Flowchart showing method used for estimating irrigated area in Wolf bay watershed area.

When the polygon of agricultural lands became covered with clouds, the irrigation shape file is modified in accordance with the closest image available in terms of time of image taken from the same growing season. This is because crops planted in a month of a growing season will also show up in the image of next month. SEBAL ET estimates from clouded area are not used. Rather, ET estimates from other cloud free pixels are used. No ground measurement data of irrigated agriculture were available for this analysis. Hence, comparison of actual irrigated area with those estimated from this method was not completed.

4.2.8 Plant water use

Seasonal volumetric ET estimates for agricultural lands are estimated using ET estimates from cloud free images and estimated irrigated areas. Average monthly and two-month ET estimates from irrigated lands are derived from SEBAL ET maps. The polygon shapefile of irrigated area is used to extract monthly or two-month ET. The average monthly or two-month ET (depth) (ET_{avg}) is used to compute total volumetric ET using total irrigated area. $ET_{avg,i}$ is estimated from cloud free area which is used as representative ET for all irrigated agriculture in

72

the watershed for the period. Volumetric ET from each period of the growing season is added to

derive the total volumetric ET during the growing season.

$$[ET_{vol} = (\sum_{i=1}^{n} ET_{avg,i} \times A_i)] \qquad (2)$$

where; ET_{vol} is the volumetric ET during growing season, measured in cubic meters, $ET_{avg,i}$

(mm) is the average ET from irrigated area for the period i, A_i (km^2) is the total irrigated area

during the period i.

4.2.9 Water demand factors

Water demand factors for major crops, turf farms, and golf courses are estimated from

randomly sampled pixels. Random pixels are generated using AlaskaPak v2.0 tool for ArcGis 9.x

(National Park Service, 2009). Each pixel is overlaid with 2008 crop layer (NRCS, USDA), 4-3-

2 combination of Landsat 5 TM imagery (USGS), and digital aerial photographs (NRCS) to

assign crop name to each pixel. Since crop layer was available for the year 2008 from NRCS, it

was assumed that cropping patterns did not changed significantly from 2005 to 2008; hence, a

corn area in 2008 also represents corn in other years. The average ET derived from all randomly

selected pixels is used as the representative seasonal ET value for the crop. Water demand

factors are estimated for dry, wet and normal years and are estimated in mm per growing season

or year since irrigation is likely to occur only during growing season.

4.2.10 Irrigation water demand projection

Because water demand factors estimates are based on the water used by the plant, future

irrigation water demand can be projected for Wolf Bay watershed area if projected irrigated area

is known. We can multiply projected irrigated area with the water demand factor to get an

estimate of future plant water demand under wet, dry and normal precipitation conditions.

Irrigation water demand can be estimated from plant water demand if efficiency of the irrigation

73

system is known. Projections of future LULC for years 2010, 2020, 2030, and 2040 were made available from Dr. Tian's group of Wolf Bay watershed project in this study. The combined area of crop land and pasture land in Wolf Bay watershed area in 2008 and 2009 from NRCS is comparable with 2010 projected LULC maps. Hence for year 2010, % coverage for major irrigated plants (crops, turf farms, and golf courses) are used from 2009 NRCS crop layer data. A future scenario of 2040 is developed using area of crop land from projected LULC of 2040 based on high population growth as shown in Table 4.4. It is assumed that most of the crop lands from Wolf Bay watershed area will be converted into turf farms and golf courses. Scenarios for years 2020 and 2030 are developed using simple linear interpolation as shown in Figure 4.4.

Table 4.4. Projected LULC scenarios (% coverage of total crop and pasture land) for year 2040 for future irrigation water demand projection.

Crop type	2009 (NRCS)	2010	2040
Peanuts	18	18	4
Cotton	1	1	1
Soybeans	24	24	5
Corn	6	6	3
Seed/sod grass	14	14	62
Golf courses	1	1	25
non-agricultural pasture land/idle crop land	32	32	0
Other crops	4	2	0
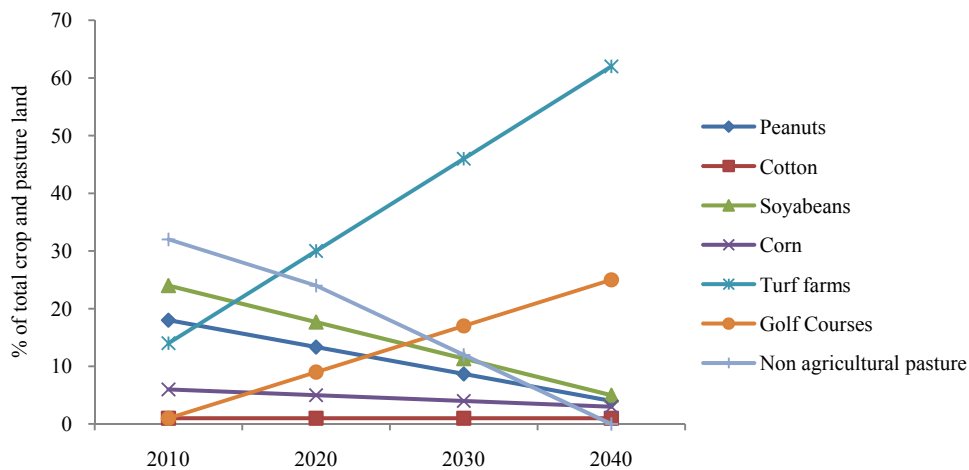
Figure 4.4. Projected LULC scenarios for irrigation water demand projection in Wolf Bay watershed area. Projected scenarios assume significantly increased turf farm and golf course use of agricultural land 2040 and assume that 100% of agricultural land is irrigated by 2040 (up from approximately 50% in 2008).

Projection of total irrigated crops is required to project irrigation water demand as not all crop lands, turf farms and golf courses are irrigated. To project future irrigated area for each crops, % irrigated area for each major irrigated plant, i.e. 100 × area irrigated of each major irrigated area/total area covered by the area, from the year 2008 is used. For year 2010, % irrigated area for each major irrigated crop is used same as year 2008. It is assumed that for year 2040, all crop land is irrigated due to higher irrigation water demand to sustain larger population. Simple linear interpolation is used to estimate % irrigated area for each major irrigated plant for year 2020 and 2030, using assumed % irrigated area data from 2010 and 2040.

Projected irrigated area for each crop is multiplied by water demand factor to estimate total plant water demand. Water demand factors estimated in this study doesn't include the water lost in the irrigation system. If an irrigation efficiency of a systems is known, that water loss during the irrigation process can be added with the plant water demand to fulfill the plant water requirement. It is assumed that the irrigation systems in Wolf Bay watershed area has an irrigation efficiency is 70%. Hence, total irrigation water demand in the watershed is estimated by dividing total plant water demand by 0.7.

4.3 Results and discussions

4.3.1 Monthly and Seasonal ET maps

ET is estimated on a monthly or two-month basis (April-May, June-July, and August-September). Total seasonal ET is estimated by summing up ET from all periods during the growing season. A seasonal ET map is prepared for year 2008 (Figure 4.5). Because of the presence of cloud cover the Landsat TM images analyzed for some of the months during year 2005-2007, seasonal ET map for these years are not processed as most of the areas in the image are covered by cloud. Total water use from irrigated areas is estimated as an aggregated

volumetric ET from the monthly or two-month ET estimates from monthly or two-month ET maps. Hence, seasonal ET maps need not need to be derived to estimate total seasonal volumetric ET from irrigated area.
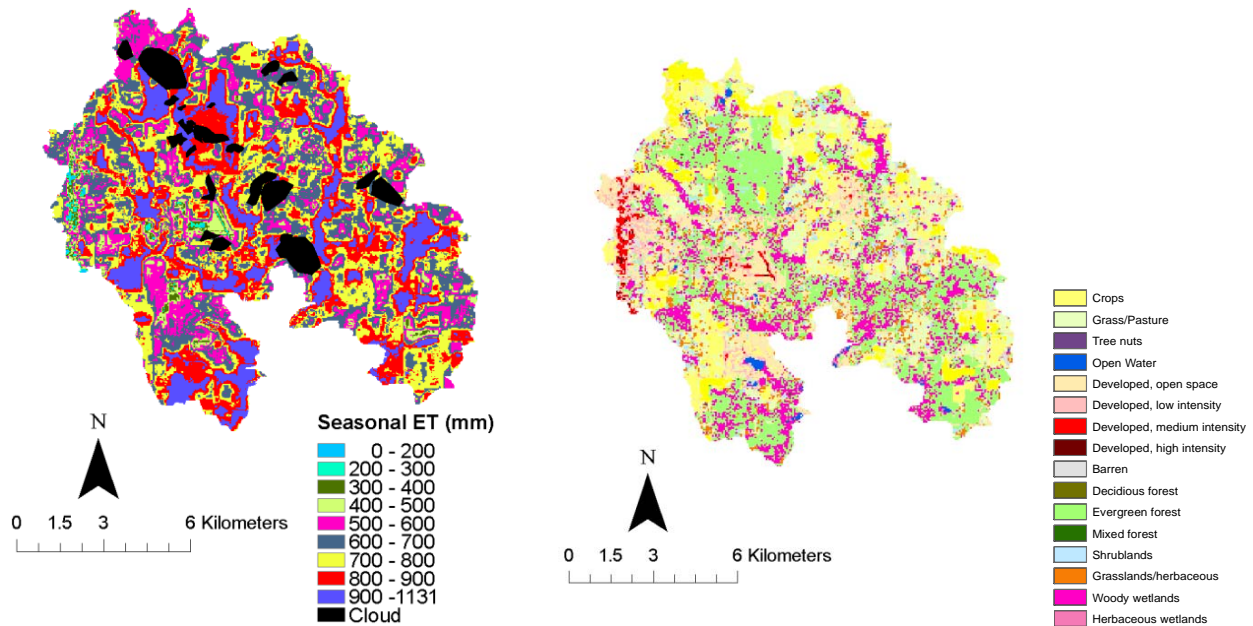
Figure 4.5. SEBAL derived seasonal ET in Wolf Bay watershed area for the growing season of 2008 in the left and LULC map from NRCS for the year 2008 in the right

4.3.2 SEBAL ET versus Potential ET and Pan ET

Figure 4.6 indicates that SEBAL ET estimates which represents actual ET are less than potential ET from modified Bair and Robertson model (Agricultural Weather Information Service, AWIS, 2009) and Pan ET from AWIS, but have same trends over time. The correlation of SEBAL ET with potential ET (r = 0.76) and Pan ET (r = 0.57) is significant (α < 0.001). This indicates that SEBAL ET values are reasonable when compared to potential and pan ET.
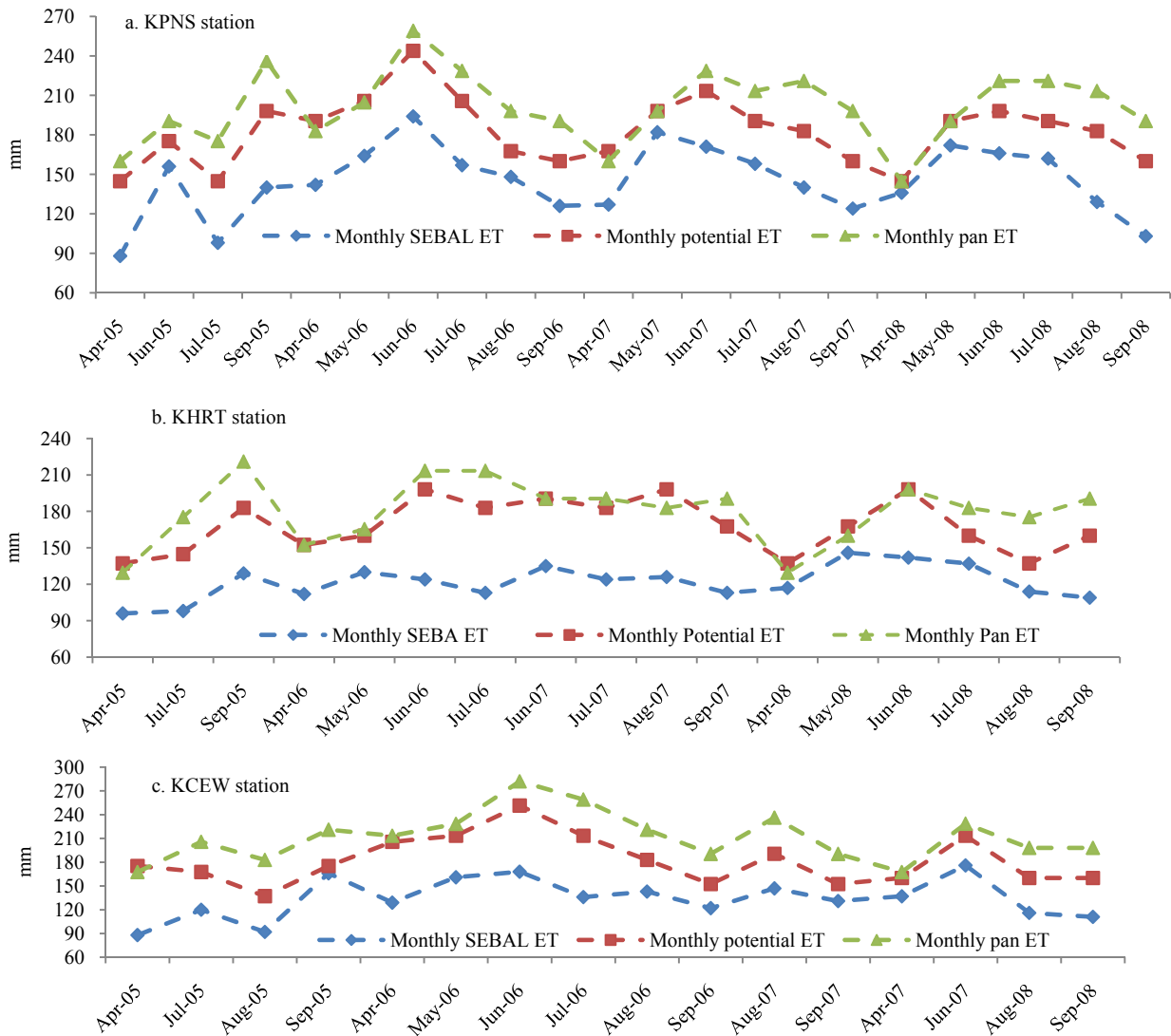
Figure 4.6. Monthly SEBAL ET estimates, AWIS potential ET and Pan ET estimates from three AWIS weather stations, KPNS-Pensacola Regional Airport, KHRT- Hurlburt Field, KCEW- Crestview Bob Sherman station (Source: AWIS).

The plot of monthly SEBAL ET with potential ET, pan ET, and available water withdrawal data indicates a positive linear relationship. The actual ET at the AWIS stations can be affected by the condition of grass present during the Landsat image acquisition which could change actual ET values. However, potential ET is estimated based on ideal condition of grass and ample availability of water, which do not fluctuate a lot. Details of method used by AWIS to estimate potential ET could not be accessed as the equations used were proprietary.

4.3.3 SEBAL ET versus water withdrawal data

Monthly SEBAL ET from golf courses is plotted with monthly water withdrawal data and monthly precipitation. The relationship suggests a positive linear relationship ($R^2 = 0.48$) as shown in Figure 4.7. Monthly ET was positively correlated with water withdrawal ($r = 0.68$, p-value <0.0001). This indicates that higher ET is associated with higher rate of water withdrawal in the golf courses.
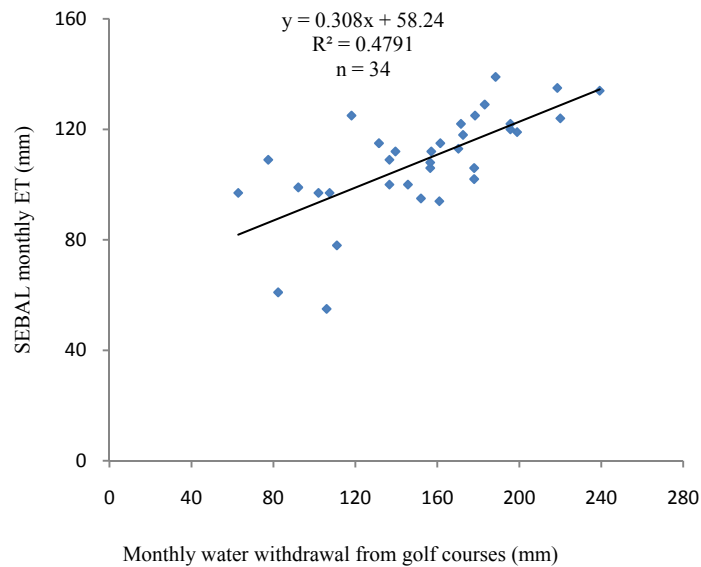
Figure 4.7. SEBAL ET versus water withdrawal from golf courses (Source: ADECA).

4.3.4 Irrigated area and SEBAL ET estimates from irrigated lands

Estimated irrigated area during April-May, June-July, and August- September from 2005 to 2008 is shown in Figure 4.8, indicating generally higher irrigated area during the mid or late growing season period. A shapefile of irrigated area is used to extract two-month ET for each growing season. Figure 4.9 indicates that ET in June-July is higher than other months confirming the expected higher rate of water use during these months.
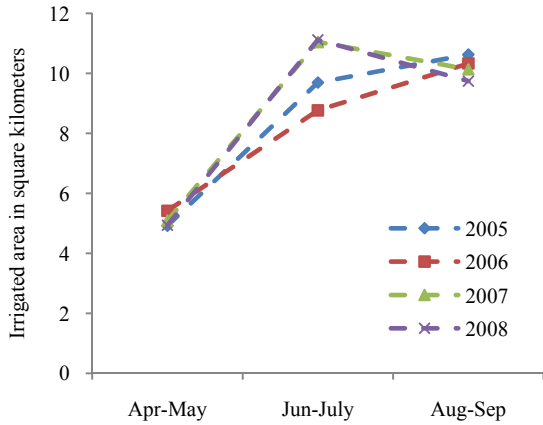
Figure 4.8. Irrigated area during growing season
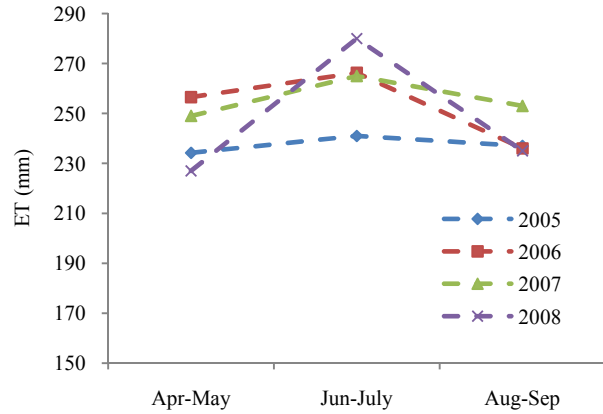
Figure 4.9. Two-month ET from irrigated area in Wolf Bay.

Total volumetric ET (million cubic meters) and total irrigated area (km^2) during growing season of 2005-2008 is shown in Figure 4.10. More area was irrigated in recent years 2007 and 2008. Estimated total irrigated areas was more in 2005 than in 2006, however, total more water was consumed in 2006 than in 2005. Figure 4.10 also indicates seasonal volumetric ET is more in dry and normal years than in wet years, as expected. Hence, Plant water use is higher in dry years than in wet years which indicates that more irrigation water is required to fulfill plant water requirements during dry years.
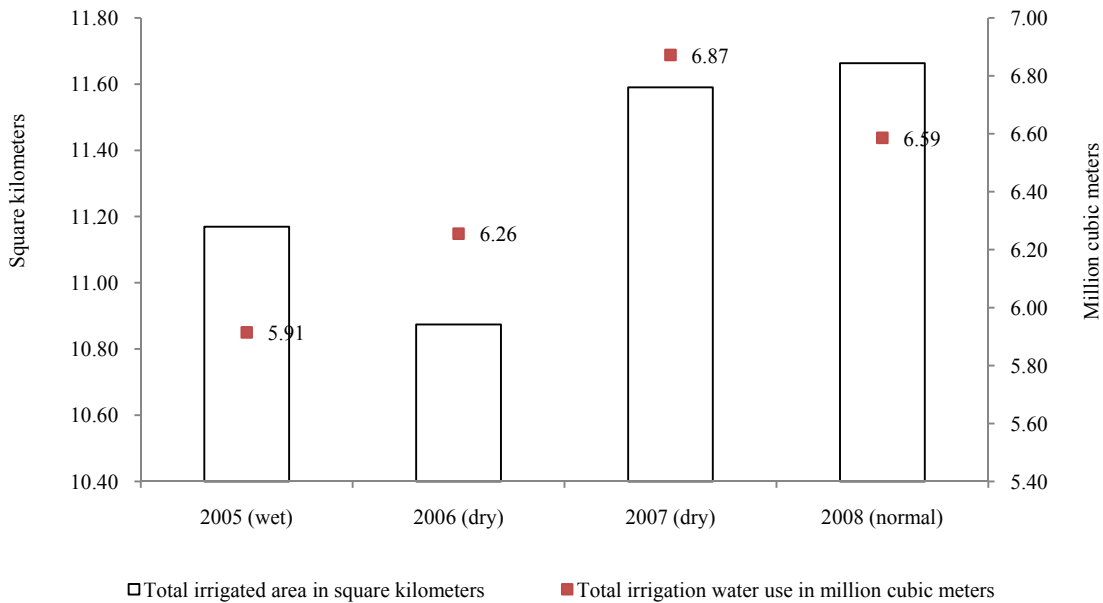
Figure 4.10. Total seasonal water use as volumetric ET and irrigated area in Wolf Bay.

79

4.3.5 Water demand factors for major plants in Wolf Bay

Average seasonal SEBAL ET depth from randomly generated pixels of each plant is used as water demand factor for each plant during wet year (2005), dry year (2007), and normal year (2008). For dry year, SEBAL ET from 2007 was used, as enough pixels from each plant were not available from seasonal ET map of 2006 due to the presence of cloud. Average seasonal ET from pixels of four major crops, turf farms, and golf courses for dry, normal, and wet year are listed in Table 4.5. The sample pixels for the plants are located in and around the wolf bay watershed area.

Table 4.5 Water demand factor (mm) from major irrigated plants in Wolf Bay watershed area for wet, dry, and normal year and mid-season crop coefficient (FAO,1998)

Crop type	2005 (Wet)	2007 (dry)	2008 (normal)	Mid-season crop Coefficients from (FAO, 1998)
Corn	629	698	645	1.15
Cotton	585	647	636	1.10-1.15
Soybeans	573	613	577	1.10
Peanuts	565	614	593	1.10
Seed/sod grass	554	593	560	0.9 (cool season), 0.8 (warm season)
Golf courses	499	665	631	NA

Corn and cotton were found to have higher ET or water consumption rate than other crops. The mid-season crop coefficient from FAO (1998) indicated that corn has highest crop coefficient among other crops considered in this study. Similarly, lower ET from turf farms were obtained also supported by the lower value of mid-season crop coefficient for turf grasses from FAO. This result suggests that the modified SEBAL method can be used to access accurate water use or ET from a crop with no need of ground information about the crop.

2008 crop layer was used to identify major irrigated plants in Wolf bay watershed area. Estimated water demand factors for each major irrigated plant is higher in dry years than in wet years. This indicates that decrease in precipitation is associated with higher use of irrigated water as indicated by higher water demand factors in the dry year. This agrees with the results from an

agricultural irrigation water demand study conducted by University of Georgia (Hook et al., 2010).

4.3.6 Irrigation water demand projection

A shape file of irrigated land was used to estimate % irrigated area of each LULC class (major irrigated plants) for year 2008. The same numbers were used for year 2010. It is assumed that as population increases crop area decreases and a higher percent of crop area is irrigated to sustain the increased population. For year 2040, it was assumed that all crop lands, turf farms, and golf courses are irrigated. Projected area % irrigated area of each LULC class for years 2020 and 2030 are estimated using linear interpolation method shown in Table 4.7.

Table 4.6 Projected irrigated area for each LULC class from 2010 to 2040

LULC type	2010	2020	2030	2040
Peanuts	3.83	2.60	1.45	0.51
Cotton	0.11	0.14	0.15	0.13
Soybeans	1.36	2.07	1.58	0.63
Corn	0.38	0.60	0.56	0.38
Seed/sod grass	1.64	4.42	6.91	7.83
Golf courses	0.35	2.39	3.29	3.16

The total projected irrigation water demand is estimated as the sum of irrigation water demand from all LULC classes representing different plants. Projected irrigation water demand is higher for dry growing seasons as plant water demand is higher during dry seasons. Total irrigation water demand for wet, normal and dry years (volumetric ET) is shown in Figure 4.11. Tables 4.7, 4.8 and 4.9 show the tabulated value of plant water demand for each LULC class representing a particular irrigated plant and total projected irrigated water demand for wet, normal and dry year respectively. A 70% irrigation efficiency was used to estimate irrigation water demand from total plant water demand.
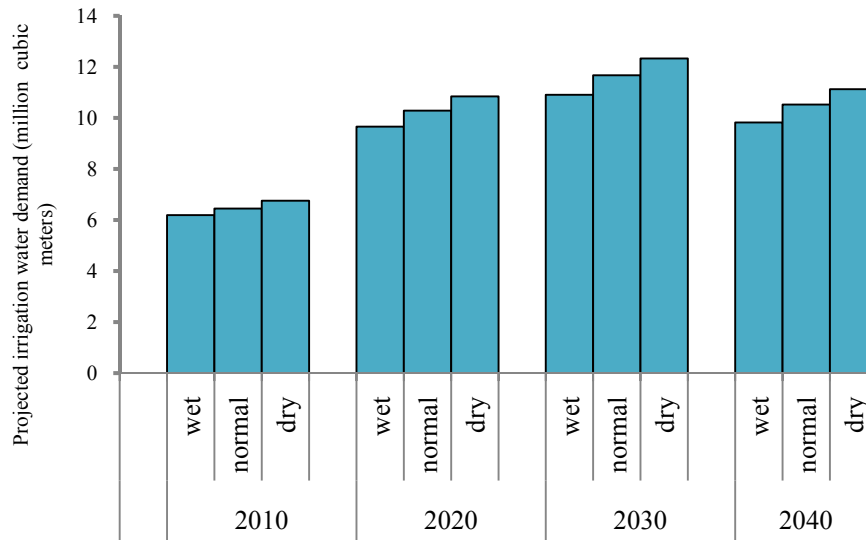
Figure 4.11. Total seasonal water use as volumetric ET and irrigated area in Wolf Bay.

Table 4.7 Projected irrigation water demand* in million cubic meters for wet year

LULC class	2010	2020	2030	2040
Peanuts	2.16	1.47	0.89	0.30
Cotton	0.06	0.08	0.10	0.08
Soybeans	0.78	1.19	0.97	0.36
Corn	0.24	0.38	0.39	0.24
Seed/sod grass	0.91	2.45	4.10	4.39
Golf courses	0.18	1.19	2.19	1.99
Total volumetric ET demand	4.33	6.76	8.63	7.37
Total irrigation water demand	6.19	9.66	12.33	10.52

* Estimated as Total volumetric ET demand divided by 0.7 (Irrigation efficiency of 70%)

Table 4.8 Projected irrigation water demand* in million cubic meters for normal year

LULC class	2010	2020	2030	2040
Peanuts	2.27	1.54	0.86	0.30
Cotton	0.07	0.09	0.09	0.08
Soybeans	0.79	1.19	0.91	0.36
Corn	0.25	0.39	0.36	0.24
Seed/sod grass	0.92	2.47	3.87	4.39
Golf courses	0.22	1.51	2.07	1.99
Total volumetric ET demand	4.51	7.20	8.17	7.37
Total irrigation water demand	6.45	10.29	11.67	10.52

* Estimated as Total volumetric ET demand divided by 0.7 (Irrigation efficiency of 70%)

Table 4.9 Projected irrigation water demand* in million cubic meters for dry year

LULC class	2010	2020	2030	2040
Peanuts	2.35	1.54	0.89	0.31
Cotton	0.07	0.09	0.10	0.08
Soybeans	0.83	1.19	0.97	0.39
Corn	0.27	0.39	0.39	0.26
Seed/sod grass	0.97	2.47	4.10	4.64
Golf courses	0.24	1.51	2.19	2.10
Total volumetric ET demand	4.73	7.20	8.63	7.79
Total irrigation water demand	6.76	10.29	12.33	11.12

* Estimated as Total volumetric ET demand divided by 0.7 (Irrigation efficiency of 70%)

Projected irrigation water demand was increased by 2040 as compared to 2010 even though crop land will be decreased significantly due to population growth and urbanization. The increase in irrigation water demand in 2040 is due to the assumption that 100% of agricultural lands will be irrigated by year 2040. It was estimated that irrigated water demand will be increased by 59% (6.19 to 9.82 million cubic meters), 65% (6.76 to 11.12 million cubic meters), and 63% (6.45 to 10.52 million cubic meters), under wet, dry, and normal climatic conditions, respectively from 2010 to 2040.

Literature shows how water demand factors have been derived using ground data of total water use and total area irrigated. In this study, remotely sensed data is used to estimate both. Projected irrigation water demand information can be useful for planners to design management plans for water resource utilization in Wolf Bay watershed area. It indicates that the remote sensing method using the modified SEBAL model has a potential to be used in irrigation water demand management studies in Wolf Bay and other watersheds in the southeastern US.

4.4 Case study

Total water demand in Wolf Bay watershed is projected for years 2010, 2020, 2030, and 2040. Total water demand is estimated as the sum of public water demand (water supplied by public water companies), private-supplied water demand (water withdrawal from privately

owned wells), and irrigation water demand described in this chapter. Public water demand and private-supplied water demand are projected using population data as described in Appendices B.1 and B.2. The projected water demand for public, private, and irrigation water demand uses for 2010, 2020, 2030, and 2040 under dry, normal and wet weather conditions are shown in Figure 4.10 and Table 4.10.
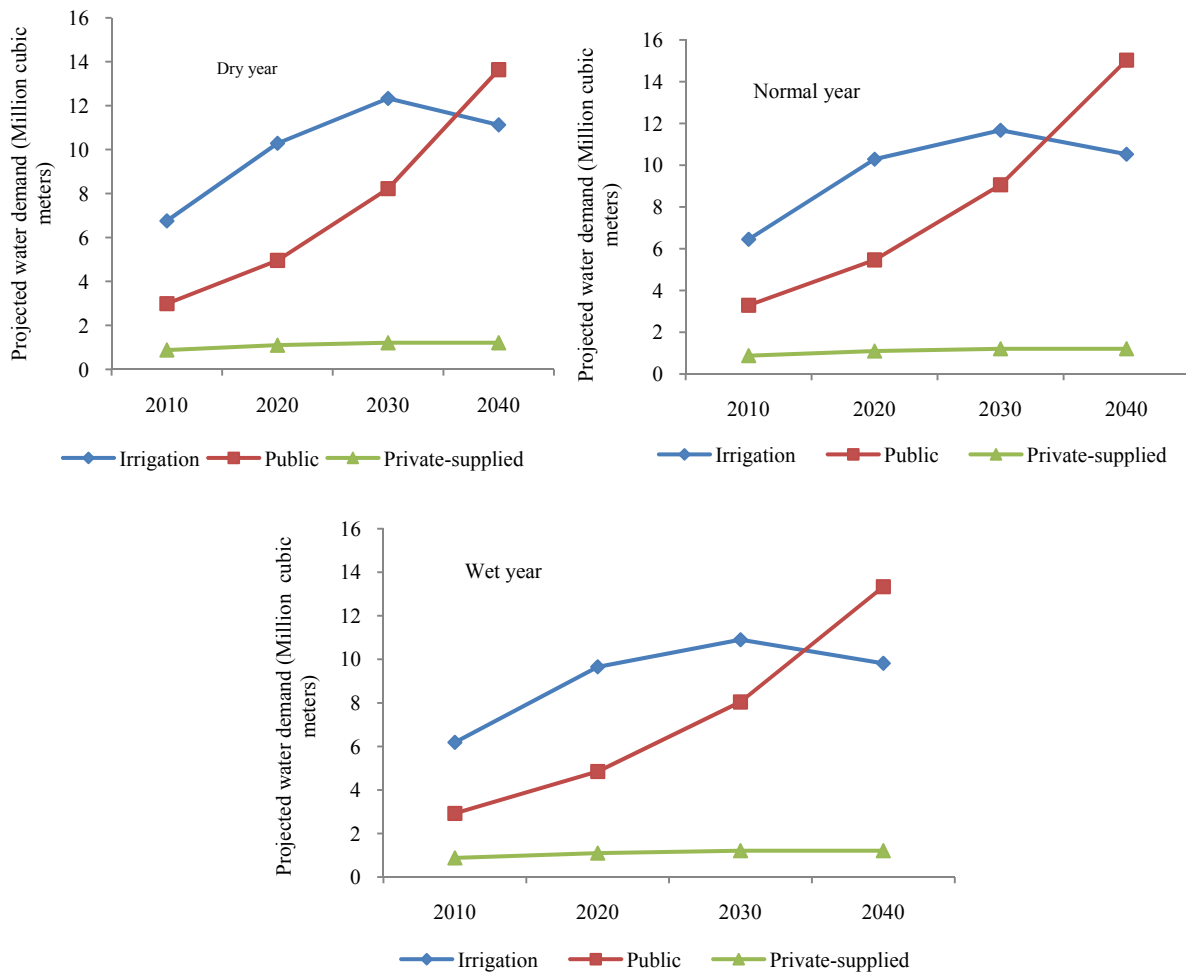
Figure 4.12 Projected water demand in Wolf Bay watershed area for years 2010, 2020, 2030, and 2040 under dry, normal and wet climatic conditions.

By 2040 public water demand will be major water use category replacing irrigation water demand in 2010. In 2010, approximately 62%, 29%, and 9 % of total water demand will be used for irrigation, public and private-supplied water, respectively. Whereas in 2040, approximately

55%, 41%, and 4 % of total water demand will be used for irrigation, public and private-supplied water, respectively. The public water demand in Wolf Bay watershed area will increase from 2010 to 2040 due to the increase in population and urbanization. The private-supplied population will not increase by the same percentage as public water demand as most of the population will be supported by public water companies in future, also an effect of increasing urbanization. The irrigation water demand will increase from 2010 to 2030, whereas it will decrease from 2030 to 2040. The increase in irrigation water demand from 2010 to 2030 is due to the increase in area of irrigated lands. However, the area of irrigated lands will be decreased from 2030 to 2040 due to urbanization which will reduce the irrigation water demand from 2030 to 2040. The increase in total water demand in Wolf Bay watershed area from 2010 to 2040 is mainly due to increase in public water demand. Hence, population growth is the major factor that will affect the total water demand in Wolf Bay watershed area in future.

Table 4.10. Projected water demand (Million cubic meters) in Wolf Bay watershed area under dry, normal and wet years.

	Dry				Normal				Wet			
	2010	2020	2030	2040	2010	2020	2030	2040	2010	2020	2030	2040
Irrigation	6.76	10.29	12.33	11.12	6.45	10.29	11.67	10.52	6.19	9.66	10.90	9.82
Public	3.29	5.46	9.06	15.03	2.99	4.96	8.22	13.64	2.92	4.85	8.04	13.34
Private-supplied	0.88	1.10	1.21	1.21	0.88	1.10	1.21	1.21	0.88	1.10	1.21	1.21
Total water demand	10.93	16.84	22.59	27.36	10.31	16.34	21.10	25.37	9.99	15.60	20.15	24.36

The projected water demand is divided by total area of watershed (Appendix B.3) to estimate water demand in terms of depth which indicates water withdrawal per unit area of the watershed. Projected water withdrawal is expected to increase from 5% of average annual precipitation to 11% of average annual precipitation from 2010 to 2040. The values of projected water demand in depth are less than long-term (39-year) average annual precipitation in Wolf

Bay watershed area (1699 mm from Pensacola Regional Airport, Robertsdale, and Fairhope NOAA stations) which indicates that projected water withdrawal in Wolf Bay watershed area will likely be sustainable into the foreseeable future. As it is expected that the total water demand in Wolf Bay watershed area will increase by approximately 146% by 2040 mainly due to increase in public water demand, water companies in Wolf Bay watershed area should make plans in the future to increase the water production rate. Similarly, for irrigation water demand in the future, effective irrigation management systems should be managed by turf farm and golf courses owners to meet the requirement of irrigation in the future. Hence, the information regarding projected water demand in Wolf bay watershed area can be used by planners to manage water resources in the Wolf Bay watershed area.

4.5 Summary and conclusions

Remotely sensed imagery provides a unique opportunity to evaluate plant water use at a local scale even in the presence of minimum ground data. The modified Surface Energy Balance Algorithm (SEBAL) model was used to quantify plant water use and project future irrigation water demand in Wolf Bay watershed area. Cloud free satellite imagery with visible, thermal and near infra-red bands were identified, some basic weather parameters such as solar radiation, temperature, relative humidity, wind speed, and precipitation were acquired for basic knowledge of the study area which was needed to process seasonal ET at a local scale. A Landsat 5 TM image is useful at this small watershed level because of its higher resolution (30 m). Availability of cloud free images is one of the major constraints in processing Landsat images for the SEBAL model. Although SEBAL can provide a good estimate of plant water use from agricultural land at a small watershed level, it should be noted that ET estimates from SEBAL are an estimation of

actual water use by the plants which does not account for water application efficiencies in the irrigation system.

Irrigated lands are identified manually using basic functions of image identification, remote sensing and GIS. The method of estimating irrigated area described in the paper has limited scope as it is best fitted for a small watershed study which involves manual labor and tremendous care to digitize individual agricultural fields. However, SEBAL parameters can be used to derive the spatial distribution of pixels representing potential irrigated areas. So the opportunity also exists for SEBAL model to identify and verify the location of irrigated lands at the regional and local scale.

It has been found that the modified SEBAL method not only provides an estimate of historical water use from irrigated lands, but also provides a means to project future water demand. In this study, result from SEBAL ET estimates indicate that plants use more irrigated water during dry years than in wet years, as expected. Therefore, it is recommended that ET estimation using images from a number of historic dry and wet years be completed. It is also recommended that integration of higher spatial but lower temporal resolution satellite imageries with lower spatial but higher temporal resolution can be used to increase the accuracy of ET estimates. This is because currently, most satellite images with higher spatial resolution have lower temporal resolution (for example spatial resolution of Landsat 5 TM is 30 m and temporal resolution is 16 days), and images with lower spatial resolution have higher temporal resolution (for example, spatial resolution of NOAA-AVHRR satellite image is 1 km but temporal resolution is at least once a day).

Instantaneous surface energy fluxes are not validated with ground measured data. However, validation of surface energy balance parameters with field data can provide further

accuracy for the assessment of the ET estimates and methods presented in this chapter. Overall, the modified SEBAL model has been identified as a useful remote sensing method to estimate plant water use and to project future irrigation water demand at a watershed scale in the humid southeastern US. Incorporation of population, water price, conservation factors with the demand factor can make the results more comprehensive and sensitive to actual conditions with respect to water use.

A case study is presented to show how the method used in this chapter can be applied to project water demand at a watershed scale. Total water demand in Wolf Bay watershed area was estimated as the sum of public, private-supplied, and irrigated water demand in Wolf Bay watershed area. Water demand projections were made for years 2010, 2020, 2030, and 2040 under wet, normal and dry climatic conditions. Total water demand in Wolf Bay watershed area are estimated to be 9.99 to 10.93, 15.60 to 16.84, 20.15 to 22.59, and 24.36 to 27.36 in million cubic meters for years 2010, 2020, 2030, and 2040, respectively. Projected water demand information is useful for planners to manage water and natural resources in Wolf Bay watershed area.

References

Abuzar, M., McAllister, A., and Morris, M., 2001, Classification of seasonal images for monitoring irrigated crops in a salinity affected area of Australia, International Journal of Remote Sensing, 22, 717–726.

Ahmad, M. D., Biggs, T., Turral, H., and Scott, C.A., 2006, Application of SEBAL approach and MODIS time-series to map vegetation water use patterns in the data scarce Krishna river basin of India. Water Science & Technology, 53 (10), 83-90.

Alcamo J, Doll P, Kaspar F, and Siebert S., 1997, Global Change and Global Scenarios of Water Use and Availability: An Application of Water GAP. Center for Environmental Systems Research (CESR), University of Kassel: Kassel.

Allen, R. G., Morse, A., Tasumi, M., Trezza, R., Bastiaanssen, W.G.M., Wright, J., and Kramber, W., 2002b, Evapotranspiration from a satellite-BASED surface energy balance for the Snake Plain Aquifer in Idaho, Proceedings of USCID Conference, USCID, Denver.

Allen, R. G., Pereira, L. S., Raes, D., and Smith, M., 1998, Crop evapotranspiration - guidelines for computing crop water requirements - FAO Irrigation & Drainage Paper 56. FAO, 1998, 301 Agriculture Organization of the U. N. (FAO), Rome, Italy.

Allen, R., Waters, R., and Bastiaanseen, W.G.M., 2002a, SEBAL Surface Energy Balance Algorithms for Land, Idaho implementation, Advance Training and Users Manual, August 2002, Version 1.0.

Allen, R.G., 2000a, REF-ET: Reference Evapotranspiration Calculation Software for FAO and ASCE standardized Equations. University of Idaho, www.kimberly.uidaho.edu/ref-et/ last accessed on April 30, 2009.

Allen, R.G., 2000b, Manual: REF-ET: Reference Evapotranspiration Calculation Software for FAO and ASCE standardized Equations. University of Idaho, http://www.kimberly.uidaho.edu/ref-et/manual.pdf last accessed on April 30, 2009.

Allen, R.G., Tasumi, M, Morse, A.T. and Trezza, R., 2005a, A Landsat-based Energy Balance and Evapotranspiration Model in Western US Water Rights Regulation and Planning, Journal of Irrigation and Drainage Systems, 19, 251-268.

Allen, R.G., Tasumi, M. and Trezza, R., 2005b, Benefits from Tying Satellite-based Energy Balance to Reference Evapotranspiration, Earth Observation for Vegetation Monitoring and Water Management, (D'Urso, G., A. Jochum, and J.Moreno (ed.)), The American Institute of Physics, 127-137.

Allen, R.G., Tasumi, M. and Trezza, R., 2007a. Satellite-based energy balance for mapping evapotranspiration with internalized calibration (METRIC) – Model, ASCE Journal of Irrigation and Drainage Engineering, 133(4), 380- 394.

Allen, R.G., Tasumi, M. Morse, A.T., Trezza, R., Kramber, W., Lorite I. and Robison, C.W., 2007b. Satellite-based energy balance for mapping evapotranspiration with internalized calibration (METRIC) – Applications, ASCE Journal of Irrigation and Drainage Engineering. 133(4), 395-406.

Allen, R.G., Tasumi, M., Morse, A., and Trezza, R., 2005a, A landsat-based energy balance and evapotranspiration model in Western US water rights regulation and Basin estimated from remote sensing measurements, Hydrological Processes, 15(9), 1585–1607.

Anderson, M.C., Norman, J.M., Mecikalski,J.R., Otkin J.A., and Kustas, W.P, 2007, A climatological study of evapotranspiration and moisture stress across the continental United States based on thermal remote sensing: 2. Surface moisture climatology, Journal of Geophysical Research 112(D11112, 1–13.

Asokan, S.M. and Dutta, D., 2008, Analysis of water resources in the Mahanadi River Basin, India under projected climate conditions, Hydrological processes, 22(18), 3589–3603.

Bastiaanssen, W. G. M., and Bos, M. G, 1999, Irrigation performance indicators based on remotely sensed data: a review of literature, Irrigation and Drainage Systems, 13(4), 291–311.

Bastiaanssen, W. G. M., Menenti, M., Feddes, R. A., and Holtslag, A. A. M., 1998a, A remote sensing surface energy balance algorithm for Land (SEBAL), Part 1: Formulation, Journal of Hydroogy, 212-213, 198–212.

Bastiaanssen, W. G. M., Noordman, E.J.M., Pelgrum, H., Davids, G., Thoreson, B.P., and Allen, R.G., 2005, SEBAL Model with Remotely Sensed Data to Improve Water-Resources Management under Actual Field Conditions, Journal of Irrigation and Drainage engineering, 131(1), 85-93.

Bastiaanssen, W. G. M., Pelgrum, H., Wang, J., Ma, Y., Moreno, J., Roerink, G. J., and Van der Wal, T., 1998b, The surface energy balance algorithm for land (SEBAL), Part 2: Validation." Journal of Hydroogy, 212-213, 213–229.

Bastiaanssen, W. G. M., Ud-din-Ahmed, M., and Chemin, Y., 2002, Satellite surveillance of water use across the Indus Basin, Water Resources Research, 38(12), 1273–1282.

Bastiaanssen, W.G.M. 2000. SEBAL-based sensible and latent heat fluxes in the irrigated Gediz Basin, Turkey. Journal of Hydrology, 229, 87-100.

Bastiaanssen, W.G.M., 1995, Regionalization of surface flux densities and moisture indicators in composite terrain. A remote sensing approach under clear skies in Mediterranean climates. 271, SC-DLO Report, Wageningen, The Netherlands.

Baumberger, L., Vincent, H., and Darkwah, S., 2007, Effect of GIS-Based Demand Allocation on Water Distribution System Modeling. Florida Water Resource Journal, December 2007, 15-19.

Brutsaert, W., 1982, Evaporation into the Atmosphere, Theory, History and Applications, 299, D. Reidel Hingham Mass.

Carlson, T.N., and Buffum, M.J., 1989, On estimating total evapotranspiration from remote surface temperature measurements. Remote Sensing of Environment, 29, 197–207.

Chander G., and Markham, B., 2003, Revised Landsat-5 TM radiometric calibration procedures and postcalibration dynamic ranges, IEEE Transactions on Geoscience and Remote Sensing, 41, 2674-2677.

Douglas, E. M., Jacobs, J. M., Sumner, D. M., and Ray, R. L., 2009, A comparison of models for estimating potential evapotranspiration for Florida land cover types. Journal of Hydrology, 373 (3-4), 366-376.

Duchon, K.K., Zieburtz, W.B. and Cornell, G.A., 1991, Use of Land Use Coefficients to Forescast Utility System Demand, Proceedings of 1991 Georgia water resource conference, March 1991.

Duffie, J.A., and W.A. Beckham. 1980, Solar Engineering of Thermal Process. John Wiley and Sons, New York.

Dziegielewski, B., and Chowdhury, F.J., 2008, Regional Water Demand Scenarios for Northeastern Illinois: 2005-2050, Project Completion Report, Southern Illinois University Carbondale, June 15, 2008.

Eckhardt, D. W., Verdin, J. P., and Lyford, G. R., 1990, Automated update of an irrigated lands GIS using SPOT HRV imagery, Photogrammetric Engineering & Remote Sensing 56, 1515–1522.

Farah, H. O., 2001, Estimation of regional evaporation under all sky conditions with satellite and routine weather data, PhD thesis, Wageningen University, The Netherlands.

Florida Automated Weather Network, University of Florida Extension, 2010, http://fawn.ifas.ufl.edu/ (Last accessed on June 10, 2010).

Garatuza-Payan, J., and Watts, C.J., 2005, The use of remote sensing for estimating ET of irrigated wheat and cotton in NorthwestMexico. Irrigation and Drainage Systems 19, 301–320.

Gowda, P. H., Chávez, J. L., Colaizzi,P. D., Evett,S. R., Howell,T. A., and Tolk,J. A., 2007, Remote sensing based energy balance algorithms for mapping ET: Current status and future challenges, Transactions of the ASABE , Vol. 50(5): 1639-1644.

Gowda, P.H., Howell, T.A., Chavez, J.L., Marek, T.H., and New, L.L., 2008a, Surface Energy Balance Based Evapotranspiration Mapping in the Texas High Plains. Sensors, 8, 5186-5201.

Gowda, P.H., Howell, T.A., and Allen, R.G., 2008b, Deriving hourly surface fluxes and ET from landsat thematic mapper data using METRIC. Pecora 17 – The Future of Land Imaging…Going Operational November 18 – 20, 2008 Denver, Colorado.

Hemakumara, H. M., Chandrapala, L., and Moene, A., 2003, Evapotranspiration fluxes over mixed vegetation areas measured from large aperture scintillometer." Agricultural Water Management, 58, 109–122.

Hook, J.E., Hoogenboom, G. and Paz,J., 2010, Agricultural Irrigation Water demand Georgia's Major and minor crops 2011 through 2050, University of Georgia.

Jacob, F., Olioso, A., Gu, X. F., Su, Z., and Seguin, B., 2002, Mapping surface fluxes using airborne visible, near infrared, thermal infrared remote sensing data and a spatialized surface energy balance model, Agronomie, 22, 669–680.

Jensen, M.E., 1969, Chapter IV: Plant and Irrigation Water requirements. USDA-ARS-SWC, Snake River Conservation Research Center, Kimberly, Idaho.

Kassam, A. H. and Doorenbos, J., 1979, Yield response to water, FAO Irrigation and Drainage Paper 33, Rome, Italy, 193.

Kite, G. W., and Droogers, P, 2000, Comparing evapotranspiration estimates from satellites, hydrological models and field data, Journal of Hydrology, 229(1-2), 3–18.

Kohsiek, W., Meijninger, W., and de Bruin, H. A. R., 2002, Long range scintillometry. Proceedings of International Symposium on Boundary Layer Physics.

Kolm, K. E. and Case, H. L., III, 1984, 'The identification of irrigated crop types and estimation of acreages from Landsat imagery', Journal of Photogrammetric Engineering and Remote Sensing, 50, 1479–1490.

Kramber, W.J., Morse, A., Allen, R.G., and Trezza, R., 2008, Landsat thermal data for water resources management in Idaho. ASPRS 2008 Annual Conference Portland, Oregon. April 28 - May 2, 2008.

Kustas, W.P., Norman, J.M., 1996, Use of remote sensing for evapotranspiration monitoring over land surface, IAHS Hydrological Sciences Journal, 41, 495–516.

Lagouarde, J. P., Jacob, F., Gu, X. F., Olioso, A., Bonnefond, J. M., Kerr, Y. H., McAneney, K. J., and Irvine, M., 2002, Spatialization of sensible heat flux over a heterogeneous landscape, Agronomie, 22, 627–633.

Leica Geosystems, 2008, http://gi.leica-geosystems.com/documents/pdf/SML.pdf (last accessed on June 10, 2010).

Lin, L., Zhihao, Q., and Li, J., 2008, Mapping the Irrigation of winter wheat farmland in North China Plain using MODIS remote sensing data. The International Archives of the Photogrammetry, Remote Sensing and Spatial Information Sciences. Vol. XXXVII. Part B4.

Martinez-Beltran, C. and Calera-Belmonte, A., 2001, Irrigated crop estimation using Landsat TM imagery in La Mancha, Spain, Photogrammetric Engineering & Remote Sensing, 67, 1177–1184.

Markham, B. L., and Baker, J. L., 1986, Landsat MSS and TM Post-Calibration Dynamic Ranges, Atmospheric Reflectance and At-Satellite Temperatures, pp.3-7. Laboratory for Terrestrial Physics-NASA/Goddard Space Flight Center, Greenbelt, MD. 20771.

Morse, A., Tasumi, M., Allen, R. G., and Kramber, W. J., 2000, "Application of the SEBAL methodology for estimating consumptive use of water and streamflow depletion in the Bear River basin of Idaho through remote sensing." Final Rep., Phase I, Submitted to Raytheon Systems, Earth Observation System Data and Information System Project, by Idaho Dept. of Water Resources and Univ. of Idaho planning. Irrigation and Drainage Systems 19, 251–268.

National Climatic Data Center (NCDC), NOAA-NCDC, http://www4.ncdc.noaa.gov (last accessed on June 15, 2010).

Natural Resource Conservation Service, USDA, 2008, http://datagateway.nrcs.usda.gov/GDGOrder.aspx (last accessed on July 9, 2010).

National Park Service, 2009, AlaskaPak v2.2 for ArcGIS 9.x, http://science.nature.nps.gov/nrgis/applications/gisapps/gis_tools/8x/alaskapak.aspx (last accessed on June 25, 2010).

Nemani, R.R., White, M.A., Thornton, P., Nishida, K., Reddy, S., Jenkins, J. and Running, S.W., 2002, Recent trends in hydrologic changes have enhanced the carbon sink in the United States,Geophysical Research Letter 29 (10) (2002), 1468.

Paulson, C.A, 1970, The mathematical representation of wind speed and temperature profiles in unstable atmospheric surface layer, Applied meteorology, 96, 587-861.

Pelgrum, H., and Bastiaanssen, W. G. M., 1996, An intercomparison of techniques to determine the area-averaged latent heat flux from individual in situ observations: A remote sensing approach using EFEDA data, Water Resources Research, 32(9), 2775–2786.

Penman, H.L, 1948, Natural evaporation from open water, bare soil and grass, Proceedings of the Royal Society of London, A193, 120-146.

Roerink, G. J., 1995, SEBAL estimates of the areal patterns of sensible and latent heat fluxes over the HAPEX-Sahel grid, a case study on 18 September 1992, DLO-Staring Centre Interne Mededeling 364, Alterra, Wageningen.

RoerinkRoerink, G.J., Bastiaanssen, W.G.M., Chambouleyron, J. and Menenti, M., 1997, Relating crop water consumption to irrigation water supply by remote sensing. Water Resour. Manag, 11 (6), 445–465.

Rosema, A., Verhees, L., Putten, E., Gielen, H., Lack, T., Wood, J., Lane, A., Fannon, J., Estrela, T., Dimas, M., Bruin, H., Moene, A., and Meijninger, W., 2001, European energy and water balance monitoring system final report April 2001. The European Community Fourth Framework Program for Research, Technological Development and Demonstration in The Field of Environment and Climate, Theme 3, Space Techniques Applied to Environmental Monitoring and Research Area 3.1.2: Pilot Projects, ENV4-CT97-0478, Scientific Report.

Rundquist, D. C., Hoffman, R. O., Carlson, M. P., and Cook, A. E., 1989, The Nebraska Center-Pivot Inventory: An example of operational satellite remote sensing on a long-term basis', Photogrammetric Engineering & Remote Sensing, 55, 587–590.

Schmugge, T. J., Jacob, F., French, A., and Kustas, W. P., 2003, Surface flux estimates with ASTER thermal infrared data, ASTER Workshop.

Seguin, B., Courault, D., and Gu´erif, M., 1994, Surface temperature and evapotranspiration: application of local scale methods to regional scales using satellite data. Remote Sensing of Environment, 49, 287–295.

Singh, R. K., Irmak, A., Irmak, S., and Martin, D.L., 2008, Application of SEBAL Model for Mapping Evapotranspiration and Estimating Surface Energy Fluxes in South-Central Nebraska, Journal of Irrigation and Drain Engineering, 134, 273.

Stisen, S., Jensen, K.H., Sandholt, I., and Grimes, D.I.F., 2008, A remote sensing driven distributed hydrological model of the Senegal River basin, Journal of Hydrology, 354, 131–148.

Sumner, D.M., and Jacobs, J.M., 2005, Utility of Penman–Monteith, Priestley–Taylor, reference evapotranspiration, and pan evaporation methods to estimate pasture evapotranspiration. Journal of Hydrology, 308, 81–104.

Tasumi M., and Allen, R. G., 2007, Satellite-based ET mapping to assess variation in ET with timing of crop development, Agricultural Water Management, 88 (1-3), 54-62.

Tasumi, M., Allen, R. G., Trezza, R., and Wright, J. L., 2005a, Satellite-based energy balance to assess withinpopulation variance of crop coefficient curves, ASCE Journal of Irrigation and Drainage Engineering, 131(1), 94-109.

Tasumi, M., Trezza, R., Allen, R.G. and Wright, J. L., 2005b, Operational aspects of satellite-based energy balance models for irrigated crops in the semi-arid U.S. Irrigation and Drainage Systems, 19, 355-376.

Teixeira, .H. de C., Bastiaanssen, W.G.M., Ahmad, M.D., and Bos, M.G., 2009, Reviewing SEBAL input parameters for assessing evapotranspiration and water productivity for the Low-Middle Sao Francisco River basin, Brazil: Part A: Calibration and validation, Agricultural and Forest Meteorology, 149 (3-4), 462-476.

The World Bank, World Development Report 1992: Development and the Environment. Oxford University Press, New York.

Trezza, R., 2006a, Estimation of Evapotranspiration from Satellite-Based Surface Energy Balance Models for Water Management in the Rio Guarico Irrigation System, Venezuela, AIP Conference. Proceedings, 852, 162-169.

Trezza, R., 2006b, Evapotranspiration from a Remote Sensing Model for Water Management in an irrigation system in Venezuela, Interciencia, 31(6), 417-423.

USGS, 2009, http://glovis.usgs.gov/ (last accessed on March 10, 2010).

USGS- Hydrologic Data Web Portal (HDWP), 2007, http://dataport.er.usgs.gov/et.html (last accessed on June 10, 2010).

Van den Kroonenberg, A., 2003, Surface flux estimates over an olive yard: SEBAL method applied to NOAA-KLM and Landsat-7, MS thesis, Wageningen University, Department of Meteorology.

Water Forum Agreement, 2000, Methodology and Assumptions used to access 2030 demand - January 2000, 336-344. http://www.waterforum.org/PDF/APPEN_B.PDF last accesed on February 21, 2009.

Waters, R., Allen, R., Tasumi, M., Trezza, and R., Bastiaanssen, W.G.M., 2002, SEBAL Surface Energy Balance Algorithms for Land, Idaho implementation, Advance Training and Users Manual, Department of Water Resources: Boise, ID, USA, 2002.

Webb, E.K., 1970, Profile relationships: the log-linear range, and extension to strong stability. Quarterly Journal of the Royal Meteorological Society, 96, 67-90.

Wiebe, Keith and Noel Gollehon, 2006, Agricultural Resources and Environmental Indicators, 2006 Edition, USDA Economic Bulletin (EIB-16), July 2006.

Wieringa, J., Davenport, A.G., Grimmond, C.S.B., and Oke, T.R., 2001, New Revision of Davenport Roughness Classification. Proceedings of the 3rd European & African Conference on Wind Engineering, Eindoven, Netherlands, July 2001, 8.

Whitman Hydro Planning Associates, 2007, Water Demand Scenarios to 2050 for 15- County East Central Illinois Region, http://www.isws.illinois.edu/iswsdocs/wsp/ppt/Methodology62907.pdf (last accessed on July 24, 2009).

Wood, E. F., and Lakshmi, E., 1993, Scaling water and energy fluxes in climate systems: Three land-atmospheric modeling experiments, Journal of Climate, 6, 839−857.

Zhang J., Yanling Hu, Y., Xiao, X., Chen, P.,Han, S., Song, G., and Yu, G., 2009, Satellite-based estimation of evapotranspiration of an old-growth temperate mixed forest, Agricultural and Forest Meteorology, 149, 976–984.

CHAPTER 5

SUMMARY AND CONCLUSIONS

5.1 Summary and conclusions

The SEBAL model developed by Bastiaanssen (Bastiaanssen, 1998; Bastiaanssen et al., 2005) and modified by Allen et al. (Allen et al., 2002a; Allen et al., 2007a) was used to estimate plant water use from Wolf Bay watershed area and derive water demand factors for major irrigated crops in Wolf Bay watershed area. The water demand factors were used to project future irrigation water demand in Wolf Bay watershed area using projected land use and land cover (LULC) maps.

The objective was to assess the validity of the modified SEBAL model in the humid southeastern US, to quantify plant water use from irrigated areas based on plant water consumption and derive water demand factors to project future irrigation water demand projection under a variety of climatic conditions. Field measurement of ET data at USGS stations in Florida was used to validate ET estimates from the modified SEBAL. The validation results revealed that the modified SEBAL model is capable of estimating daily and seasonal ET with good accuracy. Since the model performed well in Florida, it is applied in another area with subtropical humid climate of southeast, southern Alabama. Polygons of irrigated areas were created and used to quantify volumetric ET or total plant water use in Wolf Bay watershed area during growing seasons from 2005-2008. Polygons of irrigated areas were created using high quality digital aerial photographs and modified using SEBAL parameters (albedo, NDVI, and

evaporative fraction). Water demand factors (mm per growing season) under wet, normal, and dry weather conditions for each major irrigated plant in Wolf Bay watershed area were derived from randomly sampled pixels of the irrigated crops and seasonal ET estimates from the modified SEBAL model. The water demand factor for each irrigated plant was used to project future irrigation water demand for years 2010, 2020, 2030, and 2040 under wet, normal, and dry weather conditions. The objectives of the study and conclusions based on the results of the study are described below:

5.1.1 Objective 1: Assess the validity of a modified surface balance algorithm for land (SEBAL) model in the humid southeastern US.

The energy-budget eddy covariance method (EBEC) ET at USGS stations were used to validate daily and monthly ET from the modified SEBAL model. The model performed well in terms of estimating and explaining variation in measured daily, monthly, and two-month ET at USGS stations. Daily ET were estimated with a root mean square error (RMSE) of 0.48 mm/day, % RMSE of 10%, mean bias error (MBE) of 0.05 mm, Nash-Sutcliffe efficiency coefficient (ENS) of 0.82, and coefficient of determination (R^2) of 0.83. Monthly ET was estimated with a RMSE of 16 mm, % RMSE of 16%, MBE of -2 mm, ENS of 0.77 and R^2 of 0.77. Two-month ET was estimated with a RMSE of 30 mm, % RMSE of 16%, MBE of -5 mm, ENS of 0.71 and R^2 of 0.73. Results of the instantaneous surface energy fluxes compared well with results from other studies. The model was able to capture ET from agricultural lands during dry and wet months. The results confirmed that plant water demand is higher during the dry versus wet years. Overall, the modified SEBAL model was found to be a good method that can be applied for ET or crop water use related studies in the humid southeastern US.

5.1.2 Objective 2: Quantify seasonal volumetric ET as an estimate of plant water use in Wolf Bay watershed area during selected wet and dry growing season (April-September) between 2005 and 2008 using remotely sensed data.

Seasonal plant water use from irrigated areas in Wolf Bay watershed area was quantified using the modified SEBAL ET estimation method. As actual ET is the water use by the plants, seasonal water use was quantified as total volumetric ET from irrigated areas during the growing season. Monthly or two-month ET (depth) and total irrigated areas was multiplied to estimate volumetric ET during the period (monthly or two-month period). Volumetric ET from monthly or two-month period during the growing season was summed to quantify total seasonal plant water use in Wolf Bay watershed area for a given year. Total water use from irrigated area during growing seasons of 2005, 2006, 2007, and 2008 were 5.91, 6.26, 6.87, and 6.59 in million cubic meters, respectively. Seasonal plant water use was 6.41 million cubic meters or 4.64 million gallons per day (MGD), on average, in terms of volume as total irrigated areas multiplied by average seasonal ET (depth) from irrigated area. One of the findings of the study was confirmation that ET and resulting water demand from dry growing seasons was higher than from wet growing seasons. Monthly ET at Agricultural Weather Information service (AWIS) weather stations was found in good agreement with fluctuations of potential and pan ET. Comparison of monthly ET with monthly water withdrawals from golf courses showed positive linear relationship indicating that higher water withdrawal is associated with higher water use or ET.

5.1.3 Objective 3: Derive water demand factors (mm per growing season) for major irrigated plants in Wolf Bay watershed area using remotely sensed data to project irrigation water demand.

Water demand factors for each major irrigated plant in Wolf Bay watershed area were estimated as average seasonal ET from randomly sampled pixels of the irrigated plant. Water

demand factor for each plant were higher during the dry growing season, indicating that more water was applied to fulfill crop water requirement during the dry years. Corn was found to have highest water demand factor followed by cotton, soybeans, peanuts, and seed sod grass. Estimated water demand factors for dry year were 698, 647, 613, 614, 593, 665 mm for corn, cotton, soybeans, peanuts, seed/sod grass, and golf courses, respectively. Estimated water demand factors for wet year were 629, 585, 573, 565, 554, 499 mm for corn, cotton, soybeans, peanuts, seed/sod grass, and golf courses, respectively. Estimated water demand factors for normal year were 645, 636, 577, 593, 560, 631 mm for corn, cotton, soybeans, peanuts, seed/sod grass, and golf courses, respectively. This result indicates that water managers should allocate a higher rate of irrigation water application in expectation of during dry seasons in the future.

Projected landuse and land cover (LULC) projection map of Wolf Bay watershed area for years 2010, 2020, 2030, and 2040 were utilized to project future irrigation water demand for dry, normal and wet precipitation conditions based on two assumptions 1) most of the crop lands in Wolf bay watershed area are converted into golf courses and turf farms (future scenario of crop land area was developed) and 2) 100% of agricultural land is irrigated by 2040. Total projected irrigation water demand is estimated as sum of projected irrigation water demand from each major irrigated plant in Wolf Bay watershed area. Projected irrigation water demand is higher during dry years than in wet years. It was estimated that irrigation water demand will be increased from 2010 to 2040 (6.19 to 9.82 million cubic meters for wet year, 6.76 to 11.12 million cubic meters for dry year, and 6.45 to 10.52 million cubic meters for normal year. The estimates of projected irrigation water demand can be used by planners to manage water resources in Wolf Bay watershed area. It was found that remote sensing methods is useful in

estimating ET for plant water use and deriving water demand factor for projection of future water demand without the need for detailed ground survey data.

A case study was presented to describe how the method used in this study can be used to project future water demand at a watershed scale. Public and private-supplied water demand was estimated using population projections and per capita water uses. Total water demand (sum of public, private-supplied, and irrigated water demand) in Wolf Bay watershed area was estimated for years 2010, 2020, 2030, and 2040 under wet, normal and dry climatic conditions. Total water demand in Wolf Bay watershed area was higher for dry years then in wet years, as expected. Projected water demand in Wolf Bay watershed area ranged from 9.99 to 10.93, 15.60 to 16.84, 20.15 to 22.59, and 24.36 to 27.36 in million cubic meters for years 2010, 2020, 2030, and 2040, respectively. Planners can use projected water demand in Wolf Bay watershed area to manage water resources in the Wolf Bay watershed area in future.

5.2 Recommendations for future research

Based on the findings of this research and discussions in previous chapters the following future studies are recommended:

1. Validate instantaneous surface energy fluxes from the model with field measurement to assess the accuracy of the modified SEBAL model. Validation of instantaneous surface energy fluxes was not performed in this study as field measurement data was not available. Use SEBAL model application at a site where ground measured surface energy fluxes data are available to further assess the accuracy of the model.

2. Integrate high temporal resolution satellite images with low temporal resolution satellite images to provide more images for each season to increase the accuracy of model results. The integration of different satellite imagery is important because currently, most satellite

images with higher spatial resolution have relatively low temporal resolution. For example, Landsat 5 TM has spatial resolution of 30 m but temporal resolution of 16 days, while images with lower spatial resolution have higher temporal resolution. For example NOAA-AVHRR (Advanced very high resolution radiometer) satellite image has spatial resolution of 1 km but temporal resolution of at least one day. SEBAL derived parameters such as surface albedo, land surface temperature, emissivity, normalized difference vegetation index from higher resolution image may be useful in dividing 1 km temporal resolution of NOAA-AVHRR or other low spatial resolution satellite images into high resolution pixels. Aerial imagery or ground information data may also be utilized for this purpose.

3. Relate ET with water withdrawal and precipitation for modeling future irrigation water demand projection. In this study, a 70% of irrigation efficiency was assumed. However, in future the efficiency may be increased due to the advancement of the technology which may increase the errors in projected irrigation water demand. As an alternative, the actual water withdrawal data can be related to actual ET from the irrigated fields to drive empirical models that can be applied to project future irrigation water withdrawal from SEBAL derived water demand factors.

4. Estimation of ET using SEBAL model or any other remote sensing method can be tedious and time consuming. Other parameters derived during SEBAL process such as surface albedo, land surface temperature, emissivity, normalized difference vegetation index may be used an as alternative for ET estimation. A future research question can be, do we need perform the entire whole SEBAL analysis if surface albedo, land surface temperature,

emissivity, normalized difference vegetation index information is readily available or easily estimated?

5. The modified SEBAL model can be useful in land use and land cover (LULC) classification studies. SEBAL derived ET can be related to other SEBAL derived parameters such as surface albedo, land surface temperature, emissivity, normalized difference vegetation index, net surface radiation, soil heat flux, sensible heat flux, and latent heat flux to derive specific coefficient for different land use types.

References

Aase, K., and Pikul Jr, J.L., 2000, Water use in a modified summer fallow system on semiarid northern Great Plains, Agricultural water management, 43, 2000, 354–357.

Abreu, L.W. and Anderson, G.P. (Ed.), 1996, The MODTRAN 2/3 report and LOWTRAN 7 MODEL, Ontar Corporation, MA.

Abuzar, M., McAllister, A., and Morris, M., 2001, Classification of seasonal images for monitoring irrigated crops in a salinity affected area of Australia, International Journal of Remote Sensing, 22, 717–726.

Ahmad, M. D., Biggs, T., Turral, H., Scott, C.A., 2006, Application of SEBAL approach and MODIS time-series to map vegetation water use patterns in the data scarce Krishna river basin of India. Water Science & Technology, 53 (10), 83-90.

Ahmad, M.D., Magagula, T.F., Love, D., Kongo, V., Mul, M.L. and Kinoti, Jeniffer. 2005. Estimating actual ET through remote sensing techniques to improve agricultural water management: A casse study in the transboundary olifants catchment in the Limpopo basin, South Africa.

Alcamo J, Doll P, Kaspar F, Siebert S., 1997, Global Change and Global Scenarios of Water Use and Availability: An Application of Water GAP. Center for Environmental Systems Research (CESR), University of Kassel: Kassel.

Allen, R. G., Pereira, L. S., Raes, D., and Smith, M., 1998, Crop evapotranspiration, guidelines for computing crop water requirements, Irrigation and Drainage , 56, 30, FAO, Rome.

Allen, R., Waters, R., and Bastiaanseen, W.G.M., 2002, SEBAL Expert training, Idaho State University, August 19, 2002.

Allen, R., Waters, R., Bastiaanseen, W.G.M., 2002, SEBAL Expert training, The University of Idaho and the Idaho Department of Water Resources, Idaho State University, August 19-23, 2002.

Allen, R.G, Tasumi, M, Morse, A., and Trezza, R., 2005a, A Landsat-based energy balance and evapotranspiration model in Western US water rights regulation and planning, Journal of Irrigation and Drainage Systems, 19 (3-4), 251-268.

Allen, R.G. and Pruitt, W.O., 1986, Rational use of the FAO Blaney–Criddle formula, Journal of Irrigation and Drainage Engineering, ASCE 112(IR2), 139–155.

Allen, R.G., Tasumi, M. and Trezza, R., 2005b, Benefits from Tying Satellite-based Energy Balance to Reference Evapotranspiration, Earth Observation for Vegetation Monitoring and Water Management. (D'Urso, G., A. Jochum, and J.Moreno (ed.)). The American Institute of Physics, 127-137.

Allen, R.G., Tasumi, M. and Trezza, R., 2007a, Satellite-based energy balance for mapping evapotranspiration with internalized calibration (METRIC) – Model, ASCE journal of Irrigation and Drainage Engineering, 133(4), 380-394.

Allen, R.G., Tasumi, M. Morse, A.T., Trezza, R., Kramber, W., Lorite I. and Robison, C.W., 2007b, Satellite-based energy balance for mapping evapotranspiration with internalized calibration (METRIC) – Applications. ASCE journal of Irrigation and Drainage Engineering, 133(4), 395-406.

Almhab, A., Busu, I., and Cracknell, A. 2007. Comparison of regional evapotranspiration using NOAAAVHRR and LANDSAT-TM images: a case study in an arid area in the Sana'a basin, republic of Yemen, The 28th Asian Conference on Remote Sensing (ACRS) 2007P.N. 93, Kuala Lumpur, Malaysia.

Anderson, M.C., Norman, J.M., Mecikalski,J.R., Otkin J.A., and Kustas, W.P, 2007, A climatological study of evapotranspiration and moisture stress across the continental United States based on thermal remote sensing: 2. Surface moisture climatology, Journal of Geophysical Research 112(D11112), 1–13.

Baldocchi, D.D., Hicks, B.B., and Meyers, T.P., 1988, Measuring biosphere-atmosphere exchanges of biologically related gases with micrometeorological methods, Ecology, 69, 1331–1340.

Bastiaanssen, W. G. M., and Bos, M. G. 1999. Irrigation performance indicators based on remotely sensed data: a review of literature. Irrigation and Drainage Systems, 13: 291–311.

Bastiaanssen, W. G. M., Menenti, M., Feddes, R. A., and Holtslag, A. A. M., 1998a, A remote sensing surface energy balance algorithm for Land (SEBAL), Part 1: Formulation, Journal of Hydroogy, 212-213, 198–212.

Bastiaanssen, W. G. M., Noordman, E.J.M., Pelgrum, H., Davids, G., Thoreson, B.P. and Allen, R.G. 2005. SEBAL Model with Remotely Sensed Data to Improve Water-Resources

Management under Actual Field Conditions. Journal of Irrigation and Drainage engineering, 131 (1): 85-93

Bastiaanssen, W. G. M., Noordman, E.J.M., Pelgrum, H., Davids, G., Thoreson, B.P., and Allen, R.G., 2005, SEBAL Model with Remotely Sensed Data to Improve Water-Resources Management under Actual Field Conditions, Journal of Irrigation and Drainage engineering, 131(1), 85-93.

Bastiaanssen, W. G. M., Pelgrum, H., Wang, J., Ma, Y., Moreno, J., Roerink, G. J., and van der Wal, T., 1998b, The surface energy balance algorithm for land (SEBAL), Part 2: Validation." Journal of Hydroogy, 212-213, 213–229.

Bastiaanssen, W. G. M., Ud-din-Ahmed, M., and Chemin, Y., 2002, Satellite surveillance of water use across the Indus Basin, Water Resources Research, 38(12), 1273–1282.

Baumberger, L., Vincent, H., and Darkwah, S., 2007, Effect of GIS-Based Demand Allocation on Water Distribution System Modeling. Florida Water Resource Journal, December 2007, 15-19.

Blaney, H.F. and Criddle, W.D., 1950, Determining water requirements in irrigated areas from climatological and irrigation data, USDA Soil Conservation Service Technical Paper, 96, 48.

Bosch, J.M., and Hewlett, J.D., 1982, A review of catchment experiments to determine the effect of vegetation changes on water yield and evapotranspiration, Journal of Hydrology, 55, 3–23.

Cai, X., McKinney, D.C., Rosegrant, M.W., 2001, Sustainability Analysis for Irrigation water Management: Concepts, Methodology, and Applications to the Aral Sea area. Environment and Production Technology Division Dscussion paper no. 86. International Food Policy Research Institute, Washington D.C.

Calder, I.R., Narayanswamy, M.N., Srinivasalu, N.V., Darling, W.G., and Lardner, A.J., 1986, Investigation into the use of deuterium as a tracer for measuring transpiration from eucalyptus, Journal of Hydrology, 84, 345–351.

Chen, Y. H., Li, X.B., and Shi, P.J., 2001, Estimation of regional evapotranspiration over Northwest China using remote sensing, Journal of Geographical Sciences, 11 (2), 140-148.

Cuenca, R.H., Stangel, D.E., Kelly, S.F., 1997, Soil water balance in a boreal forest, Journal of Geophysical Research, D4, 29355–29365.

Daamen, C.C., Simmonds, L.P., Wallace, J.S., Laryea, K.B., Sivakumar, M.V.K, 1993, Use of microlysimeters to measure evaporation from sandy soils, Agriculture and Forest Meteorology, 65, 159–173.

Denmead, O.T., Dunin, F.X., Wong, S.C., and Greenwood, E.A.N, 1993, Measuring water use efficiency of eucalypt trees with chambers and micrometeorological techniques, Journal of Hydrology, 150, 649–664.

Doorenbos, J., and Pruitt, W.O., 1977, Crop water requirements, Irrigation and Drainage, 24, 14, FAO, Rome.

Duchon, K.K., Zieburtz, W.B. and Cornell, G.A., 1991, Use of Land Use Coefficients to Forescast Utility System Demand, Proceedings of 1991 Georgia water resource conference, March 1991.

Dziegielewski, B., and Chowdhury, F.J., 2008, Regional Water Demand Scenarios for Northeastern Illinois: 2005-2050, Project Completion Report, Southern Illinois University Carbondale, June 15, 2008.

Eastham, J., Rose, C.W., Cameron, D.M., Rance, S.J., and Talsma, T., 1988, The effect of tree spacing on evaporation from an agroforestry experiment, Agriculture and Forest Meteorology, 42, 355–368.

Eckhardt, D. W., Verdin, J. P., and Lyford, G. R., 1990, Automated update of an irrigated lands GIS using SPOT HRV imagery, Photogrammetric Engineering & Remote Sensing 56, 1515–1522.

Edwards, W.R.N., 1986, Precision weighing lysimetry for trees, using a simplified tared-balance design. Tree Physiology, 1, 127–144.

Fangmeier, D.D., Elliot, W.J., Workman, S.R., Huffman, R.L., and Schwab, G.O. (eds.), 2005, Soil and Water Conservation Engineering, Delmar Publishers Inc.

FAO, 1998, Crop evapotranspiration - Guidelines for computing crop water requirements, FAO Irrigation and Drainage Papers - 56, http://www.fao.org/docrep/x0490e/x0490e0c.htm#TopOfPage (last accessed on July 28, 2010).

FAO, 2009, http://www.fao.org/docrep/X0490E/x0490e04.htm (last accessed on April 16, 2009).

Farah, H. O., 2001, Estimation of regional evaporation under all sky conditions with satellite and routine weather data, PhD thesis,Wageningen University, The Netherlands.

Farahani, H.J., and Bausch, W.C., 1995, Performance of evapotranspiration models for maize- bare soil to closed canopy, Transactions of ASAE, 38,1049–1059.

Fritschen, L.J., 1966, Evapotranspiration rates of field crops determined by the Bowen ratio method, Agronomy Journal, 58, 339–342.

Gowda, P.H., Howell, T.A. Allen, R.G., 2008b, Deriving hourly surface fluxes and ET from landsat thematic mapper data using METRIC. Pecora 17 – The Future of Land Imaging…Going Operational November 18 – 20, 2008 Denver, Colorado.

Gowda, P.H., Howell, T.A., Chavez, J.L., Marek, T.H., and New, L.L., 2008a, Surface Energy Balance Based Evapotranspiration Mapping in the Texas High Plains. Sensors, 8, 5186- 5201.

Hemakumara, H. M., Chandrapala, L., and Moene, A., 2003, Evapotranspiration fluxes over mixed vegetation areas measured from large aperture scintillometer, Agricultural Water Management, 58, 109–122.

Hou, L.G, Xiao,H.L., Si, J.H., Xiao, S.C., Zhou, M.X., and Yang, Y.G.,2010, Evapotranspiration and crop coefficient of Populus euphratica Oliv forest during the growing season in the extreme arid region northwest China, Agricultural Water Management, 97 (2), 351-356.

Jacob, F., Olioso, A., Gu, X. F., Su, Z., and Seguin, B., 2002, Mapping surface fluxes using airborne visible, near infrared, thermal infrared remote sensing data and a spatialized surface energy balance model, Agronomie, 22, 669–680.

Jaeger, L., Kessler, A., 1997, Twenty years of heat and water balance climatology at the Hartheim pine forest Germany, Agriculture and Forest Meteorology, 84, 25–36.

Jensen, M.E., 1969, Chapter IV: Plant and Irrigation Water requirements. USDA-ARS-SWC, Snake River Conservation Research Center, Kimberly, Idaho.

Jia, L., Xi, G., Liu, S., Huang, C., Yan, Y., and Liu, G., 2009, Regional estimation of daily to annual regional evapotranspiration with MODIS data in the Yellow River Delta wetland, Hydrology and Earth System Sciences, 13, 1775–1787.

Kalma, S.J., Thorburn, P.J., and Dunn, G.M., 1998, A comparison of heat pulse and deuterium tracing techniques for estimating sap flow in Eucalyptus trees, Tree Physiology, 18, 697–705.

Kang, S.Z., Zhang, L., Liang, Y.L., Hu, X.T., Cai, H.J., and Gu, B.J., 2002, Effects of limited irrigation on yield and water use efficiency of winter wheat in the Loess Plateau of China, Agricultural water management , 55, 203–216.

Kassam, A. H. and Doorenbos, J., 1979, Yield response to water, FAO Irrigation and Drainage Paper 33, Rome, Italy, 193.

Kite, G. W., and Droogers, P, 2000, Comparing evapotranspiration estimates from satellites, hydrological models and field data, Journal of Hydroogy, 229(1-2), 3–18.

Kohsiek, W., Meijninger, W., and de Bruin, H. A. R., 2002, Long range scintillometry. Proceedings of International Symposium on Boundary Layer Physics.

Kramber, W.J., Morse, A., Allen, R.G., Trezza, R., 2008, Landsat thermal data for water resources management in Idaho. ASPRS 2008 Annual Conference Portland, Oregon. April 28 - May 2, 2008.

Kramber, W.J., Morse, A., Allen, R.G., Trezza, R., 2008, Landsat thermal data for water resources management in Idaho. ASPRS 2008 Annual Conference Portland, Oregon. April 28 - May 2, 2008.

Lagouarde, J. P., et al., 2002, Spatialization of sensible heat flux over a heterogeneous landscape." Agronomie, 22, 627–633.

Law, B.E., Falge, E., Gu, L., Baldocchi, D.D., Bakwin, P., Berbigier, P., Davis, K., Dolman, A.J., Falk, M., Fuentes, J.D., Goldstein, A., Granier, A., Grelle, A., Hollinger, D., Janssens, I.A., Jarvis, P., Jensen, N.O., Katul, G., Mahli, Y., Matteucci, G., Meyers, T., Monson, R., Munger, W., Oechel, W., Olson, R., Pilegaard, K., Paw, K.T., Thorgeirsson, H., Valentini, R., Verma, S., Vesala, T., Wilson, K., and Wofsy, S., 2002, Environmental controls over carbon dioxide and water vapor exchange of terrestrial vegetation, Agriculture and Forest Meteorology, 113, 97-120.

Li, F.R., Zhao, S.L., and Geballe, G.T., 2000, Water use patterns and agronomic performance for some cropping systems with and without fallow crops in a semi-arid environment of northwest China, Agriculture, Ecosystems, and Environment,. 79, 129–142.

Lin, L., Zhihao, Q., Li, J., 2008, Mapping the Irrigation of winter wheat farmland in North China Plain using MODIS remote sensing data. The International Archives of the Photogrammetry, Remote Sensing and Spatial Information Sciences. Vol. XXXVII. Part B4.

Malek, E., Bingham, G.E., and McCurdy, G.D., 1990, Evapotranspiration from the margin and moist playa of a closed desert valley, Journal of Hydroogy, 120, 15–34.

Marella, R. L., Mokray, M.F., and Hallock-Solomon, M., 1998, Water Use Trends and Demand Projections in the Northwest Florida Water Management District, U.S. GEOLOGICAL SURVEY, Open-File Report 98-269.

Martinez-Beltran, C. and Calera-Belmonte, A., 2001, Irrigated crop estimation using Landsat TM imagery in La Mancha, Spain, Photogrammetric Engineering & Remote Sensing, 67, 1177–1184.

Melesse, A. M., Oberg, J., Nangia, V., Berri, O., and Baumgartner, D., 2006, Spatiotemporal dynamics of evapotranspiration at the Glacial Ridge prairie restoration in northwestern Minnesota, Hydrologial Processes, 20, 1451-1464.

Menenti, M., 2000, Chapter 17: Irrigation and drainage, Remote sensing in hydrology and water management, Springer, Berlin, 377–400.

Morse, A., Tasumi, M., Allen, R. G., and Kramber, W. J., 2000, "Application of the SEBAL methodology for estimating consumptive use of water and streamflow depletion in the Bear River basin of Idaho through remote sensing." Final Rep., Phase I, Submitted to Raytheon Systems, Earth Observation System Data and Information System Project, by Idaho Dept. of Water Resources and Univ. of Idaho planning. Irrigation and Drainage Systems 19, 251–268.

Morton, F. I., 1968, Evaporation and Climate: A Study in Cause and E€ect, Scienti®c Series no. 4. Inland Water Branch, Department of Energy, Mines and Resources, Ottawa.

Murray, R.S., Nagler, P.L., Morino, K., Glenn, E.P., 2009, An Empirical Algorithm for Estimating Agricultural and Riparian Evapotranspiration Using MODIS Enhanced Vegetation Index and Ground Measurements of ET. II. Application to the Lower Colorado River, U.S, Remote Sensing, 2009, 1, 1125-1138.

Musick, J.T., Ordie, R.J., Bobby, A.S., and Donald, A.D., 1994, Water-yield relationships for irrigated and dryland wheat in the U.S. southern plains, Agronomy Journal, 86, 980–986.

National Climatic Data Center (NCDC), NOAA-NCDC, http://www4.ncdc.noaa.gov/cgi-win/wwcgi.dll?wwDI~StnSrch~StnID~20004380 (last accessed on June 15, 2010).

Natural Resource Conservation Service, USDA,
http://datagateway.nrcs.usda.gov/GDGOrder.aspx (last accessed on July 9, 2010).

Nourbaeva, G., Kazama, S., Sawamoto, M., 2003, Assessment of Daily Evapotranspiration Using Remote Sensing Data, Environmental Informatics Archives, 1, 421-427.

Obermeyer, L., 2003, Technical Memorandum: Tualatin River Water Demand Projection. Montgomery Watson Harza

Ortega-Farias, S.O., Cuenca, R.H., and English, M., 1993, Hourly reference evapotranspiration by Bowen ratio and Penman methods. In: Allen, R.G., and Van Bavel, C.M.U. (Eds.), Management of Irrigation and Drainage Systems, Integrated Perspectives. ASCE, New York, 969–976.

Pelgrum, H., and Bastiaanssen, W. G. M., 1996, An intercomparison of techniques to determine the area-averaged latent heat flux from individual in situ observations: A remote sensing approach using EFEDA data, Water Resources Research, 32(9), 2775–2786.

Penman, H.L., 1948, Natural evaporation from open water, bare soil, and grass, Proceedings of the Royal Society, London, Set. A, 193, 120-145.

Ray, S. S., and Dadhwal, V. K.,2001, Estimation of crop evapotranspiration of irrigation command area using remote sensing and GIS, Agricultural Water Management, 49 (3),239-249.

Roerink, G. J., 1995, SEBAL estimates of the areal patterns of sensible and latent heat fluxes over the HAPEX-Sahel grid, a case study on 18 September 1992, DLO-Staring Centre Interne Mededeling 364, Alterra, Wageningen.

RoerinkRoerink, G.J., Bastiaanssen, W.G.M., Chambouleyron, J. and Menenti, M., 1997, Relating crop water consumption to irrigation water supply by remote sensing. Water Resour. Manag, 11 (6), 445–465.

Romaguera, M., Hoekstra, A.Y., Su, Z., Krol, M.S., and Aalama, M.S., 2010, Potential of Using Remote Sensing Techniques for Global Assessment of Water Footprint of Crops, Remote Sensing, 2010 (2), 1177-1196.

Rosa, C.W. and Sharma, M.L., 1984, Summary and Recommendations of the Workshop on "Evapotranspiration from plant communities", Agricultural Water Management, 8, 325-342.

Rosema, A., Verhees, L., Putten, E., Gielen, H., Lack, T., Wood, J., Lane, A., Fannon, J., Estrela, T., Dimas, M., Bruin, H., Moene, A., Meijninger, W., 2001, European energy and water balance monitoring system final report April 2001. The European Community Fourth Framework Programme for Research, Technological Development and Demonstration in The Field of Environment and Climate, Theme 3, Space Techniques Applied to Environmental Monitoring and Research Area 3.1.2: Pilot Projects, ENV4-CT97-0478, Scientific Report.

Rundquist, D. C., Hoffman, R. O., Carlson, M. P., and Cook, A. E., 1989, The Nebraska Center-Pivot Inventory: An example of operational satellite remote sensing on a long-term basis', Photogrammetric Engineering & Remote Sensing, 55, 587–590.

Sadeh, A., and Ravina, I., 2000, Relationships between yield and irrigation with low-quantity water—a system approach. Agricultural systems, 64, 99–113.

Schmugge, T. J., Jacob, F., French, A., and Kustas, W. P., 2003, Surface flux estimates with ASTER thermal infrared data, ASTER Workshop.

Soppe, R. W.; Bastiaanssen, W.; Keller, A.; Clark, B.; Thoreson, B.; Eckhardt, J.; Davids, G., 2006, Use of High Resolution Thermal Landsat Data to Estimate Evapotranspiration Within the Imperial Irrigation District in Southern California, American Geophysical Union, Fall Meeting 2006.

Senay, G.B. and Henebry, G., 2007, Evaluating Vegetation Evapotranspiration (VegET) Modeling Results in South Dakota, Proceedings of the Eastern South Dakota Water Conference, October 29–31, Sioux Falls, South Dakota.

Senay, G.B., Budde , M., Verdin J.P., and Melesse,A.M., 2007, A coupled remote sensing and simplified surface energy balance approach to estimate actual evapotranspiration from irrigated fields, Sensors, 7, 979-1000.

Singh, R. K., Irmak, A., Irmak, S., and Martin, D.L., 2008, Application of SEBAL Model for Mapping Evapotranspiration and Estimating Surface Energy Fluxes in South-Central Nebraska, Journal of Irrigation and Drain Engineering, 134, 273.

Smith, D.M. and Allen, S.J., 1996, Measurement of sap flow in plant stems, Journal of Experimental Botany, 47(305), 1833–1844.

Stisen, S., Jensen, K.H., Sandholt, I., and Grimes, D.I.F., 2008, A remote sensing driven distributed hydrological model of the Senegal River basin, Journal of Hydrology, 354, 131–148.

Sun, G., Noormets, A., Chen, J., and McNulty, S.G., 2008, Evapotranspiration estimates from eddy covariance towers and hydrologic modeling in managed forests in Northern Wisconsin, USA, Agricultural and forest Meteorology, 148, 257-267.

Swift Jr., L.W., Cunningham, G.B., and Douglass, J.E., 1988, Climate and hydrology. In: Swank,W.T., and Crossley Jr., D.A. (Eds.), Forest Hydrology and Ecology at Coweeta. Springer, New York.

Tasumi M., Allen, R. G., 2007, Satellite-based ET mapping to assess variation in ET with timing of crop development, Agricultural Water Management, 88 (1-3), 54-62.

Tasumi M., Trezza R., Allen R. G., and Wright, J. L., 2003, US validation tests on the SEBAL Model for Evapotranspiration via Satellite. 2003 ICID Workshop on Remote Sensing of ET for Large Regions, 17 Sept. 2003.

Tasumi, M., Allen, R. G., Trezza, R., and Wright, J. L., 2005, Satellite-based energy balance to assess within population variance of crop coefficient curves, ASCE Journal of Irrigation and Drainage Engineering, 131(1), 94-109.

Tasumi, M., Allen, R. G., Trezza, R., and Wright, J. L., 2005a, Satellite-based energy balance to assess within population variance of crop coefficient curves, ASCE journal of Irrigation and Drainage Engineering, 131(1), 94-109.

Tasumi, M., Trezza, R., Allen, R.G. and Wright, J. L., 2005b, Operational aspects of satellite-based energy balance models for irrigated crops in the semi-arid U.S. Journal of Irrigation and Drainage Systems, 19, 355-376.

The World Bank, World Development Report 1992: Development and the Environment. Oxford University Press, New York.

Thornthwaite, C.W., 1948, An approach toward a rational classification of climate, Geographical Review, 38, 55-94.

Trezza, R., 2006, Estimation of Evapotranspiration from Satellite-Based Surface Energy Balance Models For Water Management in the Rio Guarico Irrigation System, Venezuela, AIP Conference. Proceedings, 852, 162-169.

113

Tsouni, A., Kontoes, C., Koutsoyiannis, D., Elias, P., and Mamassis, N., 2008, Estimation of Actual Evapotranspiration by Remote Sensing: Application in Thessaly Plain, Greece, Sensors, 8, 3586-3600.

USGS, 2000, http://ga.water.usgs.gov/edu/wuir.html (last accessed on April 20, 2010).

Van Bavel, C.H.M., 1966, Potential evaporation: the combination concept and its experimental verification, Water Resources Research, 2, 455-467.

Van den Kroonenberg, A., 2003, "Surface flux estimates over an olive yard: SEBAL method applied to NOAA-KLM and Landsat-7," MS thesis, Wageningen Univ., Dept. of Meterology.

Van den Kroonenberg, A., 2003, Surface flux estimates over an olive yard: SEBAL method applied to NOAA-KLM and Landsat-7, MS thesis, Wageningen University, Department of Meteorology.

Viessman, W. and Lewis, G.L. 2002, Introduction to Hydrology fifth edition), chapter 1, 4-5.

Wang, H.X., Zhang, L., Dawes, W.R. and Liu, C.M., 2001, Improving water use efficiency of irrigated crops in the North China Plain—measurements and modeling, Agricultural water management, 48, 151–167.

Wang, J., Ma, Y., Menenti, M., Bastiaanssen, W. G. M., and Mitsuta, Y., 1995, The scaling up of land surface processes over a heterogeneous landscape with satellite observations, Journal of the Meteorological Society of Japan, 73(6), 1235–1244.

Water Forum Agreement, 2000, Methodology and Assumptions used to access 2030 demand - January 2000, 336-344, http://www.waterforum.org/PDF/APPEN_B.PDF, last accessed on February 21, 2009.

Waters, R., Allen, R., Tasumi, M., Trezza, R., Bastiaanssen, W.G.M., 2002, SEBAL Surface Energy Balance Algorithms for Land, Idaho implementation, Advance Training and Users Manual, Department of Water Resources: Boise, ID, USA, 2002.

Water Technology Center (WTC), 1983, Resource analysis and plan for efficient water management — a case study of MRBC command area, Gujarat, IARI Research Bulletin. WTC, IARI, New Delhi, 359.

Whitman Hydro Planning Associates, 2007, Water Demand Scenarios to 2050 for 15- County East Central Illinois Region,

http://www.isws.illinois.edu/iswsdocs/wsp/ppt/Methodology62907.pdf (last accessed on July 24, 2009).

Wiebe, Keith and Noel Gollehon, 2006, Agricultural Resources and Environmental Indicators, 2006 Edition, USDA Economic Bulletin (EIB-16), July 2006.

Wight, J.R., Hanson, C.L., and Wright, J.L., 1993, Comparing Bowen ratio-energy balance systems for measuring ET. In: R.G. Allen and C.M.U. Van Bavel, Editors, Management of Irrigation and Drainage Systems, Integrated Perspectives, ASCE, New York, 953–960.

Wilson, K.B., Hanson, P.J., Mulholland, P.J., Baldocchi, D.D., and Wullschleger, S.D., 2001, A comparison of methods for determining forest evapotranspiration and its components: sap-flow, soil water budget, eddy covariance and catchment water balance, Agricultural and forest Meteorology, 106, 153–168.

Wood, E. F., & Lakshmi, E., 1993, Scaling water and energy fluxes in climate systems: Three land-atmospheric modeling experiments, Journal of Climate, 6, 839−857.

Xu, C.Y., and Singh, V.P. ,1998, Dependence of evaporation on meteorological variables at different time-scales and intercomparison of estimation methods, Hydrological processes, 12, 429-442.

Zhang, L., Lemeur, R., and Goutorbe,J. P., 1995, A one-layer resistance model for estimating regional evapotranspiration using remote sensing data, Agricultural and Forest Meteorology, 77 (3-4), 241-261.

Appendices

Appendix A.1

Modified SEBAL method

Surface balance equation is based on the theory that incoming net solar radiation drives all energy exchanges on the earth's surface including evapotranspiration, as shown below:

$$[R_n = G + H + \lambda ET] \tag{1}$$

where; R_n (Wm^{-2}) represents the net surface radiation which is the actual amount of energy available at the surface. G (Wm^{-2}) represents the soil heat flux which is the rate of heat storage in the soil and vegetation. H (Wm^{-2}) represents the sensible heat flux which is the rate of heat loss to the air due to temperature difference. λET (Wm^{-2}) is the latent heat flux associated with ET.

1. Extraction of thematic information

Spectral radiance, reflectance, and surface albedo

Spectral radiance (L_λ) for each band is computed from the Digital Number (DN) of each pixel from equation 2 (Chander & Markham, 2003), and the spectral reflectivity (ρ_λ) for each band is derived from equation 3:

$$[L_\lambda = L_{MIN} + [DN \times (L_{MAX} - L_{MIN}) / 255] \tag{2}$$
$$[\rho_\lambda = \pi \times L_\lambda / (E_{SUN\lambda} \times \cos\theta \times dr)] \tag{3}$$

where; L_λ is spectral radiance at the sensor's aperture in Wm^{-2}Sr^{-1}μm^{-1}, $L_{MIN\lambda}$ and $L_{MAX\lambda}$ (Wm^{2}Sr^{-1}μm^{-1}) are calibration constants for each band (Chandar and Markham, 2003); $E_{SUN\lambda}$ is the mean solar expo-atmospheric irradiance (Wm^{-2}μm^{-1}), extraterrestrial radiation on horizontal surface for each band (Markham and Barker, 1986); $\cos\theta$ is the cosine of the solar incidence computed from sun elevation angle (β) where $\theta = (90 - \beta)$; and d_r is the inverse squared relative earth-sun distance in astronomical units, from the equation by Duffie and Beckham (1980): $d_r = 1 + 0.033$

cos [DOY × 2π / 365, where; DOY is the sequential day of the year; and (DOY × 2π/365) is in radians.

Surface albedo (α) defined as the fraction of solar radiation at a surface is computed using spectral reflectivity the equations below;

$$[\alpha_{toa} = \sum (\omega_\lambda \times \rho_\lambda)] \tag{4}$$
$$[\tau_{sw} = 0.75 + 2 \times 10^{-5} \times z] \tag{5}$$
$$[\alpha = (\alpha_{toa} - \alpha_{path\_radiance})/\tau_{sw}^2] \tag{6}$$

where; α_{toa} is the albedo at the top of the atmosphere, ω_λ, is the weighting coefficient (dimensionless) for each band (Markham and Barker, 1986); $\alpha_{path\_radiance}$ (dimensionless) is the broadband path radiance, assumed to be 0.03 (Bastiaanssen, 2000); τ_{sw} (dimensionless) is the one-way atmospheric transmissivity; and z is the elevation of the weather station in meters.

NDVI, emissivity, land surface temperature, outgoing and incoming solar radiation

Normalized Difference Vegetation Index (NDVI) and surface emissivity (ε_o) are computed using equation 7 and 8 below:

$$[NDVI = (\rho_4 - \rho_3)/(\rho_4 + \rho_3)] \tag{7}$$
$$[\varepsilon_o = 1.009 + 0.047 \times \ln(NDVI)] \tag{8}$$

where; ρ_4 is the reflectivity value in the near-infrared band; and ρ_3 is the reflectivity value in the red band. Calculating NDVI results in a range of values between -1 to +1 with values closer to 0 or below indicating no vegetation and values closer to +1 indicating higher amounts of productive vegetation.

Land surface temperature (T_s) at each pixel is computed from spectral radiance in band 6 from the following equations (Markham and Barker, 1986);

$$[T_{bb} = K_2/ \ln(K_1/L_6 + 1)] \tag{9}$$
$$[T_s = T_{bb}/\varepsilon_o^{0.25}] \tag{10}$$

where; L_6 is the spectral radiance of the thermal band (band 6) of the Landsat 5 TM image; T_{bb} is effective at-satellite temperature; and K_1 (607.76 $Wm^{-2}sr^{-1}\mu m^{-1}$) and K_2 (1260.56 $Wm^{-2}sr^{-1}\mu m^{-1}$) are constants for Landsat 5 TM (Markham and Barker, 1986).

NASA (2000) defines LST is the measure of heat of the surface on the Earth according to the satellite point of view. The surface could be ice and snow, water in the sea, the grass on the lawn, roof of the building or canopy of the forest. LST is different from the air temperature that is included in the daily weather report (NASA, 2000).

30 m resolution digital elevation models (DEM) from USGS are used to derive DEM corrected LST (T_{s_dem}) using a universal lapse rate of -6°C/1000 m from the equation below:

$$[T_{s\_dem} = T_s + (0.6/100) \times DEM] \tag{11}$$

The incoming shortwave radiation ($R_s\downarrow$) is assumed to be constant at each pixel during instantaneous image time and is computed from the equation below:

$$[R_s\downarrow = G_{sc} \times \cos\theta \times d_r \times \tau_{sw}] \tag{12}$$

where; G_{SC} (1367 Wm^{-2}) is a solar constant.

"Hot" and "Cold" Pixels

Identification of "Hot" and "Cold" Pixels is an important step in the SEBAL and METRIC models. The METRIC process is followed in this study in which a "Hot" Pixel is selected as a dry, bare agricultural field where ET is assumed to be 0 (Allan et. al, 2002a; Gowda et al., 2007; Gowda et al, 2008a; Gowda et al, 2008b; Trezza, 2006b; Waters et al., 2002; Conard et al., 2007). "Cold" and "Hot" pixels are identified manually using LST map and Land use and land cover map, aerial photos, and the Landsat 5 TM image used. The process is described in detail by Waters et al. (2002). The "Cold" pixel is selected as a wet, well-irrigated crop surface with full ground cover. The x and y coordinates for identified "Hot" and "Cold" pixels are

located and used for sensible heat flux (H) computation described later in this chapter. The surface temperature of the "Cold" pixel and atmospheric emissivity (ε_a) is used to estimate the incoming longwave radiation ($R_L\downarrow$) using the Stefan-Boltzmann equation (Allen et al., 2002a, Waters et al., 2002, Allen et al., 2007):

$$[R_L\downarrow = \varepsilon_a \times \sigma \times T_a^4] \tag{13}$$

where; T_a is the near surface temperature from "Cold" pixel temperature; ε_a is the atmospheric emissivity; and is calculated from one-way atmospheric transmissivity (τ_{sw}) using the equation derived by Bastiaanssen (1995):

$$[\varepsilon_a = 1.08 \times (-\ln \tau_{sw})^{.265}] \tag{14}$$

The outgoing longwave radiation ($R_L\uparrow$) at each pixel is computed from surface emissivity (ε_o) and surface temperature (T_s) images using the Stefan-Boltzmann equation:

$$[R_L\uparrow = \varepsilon_o \times \sigma \times T_s^4] \tag{15}$$

where; ε_o is surface emissivity (dimensionless), σ is the Stefan-Boltzmann constant (5.67×10^{-8} $Wm^{-2}K^{-4}$); and T_s is the surface temperature in Kelvin.

2. Surface Energy Balance

Net surface radiation (R_n)

Surface radiance balance equation is used to compute net surface radiation (R_n) at the satellite overpass time as below:

$$[R_n = (1-\alpha) R_s\downarrow + R_L\downarrow - R_L\uparrow - (1-\varepsilon_o) R_L\downarrow] \tag{16}$$

Soil heat flux (G)

Soil heat flux (G) is computed from the empirical equation derived by Bastiaanssen as shown in equation (Bastiaanssen et. al., 2000):

$$[G/R_n = T_s/\alpha (0.0038\alpha + 0.0074\alpha^2)(1 - .98NDVI^4)] \tag{17}$$

$$[G = (G/R_n) \times R_n] \tag{18}$$

The term G/R_n at 30m pixel level is computed first; net surface radiation image is used to compute soil heat flux image using equation 18. T_s of equation 17 is in degree Celsius.

Sensible heat flux (H)

The procedure used in modified SEBAL model (Allen et al., 2002a) is followed to estimate H. The equation used by SEBAL to compute H is:

$$[H = (\rho_{air} \times c_p \times dT_{air})/r_{ah}] \tag{19}$$

where; dT_{air} is the near surface temperature difference (K), ρ_{air} is the atmospheric air density, c_p is the specific heat of air at constant pressure (1004 $Jkg^{-1}K^{-1}$), and r_{ah} is the aerodynamic resistance to heat transport.

The aerodynamic resistance to heat transport (r_{ah}) is calculated by the following equations:

$$[u^* = k \times u_x/ \ln(Z_x/Z_{om})] \tag{20}$$
$$[r_{ah} = \ln (Z_2/Z_1)/(u^* \times k)] \tag{21}$$

where; u^* is friction velocity at each 30 m pixel; k is the Von Karman's constant (0.41); Z_1 (0.1 m) is the height above zero-plane displacement height of crop canopy; and Z_2 (2 m) is the below height of surface boundary layer; u_x is the wind speed (m s^{-1}) at the height Z_x (height of the anemometer, 10 m, for all FAWN stations in this study); Z_{om} is the momentum roughness length for each pixel as is defined as the form drag and skin friction for the layer of air that interacts with the surface (Waters et al., 2002).

Z_{om} for the vegetation around the weather station is empirically estimated from average vegetation height using the equation of Brutsaert (1982):

$$[Z_{om} = 0.12h] \tag{22}$$

0.1 m for canopy height of grass is used for the FAWN weather stations for this study. Similarly, height of grasses in USGS stations is also used. 0.1 m canopy height of grass is used

in other studies (Snyder et al., 2008; Druce et al., 1997; Douglas et al., 2009; Mengistu and MJ Savage, 2010).

Z_{om} for FAWN stations calculated from equation 21 is used to compute friction velocity (u*) for each FAWN station by using average wind velocity at the anemometer height (10 m) at the image capture time (discussed in 3.2.4) using equation 20. Computed u* at the weather station and wind speed at 200 m is assumed to be constant for all pixels and is computed using equation 20.

Z_{om} is computed for each pixel by using NDVI and surface albedo from equation 23 by Bastiaanssen (Bastiaanssen et. al., 2000) and modified by Allen (Allen et al., 2002a; Allen, 2007a; Teixeira et al., 2009):

$$[Z_{om} = \exp (a \times NDVI/\alpha + b)] \tag{23}$$

Correlation constants "a" and "b" are derived by plotting $\ln (Z_{om})$ against NDVI/ α for pixels representing vegetation, with assigned Z_{om} for each pixel (Z_{om} = 0.12 h, where h is the known vegetation height). The use of surface albedo (α) helps to distinguish between tall and short vegetation which have similar NDVI values. Generally, regression analysis of tall and short vegetation is done (Allen et al., 2002a; Waters et al., 2002; Allen et al., 2007). For this study canopy heights of tall vegetation at USGS and University of Florida weather sites are used as described by Douglas et al. (2009). In case the station with vegetation is not found in the image or is covered by clouds, Z_{om} for typical forests is used as 0.5 m (Allen et al., 2002a; Waters et al., 2002; Wieringa et al, 2001).

The friction velocity (u*) for each pixel is computed using wind speed at 200 m (u_{200}) from the equation below:

$$[u^* = k \times u_{200}/\ln(200/z_{om})] \tag{24}$$

The near surface temperature difference (dT) for each pixel is derived from a linear equation between dT and DEM corrected surface (T_{s_dem}):

$$[dT = b + a \times T_{s\_dem}] \tag{25}$$

The same two anchor pixels, "Hot" and "Cold", are used to derive correlation coefficients a and b. The surface temperature (T_s), net surface radiation (R_n), soil heat flux (G), and momentum roughness length (z_{om}) for both anchor pixels are recorded from the derived images.

Evapotranspiration at the "Hot" pixel is assumed to be zero; sensible heat flux at the "Hot" pixel (H_{hot}) is calculated as $H_{hot} = R_n - G$. ET at the "Cold" pixel is assumed to be 5% more than the reference ET (ET_{ref}) (Allan et. al, 2002a; Gowda et al., 2007; Gowda et al, 2008a; Gowda et al, 2008b; Trezza, 2006b; Conard et al., 2007) in METRIC model. Hence, H for the "Cold" pixel (H_{cold}) is calculated as: $H_{cold} = R_n - G - 1.05 \times \lambda ET_{ref}$.

Air densities (ρ_{air}) for "Hot" and "Cold" pixels are calculated using DEM corrected land surface temperature image (T_{s_dem}) as:

$$[\rho_{air} = P/(R \times T_{s\_dem})] \tag{26}$$

where; R is the Gas constant = 287.05 $J/kg^{-1}K^{-1}$, T is temperature in K, P is standard pressure: P = $101325 \times (1.0 - Z \times 0.0000225577) \times 5.2559$. Where Z =Elevation above sea level (m). Aerodynamic resistance to heat transport (r_{ah}) for both anchor pixels (r_{ah_hot} and r_{ah_cold}) is obtained from equation 21 and are used in equation 19 to derive dT for the "Hot" and "Cold" pixels (dT_{hot} and dT_{cold}) as:

$$[dT_{hot} = H_{hot} \times r_{ah\_hot} /(\rho_{hot} \times c_p)] \tag{27}$$
$$[dT_{cold} = H_{hot} \times r_{ah\_cold}/(\rho_{cold} \times c_p)] \tag{28}$$

The correlation coefficients, b and a, in the Equation 6 were computed by plotting dT_{hot} versus T_{S_hot} and dT_{cold} versus T_{s_cold}.

Air temperature (T_a) for each pixel is computed as: $T_a = T_s - dT$ with air density for each pixel derived from the T_a image. H for each pixel is computed using the derived dT, air density, and r_{ah} images from Equation 21.

To correct for buoyancy effects generated by surface heating processes, Monin-Obukhov theory is applied iteratively. The Monin-Obukhov length, L, is computed to define atmospheric stability conditions using the equation below:

$$[L = - (\rho \times c_p \times u*^3 \times T_s) / (k \times g \times H)] \qquad (29)$$

where; ρ is the density of air (kgm^{-2}), c_p is the air specific heat ($1004\ Jkg^{-1}k^{-1}$), u* is the friction velocity (ms^{-1}), T_s is the temperature (K), g is the gravitational constant ($9.81\ ms^{-2}$), k is the Von Karman's constant (0.41), and H is the sensible heat flux (Wm^{-2}).

According to the Monin-Obukhov theory, if L= 0, the atmosphere is considered neutral; if L< 0, the atmosphere is considered unstable (heat flow is away from the surface); and if L>0, the atmosphere is considered stable for buoyancy effects. Stability corrections for momentum and heat transport (Ψm and Ψh) are computed using the formulations by Paulson (1970) and Webb (1970).

Stability corrected value of the friction velocity (u*) and aerodynamic resistance (r_{ah}) are computed for each successive repetition using equations below:

$$[u* = [(u_{200} \times k)/\{\ln(200/z_{om}) - \Psi_{m(200m)}\}] \qquad (30)$$
$$[r_{ah} = \{\ln (Z_2/Z_1) - \Psi_{h(2m)} + \Psi_{h(0.1m)}\}/(u* \times k)] \qquad (31)$$

where; $\Psi_{m(200m)}$ is the stability correction for momentum transport at 200 m (for L<0 or L>0 conditions, $\Psi_{h(2m)}$ and $\Psi_{h(0.1m)}$ are the stability corrections for heat transport at 2 m and 1 m, $Z_1 = 0.1$ m and $Z_2 = 2$ m, and k is the Von Karman's constant.

New dT values for "Hot" and "Cold" pixels, and new values for correlation coefficients, b and a, were computed using the stability corrected r_{ah}. These values were subsequently used to

compute a new corrected H at each pixel level. A new stability correction is done using the corrected H image. These processes is repeated until successive values for dT_{hot} and r_{ah} at "Hot" pixel (r_{ah_hot}) are stabilized, meaning the change in r_{ah} at the "Hot" pixel is less than 5% (Allen et al., 2002a). A result of iteration method used for stabilization of r_{ah} at the "Hot" pixel during SEBAL analysis of Landsat 5 TM image of August 8, 2001 (Florida) and April 26, 2008 (Alabama) is shown in Appendix A.2 and A.3, respectively. The corrected value of H at each pixel is derived by using the corrected final dT and stability corrected r_{ah} image and Equation 19.

Latent Heat Flux (λET)

Latent heat flux (λET, Wm^{-2}) for the instantaneous time of the satellite overpass is computed at each pixel using equation 32 below:

$$[\lambda ET = R_n - G - H] \tag{32}$$

3. Instantaneous, daily and seasonal ET

The instantaneous ET (ET_{inst}, $mmhr^{-1}$) also defined as the ET at the time of the satellite overpass time is computed as:

$$[ET_{inst} = 3600 \times \lambda ET/\lambda] \tag{33}$$

where; λ is the latent heat of vaporization, calculated from the surface temperature image by

$$\lambda = [[2.501 - (0.002361 \times T_o)] \times 10^6] \tag{34}$$

where; T_o is surface temperature in degree Celsius.

Evaporative fraction (ET_rF) at each pixel level is computed using reference ET at the image time as:

$$[ET_rF = ET_{inst}/ET_{ref}] \tag{35}$$

where; ET_{ref} is the ASCE Penman-Monteith standardized form of reference ET ($mm\ hr^{-1}$) at the image time derived from REF-ET software (Allen et al., 2000b).

A Daily ET (ET$_{24}$) map is derived using the evaporative fraction (ET$_r$F) and cumulative 24-hour ET for the day of the image as:

$$[ET_{24} = ET_rF \times ET_{ref\_24}] \tag{36}$$

ET for a period (monthly or two-month) is calculated by computing cumulative reference ET for the period represented by the image processed as:

$$[ET_{period} = ET_rF \times \sum_{i=1}^{n} ET_{ref\_24i} \tag{37}$$

where; ET$_{ref\_24i}$ is the cumulative reference ET for the time period from REF-ET software, and n is the number of days used for ET extrapolation.

Assumptions used while estimating seasonal ET are: ET$_r$F computed for the time of image is constant for the entire period represented by the image, and ET for the entire area of interest changes in proportion to the change in ET$_{ref}$ at the weather station. For this study, ET calculation during growing season (April to September) is considered only for irrigation volume estimation. The growing season is divided into three periods; April-May, June-July, and August-September. An image is used to extrapolate either one month or two months depending on availability of image. For example, an image in April is used to extrapolate ET for the entire month. For Wolf Bay watershed study (Chapter 4), monthly and/or two-month ET maps during growing season are combined to create a seasonal ET map for the growing season of 2005-2008.

Appendix A.2

Summary of "Hot" and "Cold" Pixel analysis (Landsat 5 TM image of August 8, 2001 image, path/row: 17/40)

Table A.2.1 SEBAL estimated parameters for "Hot" and "Cold Pixel".

Pixel	ET_rF	T_s	Ts_dem	R_n	G	U_{200}	Z_{om}	r_{ah}	λET	H*	p_{air}	dT	Description
Cold Pixel	1.05	296	296	616	53	2.335	0.0537	62.76	552	11	1.18987	0.562	Wet peanuts field
Hot Pixel	0	312	312	501	104	2.335	0.005	80.88	0	397	1.12729	28.365	Fallow crop land

"Hot" Pixel Location= 29.108322 N, -82.391885 W (Elevation = 21 m)
"Cold" Pixel location = 29.335793 N, -82.171743 W (Elevation = 24 m)
Instantaneous ET_{ref} at the satellite overpass time was 0.77 mmhr^{-1} from REF-ET software.
* H for the "Cold" pixel = $R_n - G - 1.05 \lambda ET$, and H for the "Hot" pixel = $R_n - G$
ET_rF is unitless; T_s, Ts_dem, dT are in K; R_n,G, λET, H are in Wm^2; Z_{om} is m; r_{ah} is in s/m; U_{200} is in ms^{-1}; and p_{air} is in Jkg^{-1}K^{-1}
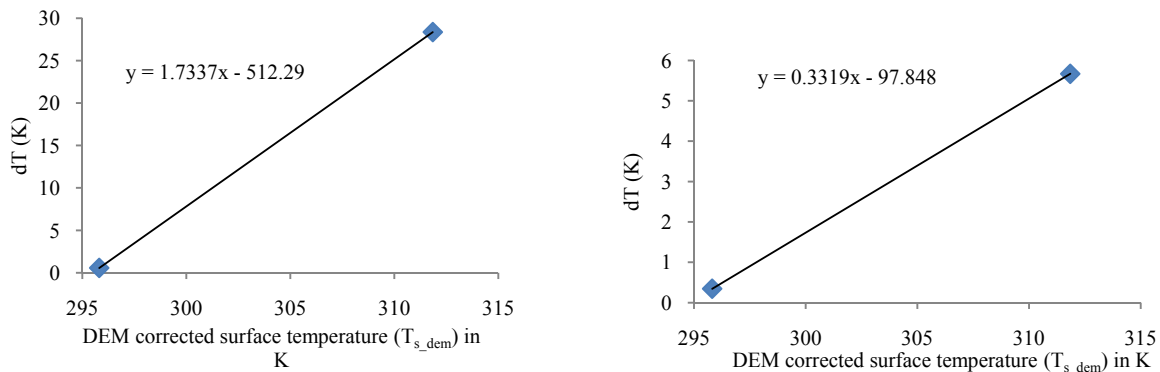
Figure A.1.1. dT versus T_{s_dem} for correlation coefficients "a" and "b" used in the modified SEBAL model using August 8, 2001 Landsat 5 TM image (left: 1st Iteration using values from Table A.1.1, right: after stabilization of r_{ah} at the "Hot" Pixel, Table A.2.2).

Table A.2.2. Results of iterations used in the modified SEBAL model to stabilize r_{ah} at the "Hot" pixel showing that the "Hot" pixel was stabilized (% change in r_{ah_hot} < 5%) after 8 iterations (August 8, 2001 Landsat 5 TM image).

a	b	r_{ah_cold}	dT_{cold}	r_{ah_hot}	dT_{hot}	% change (r_{ah_hot})
1.734	-512.290	62.757	0.562	80.875	28.365	
0.095	-27.909	25.612	0.337	5.003	1.755	-1517
0.574	-169.530	43.978	0.394	27.388	9.605	82
0.259	-76.223	35.681	0.319	12.742	4.469	-115
0.376	-110.850	39.312	0.352	18.193	6.381	30
0.318	-93.793	38.013	0.340	15.521	5.443	-15
0.343	-101.250	38.697	0.346	16.691	5.854	8
0.332	-97.848	38.535	0.345	16.162	5.668	-3

Appendix A.3

Summary of "Hot" and "Cold" Pixel analysis (Landsat 5 TM image of April 26, 2008 image, path/row: 20/39).

Table A.3.1 SEBAL estimated parameters for "Hot" and "Cold Pixel".

Pixel	ET_rF	T_s	Ts_dem	R_n	G	U_{200}	Z_{om}	r_{ah}	λET	H*	p_{air}	dT	Description
Cold Pixel	1.05	297	297	612	50	2.3	0.088	59.90	488	74	1.1831	3.73039	Wet peanuts field
Hot Pixel		319	319	419	112	2.3	0.005	82.11	0	306	1.1018	22.719	Fallow peanut field

"Hot" Pixel location = 30.445393 N, -87.516345 W (Elevation = 24 m)
"Cold" Pixel Location= 30.539392 N, -87.671777 W (Elevation = 39 m)
Instantaneous ET_{ref} at the satellite overpass time was 0.68 mmhr^{-1} from REF-ET software.
* H for the "Cold" pixel = $R_n - G - 1.05 \lambda ET$, and H for the "Hot" pixel = $R_n - G$
ET_rF is unitless; T_s, Ts_dem, dT are in K; R_n,G, λET, H are in Wm^2; Z_{om} is m; r_{ah} is in s/m; U_{200} is in ms^{-1}; and p_{air} is in Jkg^{-1}K^{-1}
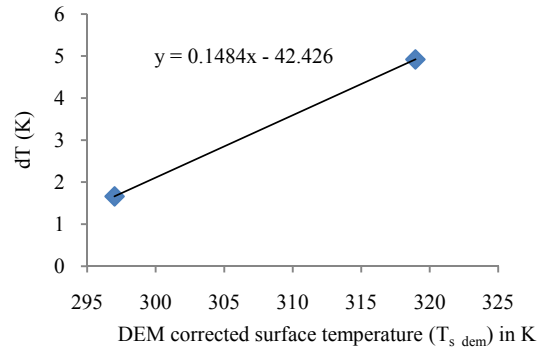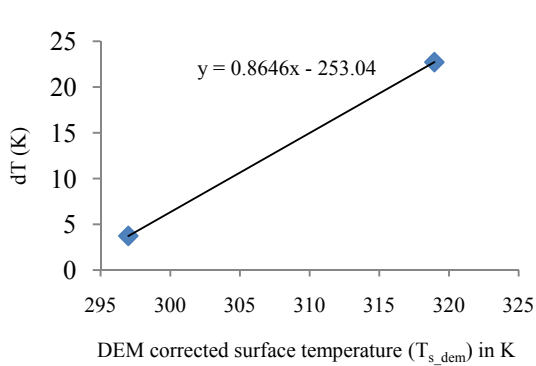
Figure A.3.1 . dT versus T_{s_dem} for correlation coefficients "a" and "b" used in the modified SEBAL model using April 26, 2008 Landsat 5 TM image (left: 1st Iteration using values from Table A.2.1, right: after stabilization of r_{ah} at the "Hot" Pixel, Table A.3.2).

Table A.3.2 Results of iterations used in the modified SEBAL model to stabilize r_{ah} at the "Hot" pixel showing that the "Hot" pixel was stabilized (% change in r_{ah_hot}< 5%) after 8 iterations (April 26, 2008 Landsat 5 TM image).

a	b	r_{ah_cold}	dT_{cold}	r_{ah_hot}	dT_{hot}	% change (r_{ah_hot})
0.865	-253.04	59.903	3.73039	82.1061	22.719	
0.036	-9.8838	13.429	0.83629	5.88736	1.6291	-1295
0.261	-75.288	35.115	2.18673	28.6088	7.9163	79
0.116	-32.976	23.164	1.44248	14.4118	3.9879	-9
0.167	-47.757	28.756	1.79073	19.714	5.455	27
0.143	-40.818	26.04	1.62161	17.203	4.7602	-13
0.153	-43.652	27.358	1.70372	18.279	5.0579	6
0.148	-42.426	26.677	1.66126	17.7865	4.9217	-3

Appendix B.1

Public water use and private-supplied water use study in Wolf Bay watershed area: methods used and results

1. Method used

1.1 Data Collection

   Public water use and private-supplied water use in Wolf Bay watershed area are quantified using water withdrawal data and population data from various sources. Water withdrawal data and population data used for the analysis are shown in Appendix B.2 (Table B.2.1).

1.2 Terminology Used

   For this study, the term "water use" and "water demand" are used as historical/current water use and future water use to be predicted, respectively. Three comparative categories of per capita water use (gallons per capita per day, GPCD) are presented:

   1. Gross per capita water use- Total water withdrawals divided by total population

   2. Gross per capita public water use – Total public water volume divided total population served by public water companies

   3. Per capita residential water use –gallons supplied per person (individual)

1. 3. Water Use categories to be quantified

   The two population based water use categories quantified in this section are,

1.3.1   Public water use – All water withdrawals by public water companies, including municipal irrigation of parks and city golf courses, and recreation areas are considered as a public water use.

1.3.2   Private-supplied water use – All non-irrigation private-supplied water withdrawals for domestic water use purpose are considered as private-supplied water use.

1.3.1 Public water use

Public water withdrawal data from companies providing public water in Wolf Bay watershed are obtained. GIS point shapefile of public water withdrawals from 1993 to 2008 is obtained from Alabama Department of Economic and Community Affairs (ADECA). Water withdrawal from three water companies: Elberta Water; Gulf Shores Water & Sewer; and Perdido Bay Water are extracted from ADECA water withdrawal data. Water withdrawal record (1983 to 2008) from Orange Beach Water & Sewer is obtained. For the City of Foley, water withdrawal records back to 1988 is obtained from Riviera Utilities, which is the largest public water purveyor in Wolf Bay watershed. In addition, detailed water rate structures and corresponding sales volumes from September 2008 to present are made available from Riviera Utilities. September 2008 to February 2010 water use data from Riviera Utilities are used to estimate average per capita residential water use.

Service area extents of water companies

The Service area extents of Elberta Water, Riviera Utilities, and Perdido Bay Water obtained in .jpg format from the respective water companies are digitized and rubber-sheeted into GIS format in ArcMap (Figure B.1.1). Public water companies within the Wolf Bay watershed boundary are Riviera Utilities, Elberta water, and a small portion of Perdido Bay water. However, the area covered by Perdido Bay water inside Wolf Bay boundary is mostly rural with no cities verified by National Land Cover dataset (NLCD) land use and land cover maps, and digital aerial orthoimages of 2006 and 2009 from Natural Resource Conservation Service (NRCS). Hence, for public water supply in the Wolf Bay watershed area, water supply from Riviera Utilities and Elberta water are considered.
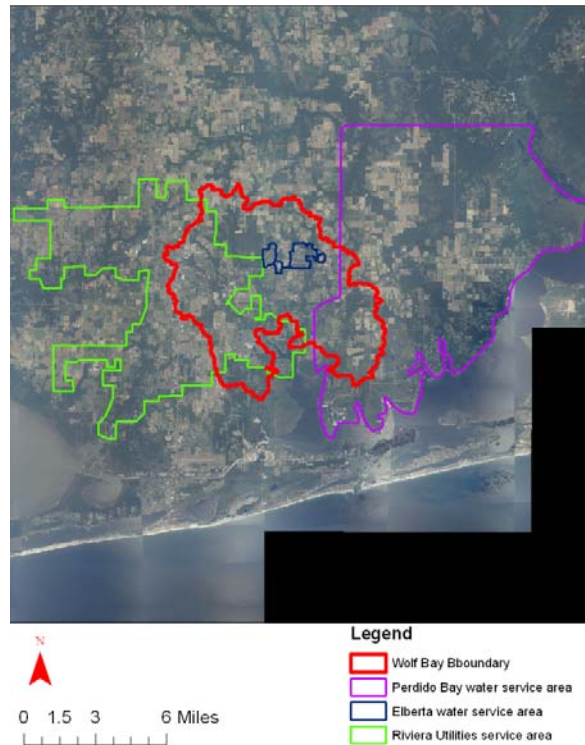
Figure B.1.1. Wolf Bay watershed boundary and service area extent of three water companies serving the area overlaid on NAIP 2009 aerial photo (Source: Riviera Utilities, Perdido Bay water, Elberta water, USDA NAIP).

GIS point shapefile of Water withdrawal data and source obtained from ADECA indicates that a total of six public well from public water companies are located inside the Wolf Bay watershed boundary which includes one well from Elberta Water, three wells from Riviera Utilities, and two wells from Orange Beach Water and Sewer. Though only three wells of Riviera Utilities are located inside the boundary of Wolf Bay watershed, water withdrawals from all wells are also considered for water use analysis for estimating water use coefficients, described later in next chapter. Though Orange Beach lies outside the boundary of Wolf Bay watershed, two wells of Orange Beach Water are located inside the boundary.

Population served by public water

Figure B.1.2 Shows that almost all of Foley is served by Riviera Utilities. Elberta population is served by Elberta water. Hence, total population of Foley and Elberta is considered as total population served by public water in Wolf Bay watershed area.

131
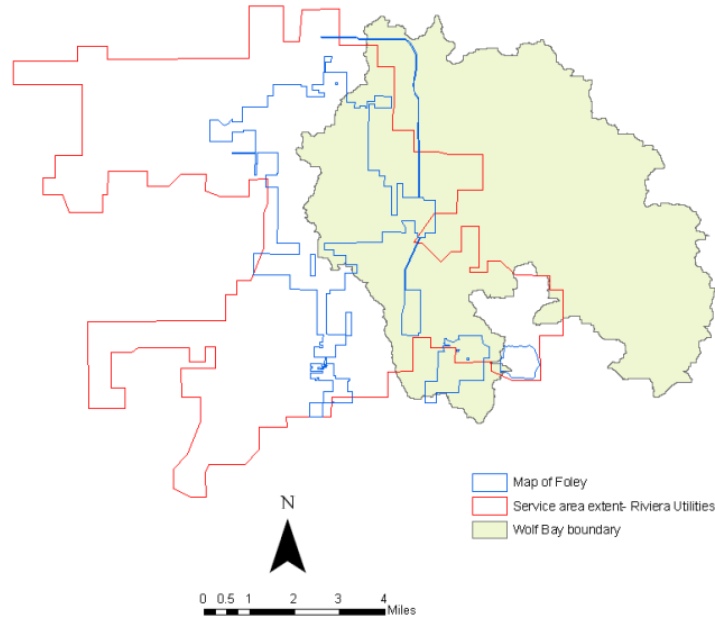
Figure B.1.2. Service area boundary of Riviera Utilities showing almost all portion of Foley is covered by it (Source: US Census Bureau for Foley city map, Riviera Utilities for service area extent).

Riviera Utilities water use per customer categories data are used to estimate the population served by Riviera Utilities (Appendix B.2, Table B.2.2). The number of meters for single-family residential customers is used to estimate single-family population served using average household size of 2.35 (US Census Bureau, 2000) and per capita residential water use (GPCD). The estimated per capita water use is used to estimate the population of multi-family residential served population by Riviera Utilities. The sum of the single and multi family served population is used as total public water served population by Riviera Utilities. The total public water served population is estimated on a monthly basis. The average monthly public water served population is assumed to be the annual public water served population for 2008 and 2009, which is used to estimate annual public water population served in 1990, 1980, and 1970. US census block level population data (1990 and 2000), boundary of Wolf Bay watershed (from Arc-SWAT), and city limits of Foley (1990 and 2000) are used to develop a GIS file of Wolf bay population in 1990 and 2000. GIS intersect function (Foley city limit and Wolf Bay boundary

population) is used to derive total Foley population within Wolf Bay boundary. Total population of Wolf Bay watershed area is derived as,

[Population in Wolf Bay watershed area excluding Foley population = Total Wolf Bay population – Foley population within Wolf Bay boundary]

[Total Wolf Bay population considering total population of Foley = Foley population (US census Bureau) + population in Wolf Bay excluding Foley population]

The population of Wolf Bay watershed between 1990 and 2008 is documented and interpolated as necessary using available population data for Baldwin County and included cities. The 10 year growth rate from 1990 to 2000 for Baldwin Country is 43% (US Census Bureau) whereas it is 83% for Wolf Bay watershed (estimated from US census block level population data). Consequently, a 4% incremental growth factor is added to the documented county growth rate to estimate annual growth rate and population for Wolf Bay watershed up to 2008. Population estimates of Wolf bay watershed area and population served by public water supply are shown in Appendix B.2 (Table B.2.3). The general population trend of Wolf Bay cities from 1970 up to the present is presented in Figure 1.1 (Chapter 1), which indicates increasing trend in Wolf Bay population since 1970.

Population-based water use coefficient for public water for public water demand projection

The per capita residential use for Foley is estimated from single-family served population and gallons sold to those customers by Riviera Utilities. This data is the best available for per capita water use estimation. Gross per capita public water use for Riviera Utilities is estimated using per capita residential use, single- and estimated multi-family residential population served (multi-family residential gallons sold divided by estimated per capita residential water use), and total gallons sold to single- and multi-family residential customers (Appendix B.2, Table B.2.2). Water withdrawal from Elberta is used to estimate gross per capita public water use (GPCD)

133

since Elberta is also inside the Wolf Bay watershed area. The average gross per capita water use

from combined water withdrawal data from Elberta and Riviera Utilities divided by sum of

population served by Riviera Utilities and Elberta Water. The average gross per capita public

water use from available years is considered as Population-based water use coefficient for public

water for public water demand projection in Wolf Bay watershed area. The coefficient can be

used to estimate future public water demand in Wolf Bay watershed if and population projections

of the cities or the watershed is known. Assumptions included are; each person uses the same

amount of water, and estimated per capita use remains constant for future years under normal

climatic conditions. This assumption is based on assumption that increased water use due to

affluence will be offset by more conservative use of water through education, outreach, and

newer water saving technologies and programs such as EPA Water Sense program.

1.3.2 Private-supplied water use

Private-supplied water use population

Private-supplied population is estimated as total Wolf Bay watershed population minus

total population served by public water. It is assumed that all the population which is not served

by water companies use privately owned wells. It is simply the population in the rural areas

where public water is not supplied. The same assumption and method is also used by USGS,

Marella et al. (1998).

Total private-supplied water use

The current average gross per capita water use and per capita residential water use from

the largest water company, Riviera Utilities, is used as the most accurate estimate of the average

per capita non-irrigated residential water use. Total private-supplied water use (MG) in Wolf Bay

watershed is estimated as total annual privately supplied population multiplied by average per capita residential water use derived from Riviera Utilities.

Population-based water use coefficient for public water for private-supplied water demand projection

Per capita water use method similar to the public water demand projection method is used to project private-supplied water demand. Future private-supplied population can be projected using projected population of Wolf Bay watershed and future city population similar to the method used for historic private-supplied water use. The population-based water use coefficient to project private-supplied water demand is the average per capita consumption (per capita residential water use) from Riviera Utilities.

1.3.3 Projected population for year 2010, 2020, 2030, and 2040 for public and private water demand projection

The population projection data for Baldwin County from University of Alabama (2005) is used for projecting Wolf Bay watershed population and public water supplied population in the watershed (Table B.1). The 10 year growth rate from 2000 to 2010 and 2010 to 2020 for Baldwin Country is estimated to be 31% and 24 %, respectively (University of Alabama, 2005). Consequently, a 40% incremental growth factor is added to the documented county growth rate to estimate annual growth rate and population for Wolf Bay watershed up to 2040. Percentage increase in Wolf Bay watershed area population is used for projecting population served by public water in Wolf Bay watershed area. It is assumed that the service area will be increased due to increasing urbanization also indicated by the LULC projected maps of Wolf Bay watershed area, and hence, private-supplied population will not be increased in a same manner as population served by public water. It is assumed that private-supplied population will be increased in a decreasing trend as shown in Table B.1.

Table B.1. Projected population (public and private water supplied) in Wolf Bay watershed area for selected years (source: University of Alabama, 2005)

Year	Baldwin County	% change in Baldwin County Population	Population of Wolf Bay watershed area	% change in Wolf Bay watershed population	% change in population served by Public water	Combined Population of Foley and Elberta	% change in population served by Public water	Private-supplied population
1990	98,280		8,406			5,395		*3,011*
2000	140,415	43	15,404	83	68	9,086		*6,318*
2010	184,375	31	*26,754*	74	*74*	*15,781*	50	*9,477*
2020	227727	24	*44,383*	66	66	26,179	25	*11,846*
2030	*281,272*	24	*NA*		66	*43,428*	10	*13,031*
2040	*347,408*	24	*NA*		66	*72,043*	0	*13,031*

Note: values in italics are estimated values

2. Results

2.1. Public water use

2.1.1 Long term average monthly public water withdrawal trend in Wolf Bay area

Figure B.1.3 shows 16-year monthly average water withdrawal from five water companies inside and outside of Wolf Bay watershed areas indicating an increasing water withdrawal rate during summer months. It indicates that water withdrawal rate in Orange Beach water is higher among all water companies especially during the summer months. Though population of Orange Beach is nearly half of the population supplied by Riviera Utilities, water withdrawal rate is higher by Orange Beach water than by Riviera Utilities during growth season months.
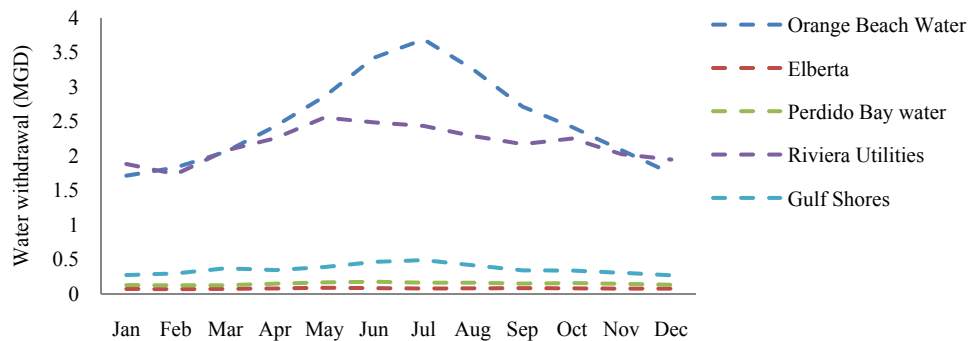
Figure B.1.3. 16-year (1993-2008) average monthly public water withdrawal trend Wolf Bay watershed (Sources: ADECA, Riviera Utilities, Orange Beach Water).

2.1.2 Gross per capita public water use for four water companies in Wolf Bay watershed

Gross per capita public water use from four water companies in Wolf Bay watershed from 1993 to 2008 indicates that Orange Beach has the highest gross per capita public water use and a high variability over the past 16 years as shown in Figure B.1.4. Historic data indicates that water withdrawals for Orange Beach are as high as Foley (16-year average water withdrawal from Orange Beach water and Riviera Utilities are 2.5 MGD and 2.8 MGD, respectively) although Orange Beach has a smaller population. This explains the relatively higher estimated gross per capita public water use in Orange Beach. The cities of Foley (Riviera Utilities) and Elberta have similar steady-state trends in gross per capita public water use over the 16-year period (Figure B.1.4). The cities of Foley and Elberta have similar steady-state trends in gross per capita public water use over the 16-year period. Gulf Shores has what appears to be a declining gross per capita public water use which could caused by its rapidly increasing population.
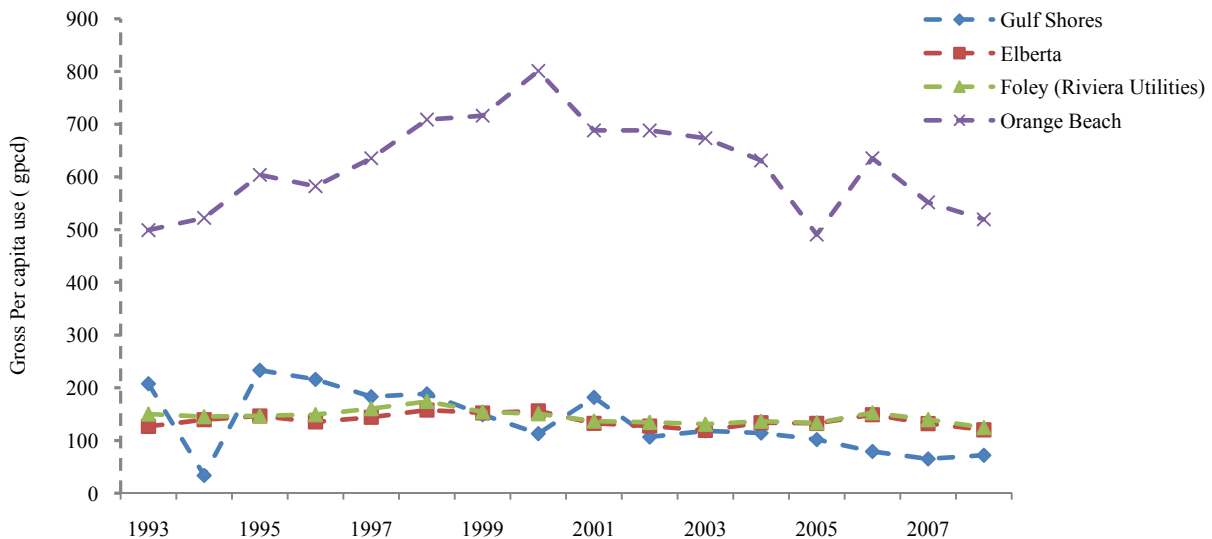
Figure B.1.4. Gross per capita public water use for four water companies in Wolf Bay watershed (Sources: Water withdrawal data of Gulf Shores, Elberta, and Perdido Bay from ADECA, Water withdrawal in Foley from Riviera Utilities, Water withdrawal in Orange Beach from Orange Beach Water, US Census Bureau for 1970,1980,1999,2000 population data from US Census Bureau, and 1990 to 2007 population from Baldwin County Commission).

2.1.3 Per capita residential water use in Riviera Utilities customers from September, 2008 to February, 2010 used for water use per capita in Wolf Bay

Per capita residential water use for Riviera Utilities is estimated by using single-family and multi-family residential served population. Estimated per capita residential water uses from September 2008 to February 2010 are shown in Appendix B.2 (Table B.2.2). Since Riviera Utilities is the largest water company serving public water in Wolf Bay watershed and the only water company for which water structures rates are available (since September 2008), the per capita residential water use of Foley customers is used as the most accurate estimate of per capita (per person) water use for Wolf Bay watershed. The available monthly data for 2008, 2009, and 2010 were used to estimate per capita residential water use (Figure B.1.5) and gross per capita public water use (Figure B.1.6). Figure B.1.5 and Figure B.1.6 indicate that both the per capita residential water use and gross per capita public water use from Riviera Utilities are increasing during summer, with expected decreases during the winter.
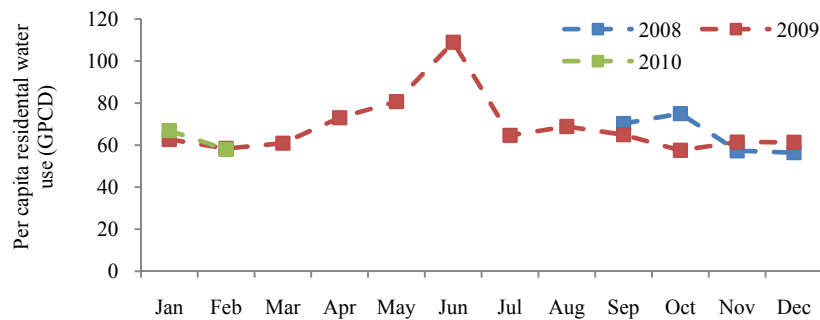
Figure B.1.5. Per capita residential water use in Foley since August 2008 (Source: Riviera Utilities).
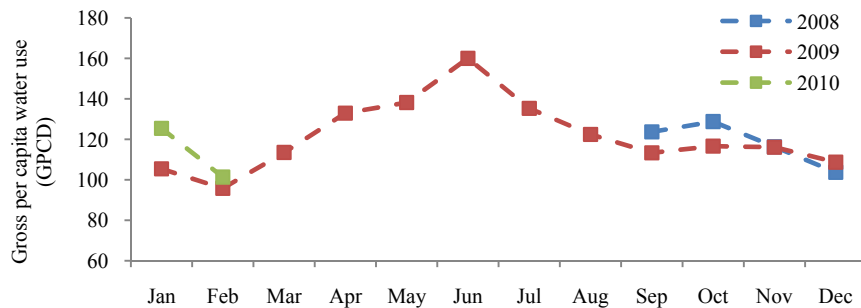
Figure B.1.6. Gross per capita public water use in Foley since August 2008 (Source: Riviera Utilities).

Both the per capita residential water use and gross per capita public water use from Riviera Utilities are increasing during summer, with expected decreases during the winter. Recent Riviera Utilities records are compared to long-term average monthly public withdrawals from the entire watershed (including adjacent cities) in Figure B.1.7, providing a useful means to estimate seasonal fluctuation of water use.
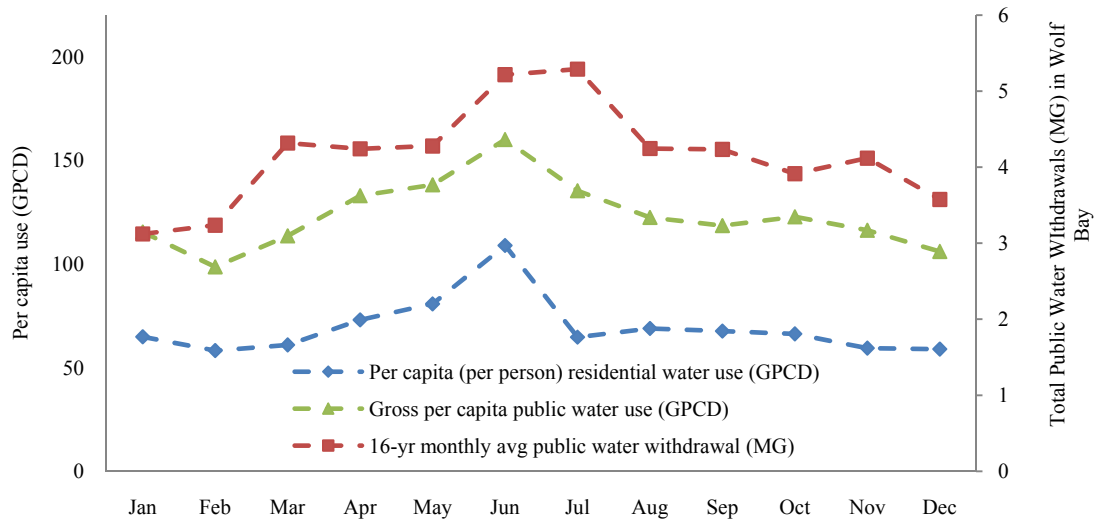
Figure B.1.7. Estimated gross per capita public water use and per capita residential water use (GPCD), Riviera Utilities, from Sep 2008 showing seasonal fluctuation (Source: Riviera Utilities, ADECA, Perdido Bay water, US Census Bureau and Baldwin County Commission).
* 16- year monthly average public water withdrawal is estimated from five water companies (Riviera Utilities, Elberta Water Utility Board, Orange Beach water, Perdido Bay Water, and Gulf Shores Water).

Figure B.1.8 shows the recent one year percentage by volume for different Riviera Utilities water use categories (September, 2008 to February, 2010). Single-Family residential customer's water use is the largest water use customer category in Foley (60% of total water use by volume), suggesting that proactive reductions in residential irrigation use through education, outreach, and reuse can be a major means to reduce water use in the watershed.
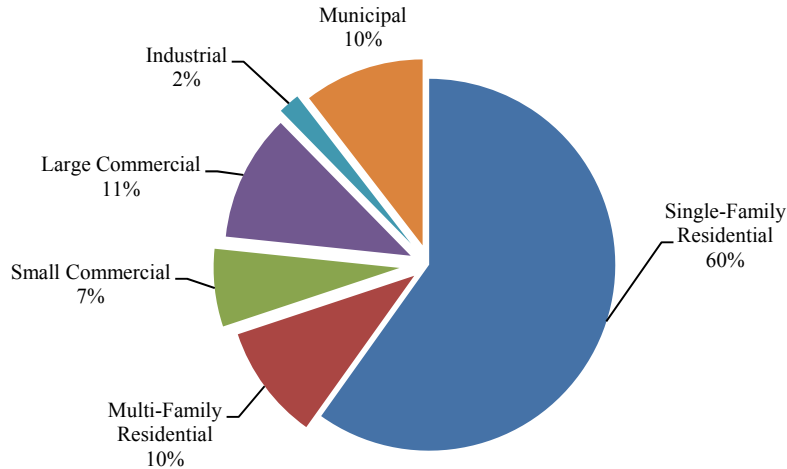
Figure B.1.8. Average volume of water use per customer categories, single-family residential categories used to estimate per capita water use. (Source: Riviera Utilities water rate structures, September 2008-Feburary 2010).

2.1.4 Population based public water demand projection

The 16-year average (1993-2008) per capita public water use coefficient of 145 GPCD is estimated by using available water withdrawal data from Riviera Utilities and Elberta Water. Gross per capita public water use coefficient from 1993 to 2008 are shown in Appendix B.2 (Table B.2.4). The per capita public water use coefficient of 145 GPCD is used for projecting future public water demand for normal years. For projection of public water in dry year, per capita public water use of 151 GPCD is used from year 2000 which received minimum growing precipitation (561 mm) from 1993-2008. For wet year, per capita public water use of 134 GPCD is used from year 2005 which received maximum growing precipitation (1493 mm) from 1993-2008. The projected public water demand is done for year 2010, 2020, 2030, and 2040 using projected population data as shown in Appendix B.2 (Table B.2.5)

Private-supplied water use

2.2.1 Private-supplied water use in Wolf Bay watershed area

Monthly per capita residential water uses from Riviera Utilities as described earlier are shown in Appendix B.2 (Table B.2.2). The average per capita residential water use from

monthly water withdrawal data is estimated 67 GPCD. Total private-supplied water withdrawal is estimated multiplying average per capita residential water use by population those not served by public water (Appendix B.2, Table B.2.3).

2.2.2 Population-based private-supplied public water demand projection

An 18-month average per capita residential water use of 67 GPCD is estimated for projecting future private-supplied water use. An important trend regarding population served by private and public water in Wolf Bay watershed is evident in Figure 1.4 (Chapter 1), indicating increasing water use patterns for public and private-supplied water use in Wolf Bay watershed area since 1970. The projected public water demand is done for year 2010, 2020, 2030, and 2040 using projected population data as shown in Appendix B.2 (Table B.2.5).

Appendix B.2

Public water use and Private-supplied water use in Wolf Bay watershed area: List of tables

Table B.2.1. Data used for estimating public water use and private-supplied water use in Wolf Bay watershed area.

DATA	AVAILABLE DATA	DATA SOURCE
Population	• Population data of Foley, Elberta, Gulf Shores, and Orange Beach from 1990 to 2007 (Source: Baldwin County Commission). • US census population data for 1970 and 1980 for Foley, Elberta, and Gulf Shores. • GIS shapefiles of Population data at US Census block level for 1990 and 2000 from National Historical Geographic Information System (NHGIS). • GIS Point shapefiles for 2004 and 2005 point population data at tract level for Baldwin County obtained from ADECA on May 28, 2009. • Population at HUC-12 level obtained from ADECA. • Population projection of four cities for 2011 by Woods & Poole Economics, Inc. • Population Projection of Elberta for 2020 by Town of Elberta Planning Commission.	US Census Bureau, ADECA, NHGIS
Water use/ withdrawals	• Withdrawal record from Riviera Utilities from 1988 to 2008. • Water rate structures available from Riviera Utilities from September 2008 to February 2010. • Water withdrawal record from Perdido Bay Water from 1999 to 2007 from Perdido Bay Water. • Water withdrawal records from Orange Beach from 1983 to 2008 • Withdrawal records from different public and private water companies in Wolf Bay area back to 1993 (Source: ADECA). • GIS point shapefiles for the locations of public water companies and private well owners (more than 70 gallons/minute) from 1993 to 2008 (Source: ADECA). • Location of irrigation water withdrawal wells in Wolf Bay. • Service area boundary map (Shapefiles) of Riviera Utilities, Elberta Water, and Perdido Bay Water.	Riviera Utilities, Perdido Bay Water, ADECA
Wolf Bay boundary	• Wolf Bay boundary based on outlet	Ruyou Wang (Dr. Latif Kalin's student), Auburn University

Table B.2.2. Per capita residential water use and gross per capita public water use, Riviera Utilities, September 2008 to February 2010 (Source: gallon sold and number of customers from Riviera Utilities, and avg. household size from US Census Bureau).

Year		Total Gallons pumped	Single-Family Residential gallons sold	No. of single family meters	Avg household size	Single-Family Population Served	Per Capita Use (GPCD)	Multi-Family Residential gallons sold	Multi-Family Population Served	Estimated Population Served *	Gross Per Capita Public water Use (GPCD)
2008	Jan-Aug	NA	NA	NA	NA	NA	NA	NA	NA	NA	*NA*
	Sep	80,965,000	40,768,700	8,228	2.35	*19,336*	*70*	5,247,000	*2,489*	*21,825*	*124*
	Oct	88,912,000	45,541,900	8,615	2.35	*20,245*	*75*	6,235,500	*2,772*	*23,017*	*129*
	Nov	82,457,700	34,612,200	8,565	2.35	*20,128*	*57*	6,013,100	*3,497*	*23,625*	*116*
	Dec	73,328,900	33,960,100	8,538	2.35	*20,064*	*56*	5,932,300	*3,505*	*23,569*	*104*
2009	Jan	74,073,899	37,690,300	8,523	2.35	*20,029*	*63*	6,395,700	*3,399*	*23,428*	*105*
	Feb	69,200,399	35,217,200	8,547	2.35	*20,085*	*58*	7,018,700	*4,003*	*24,088*	*96*
	Mar	80,605,601	36,598,100	8,521	2.35	*20,024*	*61*	6,663,400	*3,646*	*23,670*	*114*
	Apr	92,095,300	43,914,100	8,532	2.35	*20,050*	*73*	6,677,300	*3,049*	*23,099*	*133*
	May	94,887,700	48,530,600	8527	2.35	*20,038*	*81*	6,907,200	*2,852*	*22,890*	*138*
	Jun	108,533,000	65,683,400	8553	2.35	*20,100*	*109*	8,205,200	*2,511*	*22,610*	*160*
	Jul	99,421,000	38,976,700	8550	2.35	*20,093*	*65*	8,536,800	*4,401*	*24,493*	*135*
	Aug	87,216,600	41,541,600	8556	2.35	*20,107*	*69*	7,519,600	*3,640*	*23,746*	*122*
	Sep	81,674,000	39,276,100	8,579	2.35	*20,161*	*65*	7,534,100	*3,867*	*24,028*	*113*
	Oct	82,751,800	34,766,500	8,572	2.35	*20,144*	*58*	6,051,100	*3,506*	*23,650*	*117*
	Nov	82,333,700	37,179,200	8,580	2.35	*20,163*	*61*	6,411,300	*3,477*	*23,640*	*116*
	Dec	77,768,900	37,194,100	8,594	2.35	*20,196*	*61*	6,723,800	*3,651*	*23,847*	*109*
2010	Jan	85,075,900	38,837,100	8,588	2.35	*19,336*	*67*	6,588,800	*3,280*	*22,616*	*125*
	Feb	72,342,900	35,189,200	8,653	2.35	*20,245*	*58*	6,164,900	*3,547*	*23,792*	*101*

* Per capita water use (per person) is estimated by diving total single-family residential gallon sold divided by total single-family population served.
** includes communities of Summerdale, Magnolia, Bon Secour, and Elberta (Source: Riviera Utilities water rate structures September 08-February 2010)
Note: Values in italics are estimated values.

Table B.2.3. Estimated population and private-supplied water withdrawals (Source: National Historical Geographic Information System, US Census Bureau, Baldwin County Commission and Planning, Riviera Utilities).

Year	Total Population served by Riviera Utilities (A)	Population of Elberta (B)	Total Public supplied Population* A +B	Population of Foley (C)	Public water supplied population inside Wolf Bay ** D = B +C	Population of Wolf Bay (E)	Self-supplied population (F= E-D)	Per capita water use*** (GPCD)	Total Private supply (MG)
1970	2,332	395	2,727	3,368	3,763	5,079	1,316	67	32
1980	4,017	491	4,508	4,003	4,494	6,719	2,225	67	54
1990	6,633	458	7,091	4,937	5,395	**8,406**	3,011	67	74
1991	7,178	471	7,649	6,129	6,600	9,096	2,496	67	61
1992	7,757	487	8,244	6,425	6,912	9,831	2,919	67	71
1993	8,419	497	8,916	6,674	7,171	10,669	3,498	67	86
1994	9,169	511	9,680	6,955	7,466	11,620	4,154	67	102
1995	9,850	518	10,368	7,212	7,730	12,483	4,753	67	116
1996	10,612	520	11,132	7,517	8,037	13,448	5,411	67	132
1997	11,438	521	11,959	7,866	8,387	14,496	6,109	67	149
1998	12,272	519	12,791	8,319	8,838	15,552	6,714	67	164
1999	13,047	515	13,562	8,743	9,258	16,534	7,276	67	178
2000	13,840	520	14,360	8,534	9,054	**15,404**	6,350	67	155
2001	14,847	558	15,405	8,994	9,552	16,525	6,973	67	171
2002	15,765	563	16,328	9,439	10,002	17,547	7,545	67	185
2003	16,772	568	17,340	9,829	10,397	18,667	8,270	67	202
2004	18,016	576	18,592	10,579	11,155	20,052	8,897	67	218
2005	19,408	584	19,992	11,437	12,021	21,601	9,580	67	234
2006	20,949	586	21,535	12,712	13,298	23,316	10,018	67	245
2007	22,110	579	22,689	13,383	13,962	24,608	10,646	67	260
2008	23,338	671	24,009	13,807	14,478	25,975	11,497	67	281

* This is the public water supplied population based on the Riviera utilities water supply data.
** The actual public supplied water inside the Wolf Bay watershed area will be total population of Foley and Elberta.
*** Average per capita water use or per capita residential water use from Riviera Utilities.
Note: Values in Italics are estimated values.

Table B.2.4. Gross per capita public water use in Wolf Bay watershed area (Source: gallon sold and no. of customers from Riviera Utilities, ADECA, Baldwin County Commission and Planning and US Census Bureau).

year	Annual public water Withdrawal by Elberta Water (MGD) (A)	Annual public water Withdrawal by Riviera Utilities (MGD) (B)	Elberta Population (C)	Population served by Riviera Utilities (D)	Gross per capita public water use (GPCD) in Elberta (1000000 × A/C)	Gross per capita public water use from Riviera Utilities (GPCD) (1000000 × B/D)	Gross per capita public water use (GPCD) in Wolf Bay watershed area [1000000 × (A+B)/(C+D)]
1993	0.063*	1.264	497	*8419*	127	*150*	*149*
1994	0.071	1.332	511	*9169*	140	*145*	*145*
1995	0.076	1.447	518	*9850*	146	*147*	*147*
1996	0.070	1.583	520	*10612*	135	*149*	*148*
1997	0.075	1.835	521	*11438*	144	*160*	*160*
1998	0.082	2.139	519	*12272*	158	*174*	*174*
1999	0.078	2.013	515	*13047*	152	*154*	*154*
2000	0.081	2.088	520	*13840*	156	*151*	*151*
2001	0.074	2.032	558	*14847*	133	*137*	*137*
2002	0.072	2.123	563	*15765*	127	*135*	*134*
2003	0.068	2.198	568	*16772*	119	*131*	*131*
2004	0.077	2.461	576	*18016*	134	*137*	*137*
2005	0.077	2.592	584	*19408*	132	*134*	*134*
2006	0.087	3.196	586	*20949*	149	*153*	*152*
2007	0.077	3.091	579	*22110*	132	*140*	*140*
2008	0.081	2.906	677	*23338*	120	*125*	*124*

* Average from April to December 1993, since January-March, 1993 data was not available.
Note: Values in italics are estimated values.

Table B.2.5. Projected public water use and private-supplied water demand in Wolf Bay watershed area.

	Year	Public			Private- supplied		
		Population	GPCD*	Water demand in million cubic meters**	Population	GPCD***	Water demand in million cubic meters
Dry	2010	15,781	151	3.29	9,477	67	0.88
	2020	26,179	151	5.46	11,846	67	1.10
	2030	43,428	151	9.06	13,031	67	1.21
	2040	72,043	151	15.03	13,031	67	1.21
Wet	2010	15,781	134	2.92	9,477	67	0.88
	2020	26,179	134	4.85	11,846	67	1.10
	2030	43,428	134	8.04	13,031	67	1.21
	2040	72,043	134	13.34	13,031	67	1.21
Normal	2010	15,781	137	2.99	9,477	67	0.88
	2020	26,179	137	4.96	11,846	67	1.10
	2030	43,428	137	8.22	13,031	67	1.21
	2040	72,043	137	13.64	13,031	67	1.21

* Gallons per capita per day, gross per capita public water use
** Estimated as Population×GPCD×365×0.00378541178/1000000
*** Gross per capita private-supplied water use

Appendix B.3

Water demand Projection in Wolf Bay watershed area

Total projected water demand is estimated as the sum of projected water demand for public, irrigation and private supplied water use for dry, normal and wet years of 2010, 2020, 2030, and 2040. It is estimated that the total water demand in Wolf Bay watershed area will be increased by approximately 146% by 2040 as shown in Figure B.3.1. The projected total water demand in Wolf Bay watershed area and water demand in depth (mm) are shown in Table B.3.1.
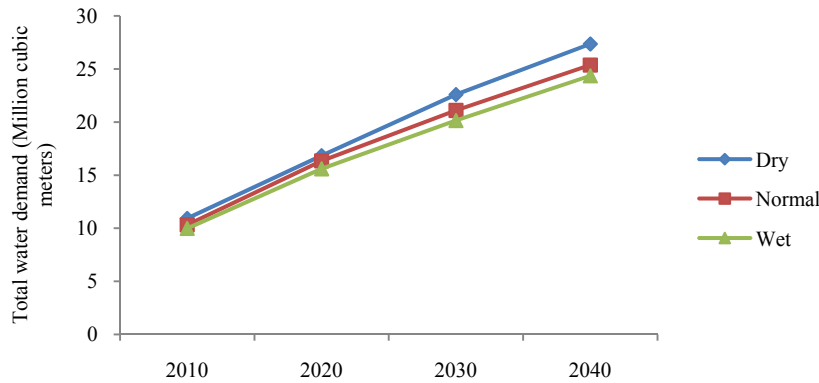
Figure B.3.1. Total projected water demand in Wolf Bay watershed area

Table B.3.1. Projected water demand (Million cubic meters) in Wolf Bay watershed area under dry normal and wet years and water demand in mm (water demand/total area of Wolf Bay watershed area, 126 km^2)

	Dry				Normal				wet			
Year	2010	2020	2030	2040	2010	2020	2030	2040	2010	2020	2030	2040
Total water demand in million cubic meters	10.93	16.84	22.59	27.36	10.31	16.34	21.10	25.37	9.99	15.60	20.15	24.36
Water demand (mm)	87	134	179	217	82	130	167	201	79	124	160	193